



**Energy Technologies Area**

# **MEASUREMENT & VERIFICATION OF THE PERFORMANCE OF SOLARIA BIPV IN FLEXLAB TEST FACILITY**

*Prepared by: Jinqing Peng, Howdy Goudey, Anothai Thanachareonkit,  
Charlie Curcija, Eleanor Lee*

*Date: May 15, 2017*

## TABLE OF CONTENTS

TABLE OF CONTENTS .....	2
1. EXECUTIVE SUMMARY .....	4
1.1 Background.....	4
1.2 Overview of the Solaria BIPV Technology.....	4
1.3 Project Results and Findings.....	5
1.4 Major Conclusions and Recommendations .....	8
2. BACKGROUND .....	9
2.1 Window Energy Consumption Status and Energy Saving Opportunity .....	9
2.2 State of the Art Window Technology .....	9
2.3 Building Integrated Photovoltaic Windows .....	12
2.4 Solaria BIPV Modules Tested in the FLEXLAB.....	14
3. PROJECT INSTALLATION AND EVALUATION .....	15
3.1 FLEXLAB XR Test Bed.....	15
3.2 Solaria BIPV Integral Glass Unit.....	17
3.3 Integrated Glass Units and Installation.....	20
3.4 BIPV System .....	26
4. PROJECT RESULTS AND FINDINGS.....	28
4.1 Testing Schedule and Measured Parameters.....	28
4.2 Power Generation Performance .....	31
4.3 Predicted Power Generation Performance.....	45
4.4 Thermal Performance & HVAC Electricity Consumption .....	46
4.4.1 Testing Results: South Orientation .....	50
4.4.2 Testing Results: Southeast Orientation .....	56
4.4.3 Testing Results: West Orientation.....	60
4.5 Daylighting Performance .....	63
4.5.1 Visual comfort.....	63
4.5.2 Lighting energy .....	65
4.5.3 Daylight adequacy .....	65
4.5.4 Discomfort glare and lighting energy use .....	65

4.6	Comparison of Overall Energy Performance .....	73
5.	CONCLUSIONS .....	75
6.	RECOMMENDATIONS.....	76
7.	REFERENCES .....	77

## 1. EXECUTIVE SUMMARY

### 1.1 Background

BIPV windows refer to the integration of electricity-producing PV elements into a window or building façade system, most commonly glazing or spandrel panels. There are several types of BIPV glazing systems available today, ranging from light redirecting layers that direct solar radiation to strategically placed PV cells, to semi-transparent PV coatings (STPV) and traditional opaque PV cells integrated into selected area of laminated glass. Compared to other advanced window technologies, BIPV glazing is distinguished by the ability to transform a portion of the incident solar irradiation into useful electrical power through the photovoltaic effect, while at the same time contributing to the regulation of solar heat gain and daylighting glare by reducing the solar transmittance through the glazing PV. BIPV windows provide a very promising alternative window choice for buildings striving to meet zero net energy goals, especially for buildings that are characterized by the large window to wall ratio (WWR) and limited useful roof area.

### 1.2 Overview of the Solaria BIPV Technology

Solaria BIPV technology consists of traditional crystalline opaque PV cells cut into strips and integrated into a glass laminate. This glass laminate is normally incorporated into the insulated glazing unit (IGU), where glass laminate with PV is outdoor-facing to maximize the conversion of solar radiation into electricity. Because the crystalline solar cell area is opaque, transparency of the glazing system is achieved by appropriately spacing PV strips, so that there is alternating transparent and opaque area, as shown in **Error! Reference source not found.** The thickness of the laminated solar cells and the width of the gap can be varied according to the requirements of the owner and building. These requirements typically seek to optimize the balance between electricity production, visible transmittance and shading, as well as aesthetics.



Window with Solaria Glazing PV

Edge areas, near the frame can be left fully transparent (i.e., without PV cells) and their size can be customized based on aesthetic or other preferences. Solaria PV strips are grouped in blocks of horizontal strips, which are connected by three vertical leads. These leads are then connected with other blocks. Each column is connected to main leads for the window

Depending on the module size and electric parameters, two windows are connected to a single micro-inverter channel. Inverters are then connected to the electrical grid. This configuration provides maximum flexibility, where failure of one of windows or inverters affects only two windows at the time. Windows can also be connected in series and onto a string-inverter.

### 1.3 Project Results and Findings

To evaluate the overall energy performance of the BIPV window relative to typical low-e coated reference windows, a side by side outdoor comparative test was conducted in FLEXLAB (Facility for Low Energy Experiments in Buildings) at Lawrence Berkeley National Laboratory (LBNL). This comparative test was conducted under several orientations (southeast, south, southwest and west), different room set point temperatures, as well as different interior venetian blind shading positions. Various energy consumption related parameters were measured during this test, including daylighting illuminance, HVAC electricity use, as well as power generation from the BIPV windows. Lighting electricity use was modeled based on measured illuminance data.

The solar heat gain coefficient (SHGC) of the BIPV insulated glazing unit (IGU) window and the reference IGU were 0.25 and 0.32, respectively. The lower solar gain of the BIPV IGU was in part because a fraction of the incident solar energy was converted into useful electrical power to serve the building electrical loads. As a portion of glazing is covered by opaque solar cells, the solar transmittance of the BIPV IGU was also much lower than that of the reference IGU. The average solar transmittance of the BIPV IGU and the reference IGU were 0.11 and 0.23, respectively. However, the BIPV IGU had a higher U-factor than the reference IGU. The U-factors were 2.68 and 1.62 for the BIPV IGU and the reference IGU, respectively. Higher U-factor means less thermal insulation which would result in larger heating load in winter and slightly higher cooling load in summer due to heat transfer based on air-to-air temperature difference. Reasons for higher U-factor were not inherent to Solaria BIPV design, though, but to the choice of placement of low-e coating in reference vs. BIPV glazing. Low-e coating was embedded in laminate of the BIPV glazing, while in reference glazing, low-e surface was exposed on surface #2. If desired, this can be solved by placing the low-e coating on different surface e.g. #4. Embedded low-e coating means that it no longer exhibits low emissivity and thus has higher thermal transmittance due to increased thermal radiation heat transfer as compared to reference glazing.

For commercial buildings that tend to be cooling energy dominated in many climates, lower SHGC means reduced HVAC electricity use, but the results can also vary by the orientation of the façade. The BIPV IGU had much better energy saving potential when it was facing the south orientation than the southeast orientation. The average HVAC electricity savings for the south facing BIPV IGU was 11.6%, but it was only 2.6% for southeast facing. The difference in energy savings for this orientation is at least in part a result of a shading discrepancy between the two test cells from an adjacent structure. The total energy saving potential of the BIPV IGU, taking the reduction of HVAC electricity use, the increase of lighting electricity use and the power generation into account, was 15.9% compared with the reference IGU when cooling was provided. In addition, the presence of an interior horizontal louvered blind affected the HVAC energy saving of the BIPV IGU. The BIPV IGU demonstrated a higher relative energy saving potential when both façades did not have the interior blinds deployed. A lower relative energy savings was demonstrated when the interior blinds were deployed in both rooms. However, in space heating case, the higher U-factor of the BIPV IGU means the larger heating load and larger HVAC electricity use. Compared with the reference IGU, the BIPV IGU consumed 19.3%

more electricity for space heating in winter. Again, this is attributed to the higher U-value that can be addressed by a different choice of low-e placement and/or width of air gap.

Compared to other advanced window technologies, the most outstanding merit of the BIPV IGU is a combination of energy efficient glazing with the local power generation delivered to the building through photovoltaic effect. To analyze the power generation performance, the incident solar irradiation and real-time power output of the BIPV IGU were measured and recorded. During the test period, the daily average incident solar irradiations were 4.53kWh/m<sup>2</sup> and 3.92kWh/m<sup>2</sup> for the south and southeast orientation, respectively. The highest daily electricity output of the BIPV IGU was 2.68kWh for entire window area, or 0.3 kWh/m<sup>2</sup>. This reading occurred on November 19, 2015 while the BIPV IGU was facing south orientation. Based on the incident solar irradiation and electricity output, the daily energy conversion efficiency of the BIPV IGU was calculated. It was about 5% on sunny days, calculated over the entire glazing area, but it was much lower on overcast days because it is well known that crystalline silicon solar cells have lower efficiency under low irradiation level. Usually, the energy conversion efficiency of crystalline silicon-based PV modules ranges from 16% to 18% under the standard test conditions. The BIPV IGU studied in this test was patterned in a form of semi-transparent array of cells, with one third of the BIPV laminate area covered by solar cells, thus the energy conversion efficiency of 5% was within expected range and manufacturer claim, since it would translate to equivalent of 15% efficiency for the solar cell area itself. Note that this particular IGU has non-ideal size that leaves more than typical unused space around the PV cells. When IGU size is better matched, efficiency is expected to be higher. Moreover, the daily average electricity outputs at different orientations were calculated for the measurement period. They were 1.58kWh, 1.94kWh and 1.91kWh for the southeast, south and southwest orientations, respectively. As expected based on solar geometry and morning versus afternoon cloud cover patterns for Berkeley, CA, a conclusion can be drawn that south and southwest orientations are typically more suitable for installing BIPV in the San Francisco Bay Area.

The impacts of solar irradiation level, incident angle and PV module temperature on the energy conversion efficiency of BIPV laminates were also analyzed during the test period. It was found that the energy conversion efficiency increased with the solar irradiation increasing, the efficiency decline was especially notable when the solar irradiation was less than 300W/m<sup>2</sup>. The relationship between solar incident angle and energy conversion efficiency showed that the energy conversion efficiency increased when the incident angle approached normal incidence, the decline in efficiency was especially notable when the incident angle was larger than 70 degrees of the plane of the window. It is well known that PV conversion efficiency declines with increased temperature. For the BIPV tested, it was found that the power output of the BIPV laminate declined by 0.42%, for each Celsius degree temperature rise (this is equivalent 0.021% absolute decline in conversion efficiency). Thus, in order to improve the energy conversion efficiency, more attention could be paid on the heat dissipation issue of BIPV IGU in future design.

For BIPV systems, one of the most concerning design problems is minimizing the performance impacts of the shading from the building itself and its surroundings. The orientation of different obstructions relative to the path of the sun will cast different patterns of shadow and result in

different impact on the power output. In this test, vertical and horizontal shade tests were conducted to analyze the impacts of the two typical shade conditions on the power generation performance of BIPV IGU.

For vertical shade case, the total energy output of the shaded BIPV array was only 4% lower than that of the unshaded BIPV array. There are two explanations why the effect of shading was relatively small in this case. The façade orientation was southwest, thus the vertical shade fin only cast shadow on the BIPV IGU during the late afternoon (a short period of the day when the solar intensity was already diminishing). Also, each PV laminate consists of 8 vertical columns of PV strings (four columns on one side are wired in parallel, together in series with the second paralleled block of four columns). In this vertical shade case, although the outermost vertical PV string was totally shaded, the remaining 3 PV strings in parallel can operate as usual, thus the total power output was reduced by 1/4 at most for this part of the array. The BIPV design, as tested, is inherently less sensitive to modest bands of shading along a vertical edge of the glazing, because of available parallel paths for current to flow.

For horizontal shade case, the total energy output of the shaded BIPV array was lower than that of the unshaded BIPV array by 28.1%. Specifically, the power output of the shaded BIPV array was only half of the unshaded BIPV array before 2:00 PM. This is because the horizontal shade device cast shadows, which impaired the current flow through all the parallel strings, effectively eliminating electricity production from this part of the array even though it was only partially shaded. However, the second BIPV IGU in series with the shaded array operated as usual because there was bypass diode--which would be installed as needed based on shading profiles--for conducting electricity in the junction box, thus the total energy output of the shaded BIPV array was half of that of the unshaded BIPV array. The power drop in horizontal shading situation can be avoided by shifting the PV strings down. Alternatively, different routing can be used to accommodate shading realities and minimize its impact. Furthermore, the use of micro-inverters can significantly reduce shading impacts altogether.

As configured in this study, the BIPV window alone is insufficient for controlling discomfort glare from the windows. When the BIPV window is used with venetian blinds, lighting energy use is greater than the same glazing without the BIPV elements. The net difference in daytime lighting energy use (8AM-6PM) is small, however, compared to the daily energy output of the BIPV due to the low power use of the efficient lighting system and low setpoint (300 lux), even when the dimmable lighting is considered across the entire 30 ft. depth of a south-facing perimeter zone. The indoor space, however, may be perceived as gloomy by some occupants since daylight availability will be reduced in proportion to the amount of BIPV used within the transparent area of the window, although good lighting design could overcome most of these problems.

Provided that measurements were done for approximately three months in late Summer and Fall of 2015, online modeling tool was used to calculate power production for the whole year. NREL's PVWatts<sup>1</sup> online software tool was used, after calibrating it with measured data for

---

<sup>1</sup> <http://pvwatts.nrel.gov/pvwatts.php>

these specific months. For the total of 8.99 m<sup>2</sup> of window vision area (i.e., exposed area of glazing) and the total of 3.05 m<sup>2</sup> of PV cells (very close to 1:3 area ratio), a total of 548 kWh, or 60.6 kWh/m<sup>2</sup> was produced.

Cost effectiveness of the glazing-integrated BIPV can be estimated from the cost premium of this technology over the reference glazing without BIPV. Using manufacturer's cost data and considering current pricing information, total installed cost per area (sq. ft.) of a window with BIPV would be approximate \$150/sf, while the total installed cost of reference window would be around \$100/sf. Both costs are fully burdened, installed costs. In the U.S.A, the difference of \$50/sf would need to be weighed by three elements – PV dedicated Federal incentives, namely the ITC and MACRS (accelerated depreciation), annual energy savings, and annual electricity production. With current pricing, ITC at 30% and MACRS at 5 years, the incremental cost difference is close to a wash. Of course, this will be true as long as ITC on a federal and/or state level is available. That would leave the value of energy savings and energy generation as a financial upside. For example, annual electricity production at 6 kWh/sf would be \$1.20/sf/yr., using conservative \$0.20/kWh cost of electricity. Payback periods, based on economic analysis would typically be achieving less than 3-year payback and double digit IRR. In case that ITC is not available, the payback period would increase to about 20 years. Novelty of the technology, various wiring requirements and subsequent safety compliance issues might bring installed cost higher, but that is difficult to determine without information about the specific project.

#### **1.4 Major Conclusions and Recommendations**

1. BIPV window has a relatively high energy conversion efficiency due to high efficiency crystalline silicon (c-Si) solar cells being used. The daily average energy conversion efficiency of the BIPV IGU under test was about 5% on sunny days. The daily average electricity outputs at different orientations were 1.58kWh, 1.94kWh and 1.91kWh for the southeast, south and southwest orientations, respectively. Thus, south and southwest orientations are definitely more favorable for installing BIPV IGU in terms of increasing power generation. Furthermore, using higher efficiency c-Si cells would further increase the energy yield.
2. Compared to the test cell with reference IGU, the test cell with BIPV IGU had lower overall energy use. On average, BIPV IGU showed a 15.9% total energy saving potential (including power generation) during the test period.
3. Electricity production on vertical window surfaces yield relatively uniform monthly energy throughout the year. This is due to the interesting coupling of solar angles and incident solar radiation intensity, so when intensity is lower, the incident angle closer to normal and vice versa, resulting in relatively constant output.
4. Discomfort glare is lower with the BIPV window compared to the reference window due to the combined effect of both the visible transmittance of the transparent glass and the lower percentage of transparent window area. However, a combination of a lower transmittance glazing and/or suitable shading system will be needed to bring overall discomfort levels in both rooms to below the “just perceptible” glare level of 0.35

5. Leveraging its high uniformity, the Solaria BIPV IGU has agreeable visual appearance, both looking from indoors and outdoors. View through the BIPV window does not appear significantly obstructed and it has the overall appearance of fritted striped glazing.

## 2. BACKGROUND

### 2.1 Window Energy Consumption Status and Energy Saving Opportunity

Windows present a significant energy load to buildings, especially in modern high-rise buildings with large window wall ratio (WWR). It was estimated by the United States (U.S.) Department of Energy (DOE) that 30% of the energy used to heat and cool all buildings in the U.S. is lost through inefficient windows, which resulted in a cost of \$42 billion per year [1-2]. Previous studies by Lawrence Berkley National Laboratory (LBNL or Berkeley Lab) have estimated that, averaged over the contemporary building stock in the U.S., roughly 39% of heating energy BTUs consumed in commercial buildings annually, or 0.96 quadrillion BTUs (quads) out of 2.45 quads, is associated with windows. Windows are also a significant factor in the cooling energy used in buildings, with 0.52 out of 1.9 quads, or 28%, of building cooling energy demand attributed to windows (see Table 1, [3]). In this context, developing advanced windows and then replacing or retrofitting the existing inefficient window systems has a huge energy saving potential in the U.S. It has been estimated that replacing the entire existing commercial building window systems with typical low-e double pane windows ( $U=0.4$  BTU/hr-ft<sup>2</sup>-F and SHGC=0.29) could save 0.32 quads (or 62%) of the annual commercial building cooling energy [3], which is equivalent to the annual energy consumed by roughly 1.8 million U.S. households [4].

**Table 1** U.S. Annual Commercial Building Window Energy Use - reported in quadrillion BTUs (quads) of primary (source) energy [3]

Modes	Building HVAC energy consumption	Window-related energy consumption	Percent of building HVAC energy-related to windows
Heating	2.45	0.96	39%
Cooling	1.90	0.52	28%
Total	4.35	1.48	34%

### 2.2 State of the Art Window Technology

High-performance window technology development over the years has achieved significant reductions of heat flow through windows by means of controlling thermal conduction, convection, and radiation. Some of the established high-performance design elements include multiple glazing layers that enclose hermetically sealed insulating gas layers or vacuum glazing technology to reduce conduction and convection, low-emissivity (low-e) films to reduce radiant heat exchange between the layers and more insulating frames and edge of glass spacer materials to reduce conduction at the perimeter of the glass area. These measures address the

thermal transfer due to the interior-exterior temperature difference, typically reported as a resistance (R-value) for walls, or as a U-factor (inverse of R-value) for windows.

Except for thermal insulation performance, windows, as distinct from opaque walls, have additional functions, such as the acquisition of daylighting, visual contact between indoors and outdoors, and so on. Thus, additional performance criteria are necessary to evaluate the overall performance of a window system. The first assessment criterion is solar heat gain coefficient (SHGC), which evaluates the amount of solar energy gained through the window. SHGC is a dimensionless number from zero to one that represents the fraction of solar energy incident on the exterior of a window and frame that is transmitted to the interior. Another important criterion is the visible light transmittance ( $T_{vis}$ ) of a window, which represents the amount of useful daylight transmitted through the window unit, factoring in shading from window framing. High visible light transmittance through windows can reduce electric lighting loads and improve the quality of light and occupant enjoyment of the space, although too much direct light transmission can cause discomfort from glare.

In short, most of the research related to window glazing focuses on optimizing SHGC, ( $T_{vis}$ ) and U-factor based on the climate, occupancy type and orientation of the building. Good thermal design coupled with good daylighting design that maximizes useful visible light while controlling glare, can significantly reduce energy consumption for heating, cooling and lighting. Common window technologies include low-e coatings, multi-pane layers, inert gas fill (e.g., Argon, Krypton), and low-conductance spacer and frame technologies. Technologies under development and partial deployment include vacuum glazing, electrochromic or thermochromic glazing, Nanoparticle coatings, etc.

Low-emissivity (low-e) coatings are a common window technology used to improve the insulating performance of double pane windows (i.e., lowering the radiative portion of U-factor). Low-e coatings function by reducing the long wave infrared radiation exchange between glazing layers that would otherwise occur under a layer to layer temperature difference. Low-e coatings can be also designed to reflect portions of solar spectrum as well, principally in the infrared wavelengths, resulting in lower solar heat gains, without significantly increasing glass temperature or reducing visible transmittance. A low-e coating with these properties is called a spectrally selective, or low solar gain, low-e coating. It preserves a relatively high visible transmission, maintaining the appearance of clear glass, while reflecting most of the invisible, near-infrared, portion of sunlight, which carries about half of the radiant energy in the solar spectrum. This combination of properties, available in low-e coatings, can reduce both heating and cooling loads in buildings, leading to energy savings potential in both winter and summer.

Double-glazing is a norm today in the United States. Most of the energy codes now require at least double pane glazing and in many cases in the heating climates in the north, triple or quadruple glazing is used. When combined with Argon or Krypton gas fill, these windows can achieve a thermal resistance of R-5 or higher. Insulating spacers not only reduce heat transfer through the frame, but also vastly improve condensation resistance of a window, because it insulates glazing edges, where condensation usually occurs.

Vacuum glazing consists of two flat sheets of glass hermetically sealed together around the edges, and separated by a narrow ( $\sim 0.2$  mm) evacuated space, as shown in Figure 1 [5]. Under the influence of atmospheric pressure, the internal surfaces of the glass sheets are kept apart by an array of small support pillars which are high strength material [5]. As the vacuum eliminates heat conduction and heat convection in the gap between the two glass plates, and the internal low-e coating reduces radiative heat transfer, the thermal insulation performance of vacuum glazing is very good, whose U-value can be as low as  $0.4\text{W}/(\text{m}^2\text{K})$  or less [6].

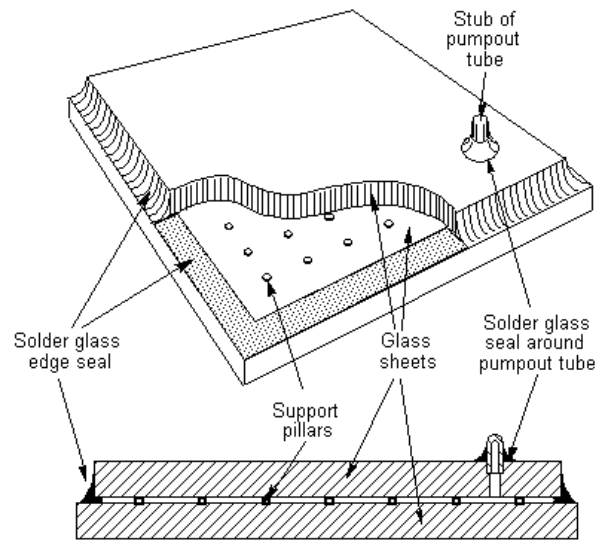


**Figure 1** Structure diagram of vacuum glazing

Electrochromic glass, also known as smart glass or electronically switchable glass, is an innovative glass that can be used to produce windows, skylights and curtain walls. Electrochromic glass is developed based on the principle of electrochromism, which is the phenomenon displayed by some materials of reversibly changing color (or switch from transparent to opaque) by using bursts of charge to cause electrochemical redox reactions. In one form of electrochromic technology, as shown in Figure 2, when lithium ions exist in the inner electrode (close to room side), the glass is clear, when a voltage is applied to the electrodes, the ions transfer through the separator to the outside electrode, where they scatter away most of the incoming light and thus turn the glass dark or even opaque [7]. The process of ion migration is reversible when polarity is reversed. A prominent advantage of electrochromic glass is that occupants can control the amount of heat or daylight passing through the window by flicking a switch and then a thermal and visual comfortable indoor environment is realized.

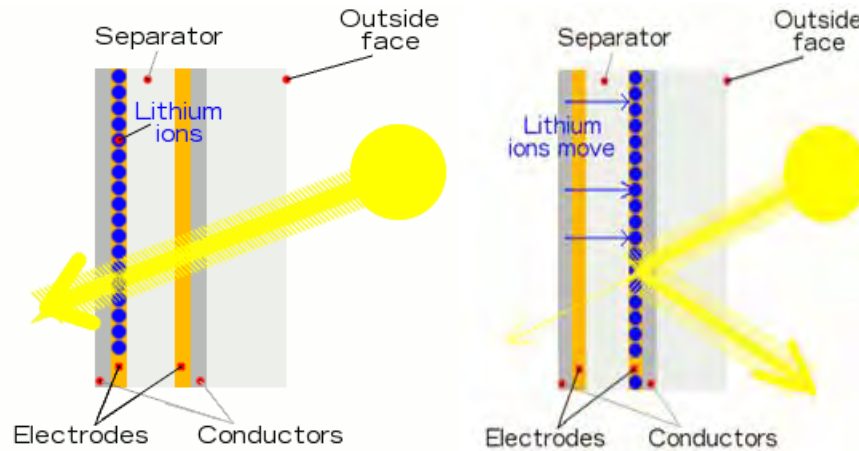


**Figure 2** An example of electrochromic glass [7]

Thermochromic windows dynamically shift from clear to dark using adhesive coating to adjust tinting passively in response to outdoor temperature and solar radiation. Compared to electrochromic glass, thermochromic glass uses heat from sunlight to tint the windows, thus it is more simpler and “automatic”. The more solar irradiation is shining on the window, the darker the window will become [8]. This function allows the windows to significantly reduce the solar heat gain and daylighting glare when necessary. A GSA pilot evaluation reported that the thermochromic windows can reduce about 10% of annual HVAC cooling electricity use compared to low-e windows [9].

As mentioned above, many high-performance window technologies, such as low-e windows, chromogenic windows and vacuum glazing windows, have been developed and utilized to reduce the window related building energy consumption in recent years. However, all these technologies can only reduce energy consumption by passively reflecting or preventing superfluous heat gain and daylighting illuminance. They can't reduce solar heat gain and daylighting glare, while actively producing electric power in the way that building integrated photovoltaic windows (BIPV windows) can.

### 2.3 Building Integrated Photovoltaic Windows

BIPV windows refer to the use of glass-laminated semi-transparent PV (STPV) modules to substitute for conventional glazing in framed window and curtainwall systems. These PV modules can be comprised of full poly- or mono-crystalline cells or, as in the case of Solaria, strips of mono-crystalline cells tied together into strings via a busbar. Varying the width of the strips, as well as varying the gaps between the strips allows designers to balance SHGC,  $T_{vis}$  and DC power production. An optimally designed BIPV window can not only reduce unnecessary solar heat gain and undesirable daylighting glare, but also actively convert the part of undesirable and excessive incident solar energy into electricity rather than passively reflect, discard or prevent it like the other commonly used window technologies. To some extent, BIPV windows are characterized by both functions of building energy efficiency and distributed renewable energy generation. Thus, they provide pretty good alternative choices for high-rise office buildings which are characterized by large window area, high solar heat gain as well as

big peak load. With the further improvement of energy conversion efficiency and reduction of cost of solar cells, semi-transparent BIPV windows with customized sizes, patterns and colors should achieve a much better overall energy performance and economic returns in future.

The transparency of semi-transparent PV modules is normally achieved by three different ways. For thin-film PV modules, the solar cell layer can be so thin that it is see-through [10], as shown in Figure 3. However, the visible transmittance of this kind of semi-transparent PV modules is usually as low as 5%, which is unable to meet daylighting requirements as well as to achieve an acceptable visual view. Thus, it is usually adopted in locations where the daylighting demand is not really a concern. In addition, the thin-film solar cell layer can also be grooved by laser to increase transparency, as shown in Figure 4. Compared to earlier versions of semi-transparent PV modules, the transmittance of the laser grooved PV modules is much higher and theoretically any transmittance can be achieved for this kind of PV modules by adjusting the width of groove. Usually, 20%-30% transmittances were adopted for BIPV window applications to maximize the overall energy performance, which includes the power generation performance, daylighting performance and thermal insulation performance.

Even though the transmittance of the second kind of PV modules can be customized according to the daylighting requirement, their energy conversion efficiency would be very low if the high visible transmittance is required. Typically, the energy conversion efficiency would be lower than 5% if the transmittance is higher than 30%. For semi-transparent crystalline silicon PV modules, as shown in Figure 5, the transparency is achieved by placing the opaque solar cells in the laminate with a certain interval so that partial light could penetrate through the PV module and illuminate the indoor room. Compared to thin-film semi-transparent PV modules, the advantage of this kind of semi-transparent PV modules is the relatively high energy conversion efficiency due to crystalline silicon solar cells being used. However, the using of big opaque solar cells (156x156 mm<sup>2</sup>) in the laminate on the one hand would cast shadow in indoor room and result in uncomfortable illuminance distribution as shown in Figure 5, on the other hand may block the sight of occupants. It is obvious that the second semi-transparent thin-film PV module seems to be much more aesthetically and optically pleasing than the semi-transparent crystalline silicon PV module due to its uniform appearance and color.



**Figure 3** Semi-transparent thin-film PV module with see-through solar cell (5% transmittance)



**Figure 4** Semi-transparent thin-film PV module with laser grooved (20% transmittance)



**Figure 5** Semi-transparent crystalline silicon PV modules with uncomfortable illuminance distribution

#### **2.4 Solaria BIPV Modules Tested in the FLEXLAB**

In summary, as mentioned above, both the semi-transparent thin-film PV modules and crystalline silicon PV modules have advantages and disadvantages in terms of energy conversion efficiency, appearance aesthetics and visual effect. However, a novel semi-transparent crystalline silicon PV module which combined the advantages of both the laser groove thin-film PV modules and the conventional crystalline silicon semi-transparent PV modules has been developed by the Solaria Corporation. Solaria's semi-transparent PV module was produced by cutting standard crystalline silicon solar cells into small strips and then automatically welding and connecting the strips into strings for laminating. This kind of PV module not only has the same beautiful appearance and pretty good visual effect as the laser grooved thin-film PV modules, but also has a relatively high energy conversion efficiency due to high efficiency crystalline silicon solar cells being used. The Solaria semi-transparent PV

module has much higher energy conversion efficiency than the laser grooved thin-film PV modules when achieving the same visible transmittance.

To evaluate the overall energy performance of the Solaria semi-transparent BIPV window, as well as identify its energy saving potential compared with low-e coating windows, a comparative field test was conducted in the FLEXLAB (Facility for Low Energy Experiment in Buildings) at Lawrence Berkeley National Laboratory (LBNL). Various energy consumption related parameters were measured during this test, including daylighting illuminance, lighting electricity use, HVAC electricity use as well as power generation data of the BIPV windows. This report mainly compares and analyzes the daylighting and thermal performance of both the BIPV window and the low-e coating reference window. The power generation performance of the BIPV windows under different orientations and different shade conditions was also presented and analyzed. In addition, the overall energy performance of the BIPV windows was evaluated and its energy saving potential compared to the low-e coating reference window was identified. Finally, based on the test results, some important conclusions and recommendations were presented.

### **3. PROJECT INSTALLATION AND EVALUATION**

#### **3.1 FLEXLAB XR Test Bed**

DOE's FLEXLAB at Berkeley Lab, as shown in [Figure 6](#), is the most flexible, comprehensive, and advanced building efficiency simulator in the world and it's unleashing the full potential of energy efficiency in buildings. FLEXLAB lets users test energy-efficient building systems individually or as an integrated system, under real-world conditions. FLEXLAB test beds can test HVAC, lighting, windows, building envelope, control systems, and plug loads, in any combination. Users can test alternatives, perform cost-benefit analyses and ensure a building will be as efficient as possible — before construction or retrofitting even begins. Last, but not least, FLEXLAB can also conduct comparative studies in real-world conditions for different building components and equipment, such as windows, building envelope, HVAC, lighting systems, in order to identify the full energy saving potential of emerging building technologies. The main objective of this comparative test is to identify the energy saving potential of the Solaria building integrated photovoltaic (BIPV) window compared to the most representative glazing windows on buildings.



**Figure 6** Facility for Low Energy Experiment in Buildings (FLEXLAB) at Berkeley Lab

FLEXLAB consists of four test beds, viz. X1, X2, X3 and XR. Each test bed includes two identical test cells, which can be used for comparative study. For the X1 to X3 test beds, the orientation is fixed to due south. The XR test bed, where the test was conducted, is set on a turntable, which allows the test bed to rotate from a southeastern orientation to a northern orientation to test the overall energy performance of the BIPV window in different orientations. [Figure 7](#) presents the layout of the rotatable XR test bed. There are two identical test cells, the left one is designated as XRA, where the Solaria BIPV windows were installed; the right one is designated as XRB where the reference windows were installed for comparison.

To comprehensively evaluate the energy performance of the BIPV window, the following sensors were adopted for measuring various energy-related parameters in the XR test bed:

- Built-in water flow meters measure heating and chilled water flows
- Built-in temperature sensors measure supply and return water temperature in heating and chilled water loops
- Built-in velocity sensor measures air flow in supply and return ductworks
- Built-in temperature sensors measure supply and return air flow temperatures
- Portable window energy meter (PWEM) measures the solar heat gain coefficient (SHGC) and U-value
- Pyranometers measure the vertical façade incident solar irradiation
- Weather station measures horizontal global solar radiation, diffuse radiation, cloud coverage, dry bulb temperature, relative humidity, wind speed and wind direction

- Power meters measure electrical power produced by the Solaria BIPV windows and lighting energy use

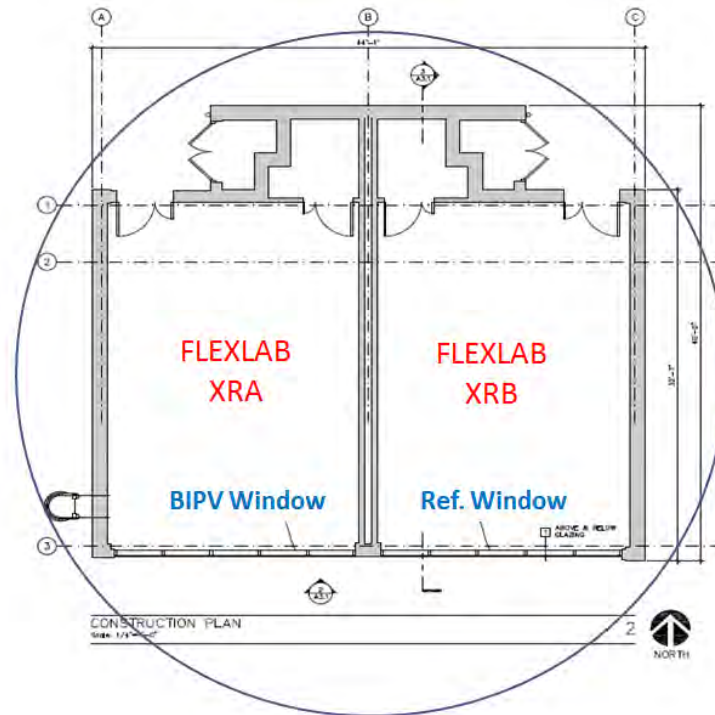


**Figure 7** Layout of the rotatable XR test bed

### 3.2 Solaria BIPV Integral Glass Unit

Solaria semi-transparent PV modules are produced based on standard mono-crystalline silicon solar cells. Figure 8 illustrates the technical procedures for manufacturing this kind of BIPV modules. First, the standard crystalline silicon solar cells are produced and then cut into strips with customizable width, spacing and length according to different applications and daylighting requirements. Second, the small strips are interconnected strings automatically and then the strings are connected in series or parallel according to the required voltage and current. Third, the connected strings are laminated between glass panes. Finally, the laminates are installed directly on buildings or integrated into insulated glass units (IGUs), as shown in Figure 9. The transmittance and energy conversion efficiency of this kind of PV module can be customized by changing the spacing of adjacent strips. Its thermal insulation performance can be improved by integrating different kinds of glazing units on the back side, such as low-e insulating glazing, vacuum glazing and so on.

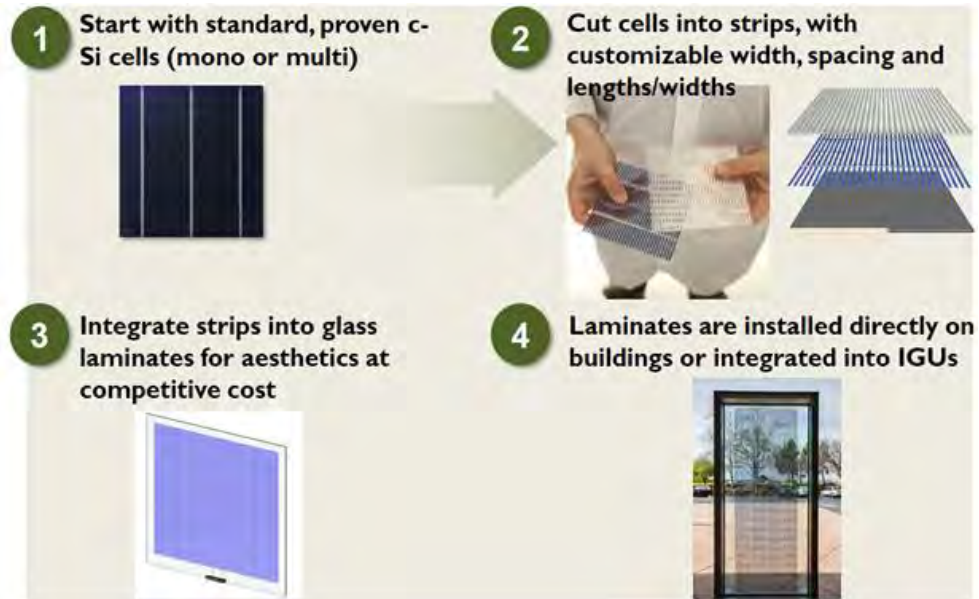


**Figure 8** Technical procedures of manufacturing the Solaria semi-transparent BIPV window



**Figure 9** Solaria semi-transparent BIPV IGU

**Figure 10** presents the structure diagram of the Solaria semi-transparent PV laminate. It is seen that the PV laminate consists of two glass lites, two layers of PVB and the PV strings. For BIPV applications, the external and internal glass lites are usually tempered glass. The function of the PVB layers is to protect the solar strings from the erosion of external environment, especially humidity, which could accelerate aging and deterioration of PV modules.

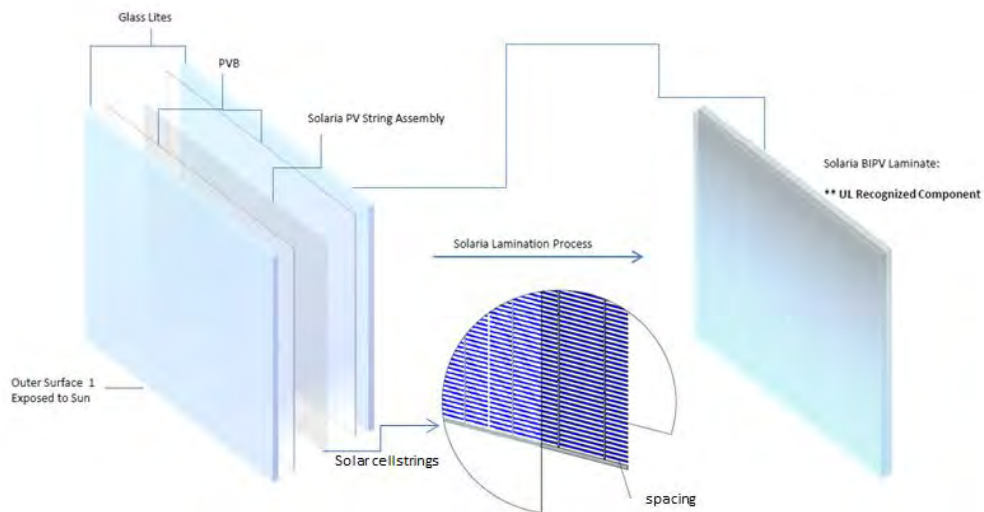


**Figure 10** Construction diagram of Solaria BIPV laminate

As both the current and voltage of a single strip solar cell are very low, it is necessary to connect the strips in series or parallel to get the required current and voltage. **Figure 11** illustrates the PV strings arrangement and connection layout of the BIPV laminate used in FLEXLAB testing. It is seen that there are totally 8 strings, and the left side four strings and the right side four strings are firstly connected in parallel to increase the current output and then connected each other in series to increase voltage output. The electrical specifications of the semi-transparent BIPV laminate under standard test conditions (STC, viz. solar irradiation  $1000\text{W}/\text{m}^2$ , air mass 1.5 and module temperature  $25^\circ\text{C}$ ) are listed in **Table 2**. As mono-Si solar cells were used, the fill factor was relatively high, reaching to 0.76, which means that the quality of solar cells was pretty good. The PV area efficiency under STC was 7% (only one third of the laminate was covered by solar cells), which is much higher than that of thin film based PV laminates with the same transmittance.

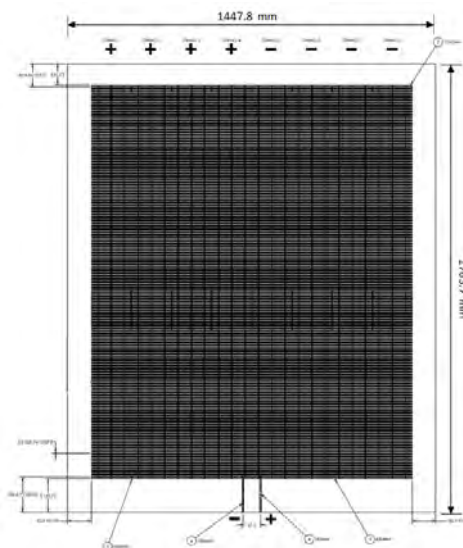


**Figure 11** PV string arrangement and connection layout

Notice all the empty space around the cells. These windows were designed to fit in the existing opening. When window design takes BIPV into consideration, energy production per unit area will be somewhat higher. Also, notice the large empty space at the bottom. The energy reduction due to horizontal shading discussed earlier can be completely eliminated by shifting PV cells down. Solaria was not aware of the plan for shading experiment at the time of submission of IGUs.

**Table 2** Electrical specifications of the BIPV laminate under standard test conditions

Electrical specifications under (STC)	
Maximum power output, ( $P_{\max}$ )	137 W
Open circuit voltage, ( $V_{oc}$ )	23.9 V
Short circuit current, ( $I_{sc}$ )	7.6 A
Voltage at the maximum power point, ( $V_{mp}$ )	19.6 V
Current at the maximum power point, ( $I_{mp}$ )	7.0 A
Fill factor	0.76
PV area efficiency, ( $\eta$ )	7%

### 3.3 Integrated Glass Units and Installation

It is well known that BIPV laminates absorb the vast majority of incident solar irradiation but only convert a small part of solar energy into DC power (usually less than 18% for commercialized crystalline silicon PV modules), and the remaining large part of energy is converted into waste heat, which not only decreases the energy conversion efficiency, but also increase the heat gain of buildings. In addition, the high infrared emittance of PV modules also results in a high U-value, which leads to severe heat loss in winter. Therefore, in order to improve the thermal insulation performance of single pane PV modules, a low-e insulating glazing was adhered to the back side of the Solaria BIPV laminates to form an BIPV insulated integrated glass unit (IGU). **Figure 12** presents the structure diagram of the BIPV IGU, which was 11.25 mm BIPV outboard laminate on 5mm clear inboard glass lite with 12mm air gap. The BIPV laminate, from outside to inside, was constituted by 5mm Starphire lite/ 0.5 mm PVB interlayer/ 0.25 mm solar strings/ 0.5 mm PVB interlayer/ 5mm Starphire lite. The Solarban 70XL low-e coating was deposited on the third surface to improve its thermal performance. The cross-section diagram of the BIPV IGU is shown in **Figure 13**, which clearly illustrate its configuration and dimension. The total thickness of the BIPV IGU is 28.25 mm.

In order to evaluate the energy saving potential of the BIPV IGU, a reference IGU, which not only represents the most common advanced technology available today, but also has a similar structure with the BIPV IGU, was adopted for comparative study in this test. The configuration diagram of the reference IGU is illustrated in **Figure 14**. It is seen that the reference IGU stack is constituted by a 6mm Starphire with Solarban 70XL outboard lite on a 6mm clear inboard lite with 12mm air gap. The total thickness is 24mm, thinner than the BIPV IGU by 4.25mm.

BIPV Glazing (XRA) - Total Thickness: 28.25		Outdoor
LITE	PPG Starphire Thickness = 5mm	#1 ----- #2 -----
Solar	Interlayer 0.5mm Solaria PV Cells 0.25mm Interlayer 0.5mm	
LITE	PPG Starphire Thickness = 5mm	#3 PPG Solarban 70XL #4 -----
GAP	100% air - 12mm	
LITE	Clear Thickness = 5mm	#5 ----- #6 -----
		Indoor

Figure 12 Configuration of the Solaria BIPV IGU

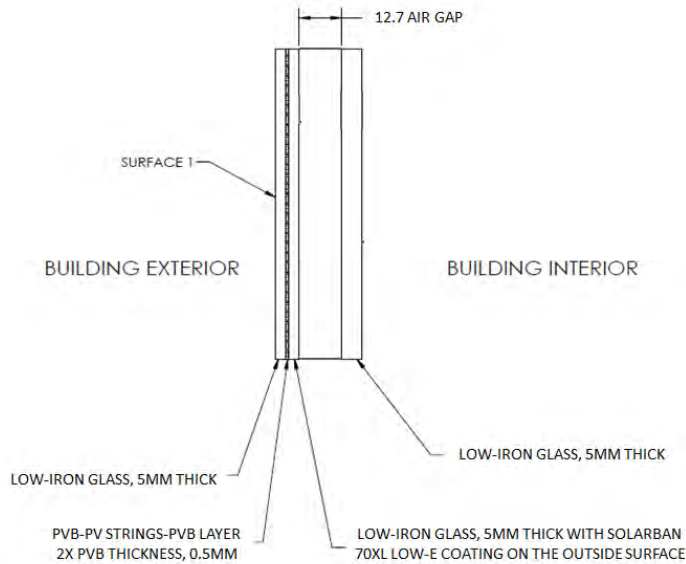


Figure 13 Cross section diagram of the BIPV IGU

Reference Glazing (XRB) Total Thickness: 24mm		Outdoor
LITE	PPG Starphire Thickness = 6mm	#1 ----- #2 PPG Solarban 70XL
GAP	100% air - 12mm	
LITE	Clear Thickness = 6mm	#3 ----- #4 -----
		Indoor

Figure 14 Configuration of the low-e reference IGU

The thermal and optical properties of the reference IGU was simulated by WINDOW v7.3 under the environmental conditions of NFRC 100-2010. Table 3 lists the calculated values of optical and thermal parameters. The solar heat gain coefficient, and light transmittance are 0.275 and 0.64, respectively. The U-factor is 1.62 W/(m<sup>2</sup>·K) (0.29 Btu/(hr·ft<sup>2</sup>·F). Therefore, it is seen that the thermal insulation performance and optical characteristics of the reference IGU are pretty good, and representative of the typical state-of-the-art technology in building window industry.

**Table 3** Simulated optical characteristics and thermal performance

ID	Name	# Layers	Layer 1	Gap 1	Layer 2	Tilt	Thickness	Tsol	Rsol	U	SHGC	Tvis
						Deg	mm	-	-	W/m <sup>2</sup> K	-	-
101	XRA - BIPV	2	Solaria Lami	Air 12 mm	Clear 5 mm	90	26.361	0.236	0.333	2.675	0.314	0.628
102	XRB - Reference Glazing	2	PPG SB70XL 6 mm	Air 12 mm	Clear 6 mm	90	23.328	0.246	0.524	1.623	0.275	0.640

Note that modeled SHGC for BIPV glazing did not include energy converted to electricity, which would lower absorbed heat, thus reducing SHGC by couple of points (i.e., 0.29 vs. 0.31).

As a practical matter the BIPV IGU’s framing system should be designed to facilitate electrical junction box placement and wiring. In addition, the mullion cap should not cast any shadow on the PV laminates.

To accommodate these requirements and ensure comparability between the two framing systems, both the BIPV IGU and the reference IGU were assembled with the identical Inviso framing system for this testing. It was a four-side window frame, however, the glass was captured only at the sill and header. Figure 15 illustrates the frame structure.

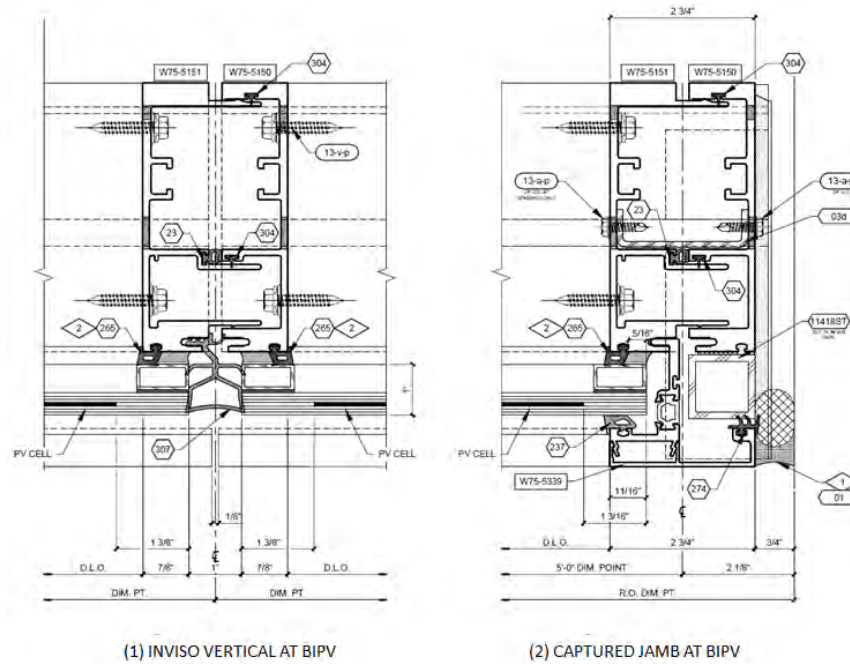


**Figure 15** Structure diagram of the BIPV friendly frame

The IGUs were glazed on top of the unit frame using a structural adhesive and when the units were installed the vertical mullions interlocked behind the glass. As a result, there was no mullion cap on the exterior vertical gaps but rather simply a gasket which filled the 1" gap between the adjacent IGU's. The glass was captured at the jambs but not between the individual units. This design is ideal for BIPV IGU because it eliminates any vertical mullions which may cast shadow on the active area of PV laminates and results in severe degradation of energy output. It also increases the available area for active PV. The electrical junction box for each laminate, which was mounted on front side bottom of the laminate, was embedded in the sill of frame. Wires run through the BIPV friendly frame and came out through the strain relief connectors on the back of the frame into the XRA test cell where inverters and communicate gateway were mounted.

In order to fill the window opening size of XR test cells, four pieces of BIPV IGU were installed in XRA test cell. **Figure 16** illustrates the layout and dimensions of the BIPV IGU.

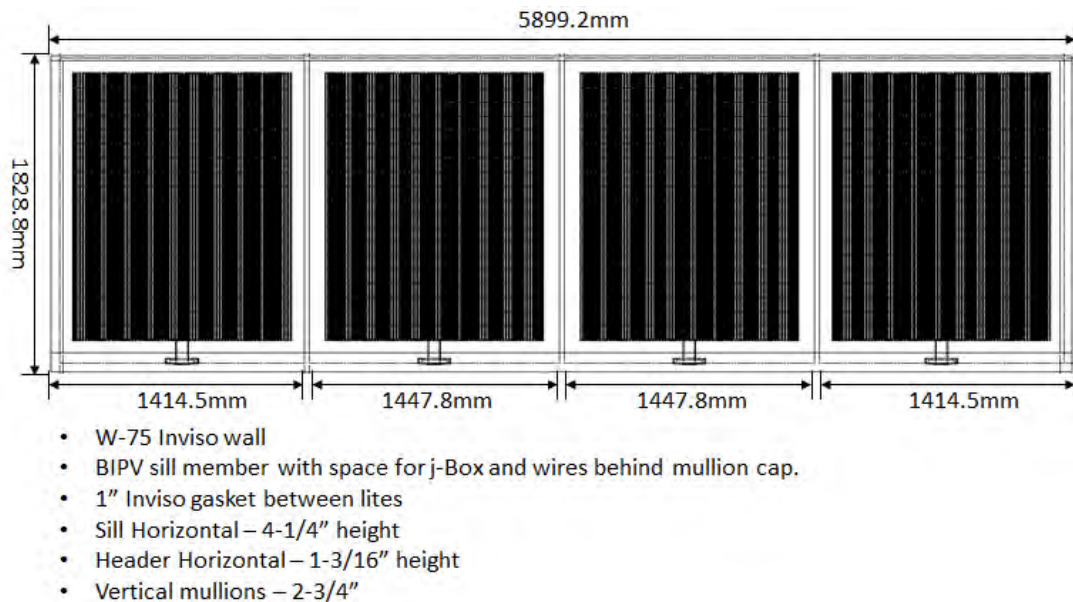


**Figure 16** Layout and dimensions of the BIPV IGU

Even though the laminates' width at both sides was little bit smaller than the middle two, the active area of solar cells in each BIPV laminate was the same. Thus, the power output of each laminate was almost identical. The total width and height of the BIPV IGU were 5899.2mm and 1828.8mm, respectively. The total glazing area and active PV area were 9m<sup>2</sup> and 3m<sup>2</sup>, respectively. The reference IGU as the same layout and dimensions as the BIPV IGU was installed on XRB cell for comparative testing. The photograph of these two IGUs is shown in **Figure 17**. The left one is XRA test cell equipped with Solaria BIPV IGU, the right one is XRB cell equipped with low-e reference IGU. It is seen that there is almost no difference in terms of outside appearance between BIPV IGU and reference IGU.



**Figure 17** Picture of the BIPV IGU and the reference IGU installed on the XR rotatable test bed

**Figures 18 and 19** show the views from inside to outside of the BIPV IGU and the reference IGU, respectively. As the existing of small solar cell strips in the laminate, the uniformity and visual effect of the BIPV IGU were obviously worse than that of the reference IGU, which was constituted by low-iron clear glasses with low-e coating. However, as shown in **Figure 19**, no matter the visual comfort or the daylighting performance of the BIPV IGU was largely acceptable especially when the merits of energy generation and energy saving are taken in account. The comparison of thermal, power and daylighting performance between the BIPV IGU and reference IGU will be elaborated in next section.



**Figure 18** Inside to outside view of the BIPV IGU

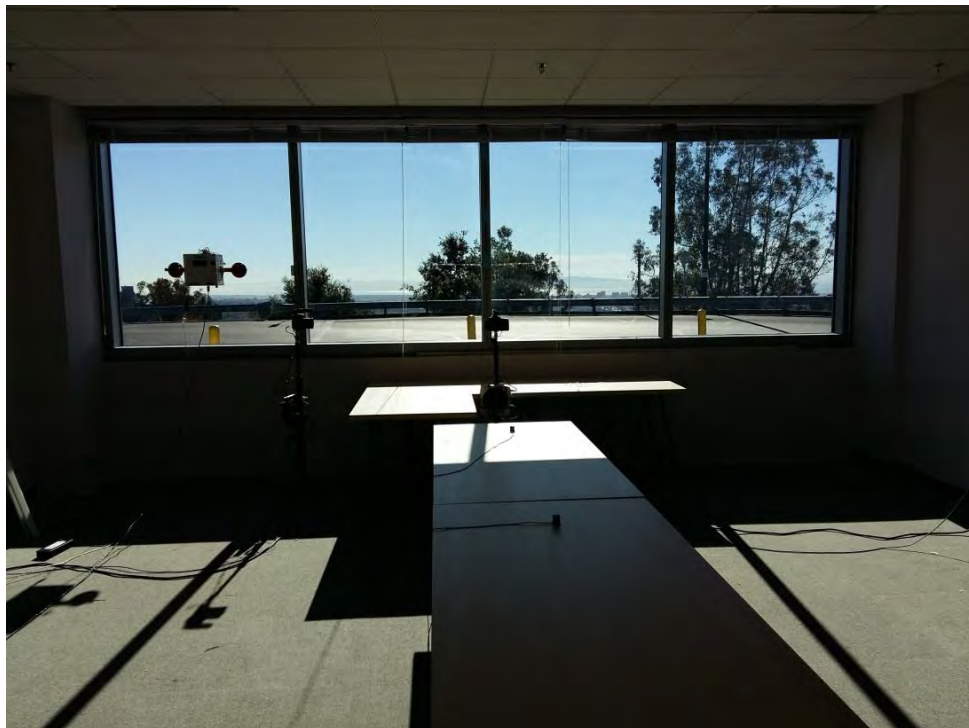


**Figure 19** Inside to outside view of the reference IGU

### 3.4 BIPV System

Wires from electrical junction box of each BIPV laminate run through the BIPV friendly frame and came out through the strain relief connectors on the back of the frame into the XRA cell where inverter and communicate gateway were mounted. In this test, a microinverter was used to convert DC electricity from PV modules into AC electricity. Compared with traditional string inverters, microinverters can track each PV module's maximum power point alone, thus, it is more productive. Moreover, microinverters are independent of the impacts of partial shading, module mismatching and different installation orientations, hence it is very suitable for building-integrated PV systems.

The electrical diagram of the BIPV power generation system is shown in [Figure 20](#). It is seen that both the left side two PV laminates (BIPV Array 1) and the right side two PV laminates (BIPV Array 2) were first connected in series and then connected to the APS YC500A grid-tied microinverter in parallel. As this microinverter has dual maximum power point tracking (MPPT), it can handle two PV modules/arrays under different operating conditions simultaneously. The dual MPPT brings a big advantage of halving the inverters and halving the installation, which means real cost savings for residential and commercial solar PV systems. The key parameters of the microinverter are listed in [Table 4](#). According to the electrical specifications of the BIPV laminate, as shown in [Table 2](#), two PV laminates connecting in series just reach the MPPT voltage range of the microinverter. [Figure 21](#) presents the real picture of the BIPV power generation system. DC power from BIPV laminates was converted into 240V and 60Hz AC electricity in the microinverter and then transferred to the AC distribution panel, in which AC electricity was prior supplied to local AC loads and the surplus electricity if any would be uploaded to the utility grid. This system also incorporated an APsystems energy communication unit (ECU) functioned as the information gateway for the microinverters. This unit collected module performance data from the microinverter via a power line cable (PLC) and then transferred this information to an Internet database in real time via a router. Through the APsystems monitor software, the ECU provides precise analysis of the performance of the microinverter and each BIPV array. In addition, the user can check and download power generation information of the microinverter at any time by remote login to the specified server. In addition to using the ECU to record the power generation data of the BIPV IGU, a local power measuring system was also set up to test and record the real time power output data.

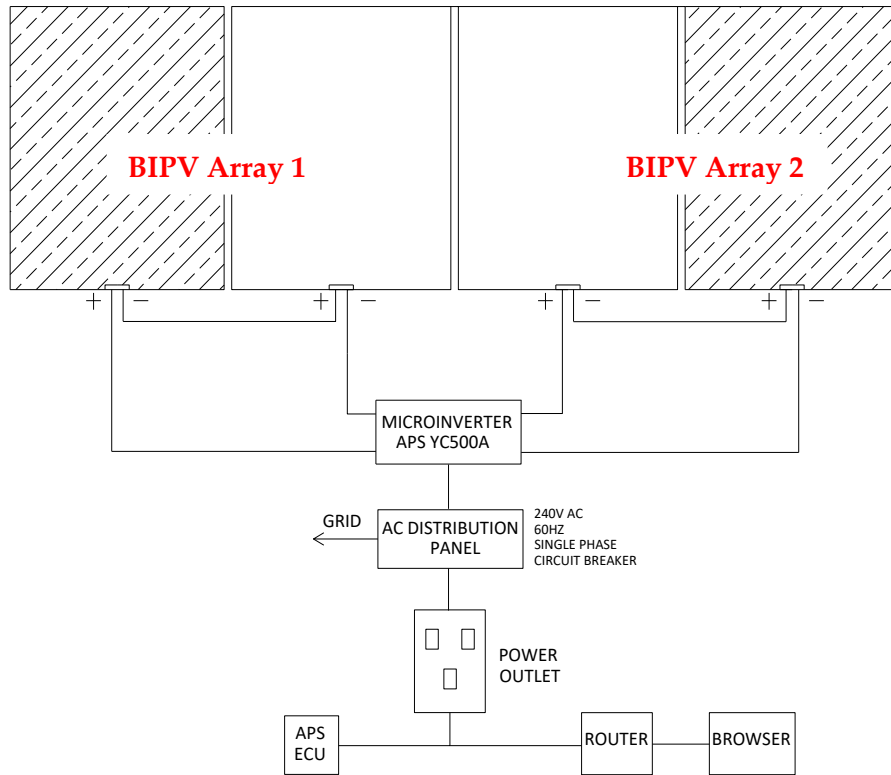


**Figure 20** Electrical diagram of the BIPV power generation system

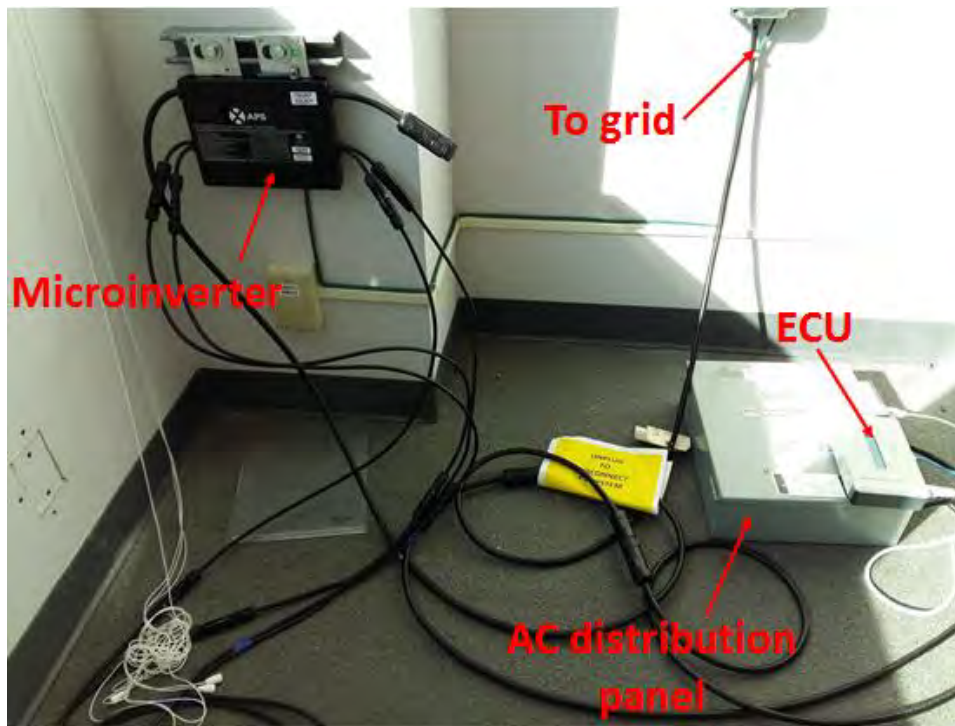


**Figure 21** Photo of the BIPV power generation system

**Table 4** Key parameters of the APS microinverter

APsystems YC500A microinverter datasheet	
<b>Input data (DC)</b>	
Recommended PV module power range (STC)	180-310W
MPPT voltage range	22-45V
Maximum input voltage	55V
Maximum input current	12A x 2
<b>Output data (AC)</b>	
Rated output power	500W
Maximum output current	2.08A @ 240V 2.4A @ 208V
Nominal output voltage/range-240V	240V/211V-264V
Nominal output voltage/range-208V	208V/183V-229V
Nominal output frequency/range	60Hz/59.3-60.5Hz
<b>Efficiency</b>	
Peak efficiency	95.5%
CEC weighted efficiency	95%
Nominal MPP tracking efficiency	99.5%

## 4. PROJECT RESULTS AND FINDINGS

### 4.1 Testing Schedule and Measured Parameters

In order to fully evaluate the energy saving potential of the Solaria BIPV IGU, a comparative test between the BIPV IGU and the reference IGU was conducted on the XR test bed of FLEXLAB at Lawrence Berkeley National Laboratory from Sep. 30 to Dec. 7, 2015. The schedule of the BIPV IGU energy performance test is listed in [Table 5](#). The comparative test was conducted under different orientations (southeast, south, southwest and west), different set point temperatures as well as different interior venetian blind shade positions in order to fully understand the energy generation and energy saving potential of the BIPV IGU under a full set of different conditions.

**Table 5** Schedule of the BIPV IGU energy performance test

Month	Date	Orientation of XR test bed	Indoor set point temperature	Light	Test configuration		
					XRA (BIPV)	XRB (Ref.)	Weather
					Blinds	Blinds	
SEP	30	South	21 °C	off	Down	Down	Overcast
OCT	1	South	21 °C	off	Down	Down	Dynamic+Clear
OCT	2	South	21 °C	off	Down	Down	Clear
OCT	3	South	21 °C	off	Down	Down	Clear
OCT	4	South	21 °C	off	Down	Down	Clear
OCT	5	South	21 °C	off	Down	Down	Clear
OCT	6	South	21 °C	off	Down	Down	Clear
OCT	7	South	21 °C	off	Down	Down	Clear
OCT	8	South	15 °C	off/on	Down	Down	Dynamic
OCT	9	South	15 °C	on	Down	Down	Clear
OCT	10	South	15 °C	on	Down	Down	Clear
OCT	11	South	15 °C	on	Down	Down	Clear
OCT	12	South	15 °C	on	Down	Down	Clear
OCT	13	South	15 °C	on	Down	Down	Clear
OCT	14	South	16 °C	on	Down	Down	Clear
OCT	15	South	16 °C	on	UP	Down	Dynamic
OCT	16	South	16 °C	on	UP	Down	Clear
OCT	17	South	16 °C	on	UP	Down	Overcast
OCT	18	South	16 °C	on	UP	Down	Dynamic
OCT	19	South	16 °C	on	UP	Down	Dynamic+Clear
OCT	20	South	17 °C	on	UP	UP	Clear
OCT	21	South	17 °C	on	UP	UP	Clear
OCT	22	South	17 °C	on	UP	UP	Clear
OCT	23	South	17 °C	on	UP	UP	Dynamic
OCT	24	South	18 °C	on	UP	UP	Dynamic
OCT	25	South	18 °C	on	UP	UP	Clear
OCT	26	South	18 °C	on	UP	UP	Clear
OCT	27	South	18 °C	on	UP	UP	Cloudy
OCT	28	Southeast	18 °C	on	UP	UP	Dynamic
OCT	29	Southeast	18 °C	on	UP	UP	Clear
OCT	30	Southeast	18 °C	on	UP	UP	Clear
OCT	31	Southeast	18 °C	on	Down	Down	Clear
NOV	1	Southeast	18 °C	on	Down	Down	Dynamic
NOV	2	Southeast	18 °C	on	Down	Down	Dynamic
NOV	3	Southeast	18 °C	on	Down	Down	Clear

Month	Date	Orientation of XR test bed	Indoor set point temperature	Light	Test configuration		
					XRA (BIPV)	XRB (Ref.)	Weather
					Blinds	Blinds	
NOV	4	Southeast	18 °C	on	Down	Down	Clear
NOV	5	Southeast	18 °C	on	Down	Down	Dynamic
NOV	6	Southeast	18 °C	on	Down	Down	Clear
NOV	7	Southeast	18 °C	on	UP	Down	Clear
NOV	8	Southeast	18 °C	on	UP	Down	Dynamic
NOV	9	Southeast	18 °C	on	UP	Down	Dynamic
NOV	10	Southeast	18 °C	on	UP	Down	Dynamic
NOV	11	Southeast	18 °C	on	UP	Down	Clear
NOV	12	Southeast	18 °C	on	UP	Down	Clear
NOV	13	Southeast	18 °C	on	UP	Down	Clear
NOV	14	Southeast	18 °C	on	UP	Down	Clear
NOV	15	Southeast	18 °C	on	UP	Down	Dynamic
NOV	16	Southeast	18 °C	on	UP	Down	Clear
NOV	17	Southeast	18 °C	on	UP	Down	Clear
NOV	18	South	18 °C	on	disturbed	disturbed	
NOV	19	South	18 °C	on	UP	UP	
NOV	20	South	18 °C	on	UP	UP	
NOV	21	South	18 °C	on	UP	UP	Vertical shade test
NOV	22	South	18 °C	on	UP	UP	Vertical shade test
NOV	23	South	18 °C	on	UP	UP	Vertical shade test
NOV	24	South	18 °C	on	UP	UP	Vertical shade test
NOV	25	Southwest	fluctuation	on	UP	UP	Horiz. shade test
NOV	26	Southwest	fluctuation	on	UP	UP	Horiz. shade test
NOV	27	Southwest	fluctuation	on	UP	UP	Horiz. shade test
NOV	28	Southwest	fluctuation	on	UP	UP	Horiz. shade test
NOV	29	Southwest	fluctuation	on	UP	UP	Horiz. shade test
NOV	30	Southwest	fluctuation	on	UP	UP	
DEC	01	Southwest	16 °C	on	UP	UP	
DEC	02	West	17 °C	on	UP	UP	
DEC	03	West	increasing	on	UP	UP	
DEC	04	West	25 °C	on	UP	UP	Space heating
DEC	05	West	25 °C	on	UP	UP	Space heating
DEC	06	West	25 °C	on	UP	UP	Space heating
DEC	07	West	25 °C	on	UP	UP	Space heating
DEC	08	West	25 °C	on	UP	UP	Space heating
DEC	09	West	25 °C	on	UP	UP	Space heating

During the outdoor comparative test, the following parameters and data were measured and recorded:

**i) Weather data**

- Ambient temperature & humidity
- Wind speed and wind direction
- Horizontal global solar irradiation
- Horizontal diffuse solar irradiation
- Incident solar irradiation

**ii) HVAC & Thermal performance**

- Various surface temperatures of the BIPV IGU and reference IGU
- Water flow rates of heating and chilled water flows
- Supply and return water temperatures of heating and chilled water flows
- Supply, return and mixed air flow temperatures
- Velocity of air flow in supply and return ductwork
- Heat flux through the BIPV IGU
- SHGCs of BIPV IGU and reference IGU

**iii) Daylighting & glare**

- Daylighting illuminance
- HDR imaging
- Lighting energy use

**iv) Power generation**

- Energy output of each BIPV array

With the measured data, the overall energy performance including thermal, power and daylighting performance of the BIPV IGU was completely analyzed and evaluated

## **4.2 Power Generation Performance**

Compared to other advanced window technologies, the most outstanding merit of the BIPV IGU is the power generation ability in situ of buildings through photovoltaic effect. During this test, the DC power generated by the BIPV IGU was first converted into AC power via a microinverter and then transferred to the AC distribution panel. To analyze the power generation performance, the incident solar irradiation and real time power output of the BIPV IGU were measured and recorded.

Tables 6 and 7 present daily incident solar radiation, electricity output, solar cell efficiency, and the whole BIPV IGU efficiency in late September and early-mid October, respectively. The

second column of the table is the available solar resource (radiant energy) falling on the vertical window façade (measured with a pyranometer). The third column is the electrical energy produced by the BIPV and inverter onto the utility grid. The fourth column multiplies the solar resource in the second column by the active BIPV cell area as a reference for the efficiency calculation. The fifth column uses the area basis of the whole glass rather than just the active PV cell area. The sixth and seventh columns calculate conversion “efficiencies” based on either the cell area or glass area basis.

**Table 6** Daily incident solar radiation and BIPV energy generation in late September

Dates	Daily Vertical Radiant Energy (kWh/m <sup>2</sup> -day)	Daily BIPV Electrical Energy Production (kWh/day)	Daily Vertical Radiant Energy on PV Cell Area (kWh/day)	Daily Vertical Radiant Energy on Glass Area (kWh/day)	Incident Radiation to Electrical Production BIPV Cell Efficiency	% Energy Incident on Glass Area Converted to Electricity
9/20/2015	4.24*	1.95	12.93	38.13	15.10%	5.10%
9/21/2015	4.23*	1.95	12.88	37.99	15.10%	5.10%
9/22/2015	2.61	1.23	7.96	23.47	15.40%	5.20%
9/23/2015	4.34*	2.09	13.21	38.97	15.80%	5.40%
9/24/2015	4.15*	1.94	12.66	37.33	15.30%	5.20%
9/25/2015	4.42*	2.12	13.47	39.71	15.70%	5.30%
9/26/2015	4.30*	2.05	13.1	38.65	15.60%	5.30%
9/27/2015	3.42	1.72	10.42	30.73	16.50%	5.60%
9/28/2015	3.58*	1.72	10.91	32.18	15.80%	5.30%
9/29/2015	3.24	1.56	9.88	29.15	15.80%	5.40%
9/30/2015	0.51	0.25	1.57	4.63	15.70%	5.30%
Selected average (*)	4.18	1.97	12.74	37.57	15.50%	5.30%
<b>NREL PVWatts model avg. results for Sept.</b>	<b>4.2</b>	<b>1.95</b>	<b>12.8</b>	<b>37.75</b>	<b>15.30%</b>	<b>5.20%</b>

**Table 7** Daily incident solar radiation and BIPV energy generation in early-mid October

Dates	Daily Vertical Radiant Energy (kWh/m <sup>2</sup> -day)	Daily BIPV Electrical Energy Production (kWh/day)	Daily Vertical Radiant Energy on PV Cell Area (kWh/day)	Daily Vertical Radiant Energy on Glass Area (kWh/day)	Incident Radiation to Electrical Production BIPV Cell Efficiency	Percent of Energy Incident on Glass Area Converted to Electricity
10/1/2015	3.61	1.76	11	32.44	16.00%	5.40%
10/2/2015	4.6	2.24	14.03	41.39	15.90%	5.40%
10/3/2015	4.73	2.34	14.42	42.52	16.20%	5.50%
10/4/2015	4.54	2.23	13.82	40.77	16.10%	5.50%
10/5/2015	4.57	2.25	13.93	41.09	16.20%	5.50%
10/6/2015	4.02	1.93	12.24	36.11	15.80%	5.40%
10/7/2015	4.43	2.2	13.5	39.82	16.30%	5.50%
10/8/2015	4.07	1.97	12.39	36.56	15.90%	5.40%
10/9/2015	4.9	2.37	14.94	44.06	15.90%	5.40%
10/10/2015	3.64	1.75	11.09	32.72	15.80%	5.30%
10/11/2015	4.8	2.36	14.64	43.17	16.10%	5.50%
10/12/2015	4.79	2.34	14.59	43.04	16.10%	5.40%
10/13/2015	4.57	2.27	13.93	41.09	16.30%	5.50%
10/14/2015	4.09	2.08	12.45	36.72	16.70%	5.70%
10/15/2015	2.18	1.08	6.63	19.56	16.30%	5.50%
10/16/2015	4.47	2.26	13.61	40.14	16.60%	5.60%
10/17/2015	0.59	0.26	1.8	5.3	14.60%	5.00%
10/18/2015	3.99	2.06	12.15	35.82	17.00%	5.80%
average (all)	4.03	1.99	12.29	36.24	16.20%	5.50%
<b>NREL PVWatts model avg. results for Oct.</b>	<b>3.89</b>	<b>1.86</b>	<b>11.85</b>	<b>34.96</b>	<b>15.70%</b>	<b>5.30%</b>

Figures 22 and 23 present the daily incident solar irradiation and electricity output in October and November, 2015. The largest daily incident solar irradiation was 6.38kWh/m<sup>2</sup>, occurred on Oct. 11, 2015. The daily average incident solar irradiation was 4.53kWh/m<sup>2</sup> for the south orientation, was 3.92kWh/m<sup>2</sup> for the southeast orientation. The highest daily electricity output was 2.68kWh, occurred on Nov.19, 2015 when the BIPV IGU was facing the southern orientation. Based on the incident solar irradiation and electricity output, the daily energy conversion efficiency was calculated. As shown in Figures 24 and 25, the daily energy conversion efficiency of the BIPV IGU was more or less 5% on sunny days, but it was much

lower on overcast days because it is well known that crystalline silicon solar cells have lower efficiency under low irradiation level. Usually, the energy conversion efficiency of crystalline silicon based PV modules ranges from 16% to 18% under the standard test conditions. Because the BIPV IGU studied in this test was semi-transparent--only one third of the BIPV laminate was covered with solar cells--thus the measured overall areal energy conversion efficiency of 5% was reasonable.

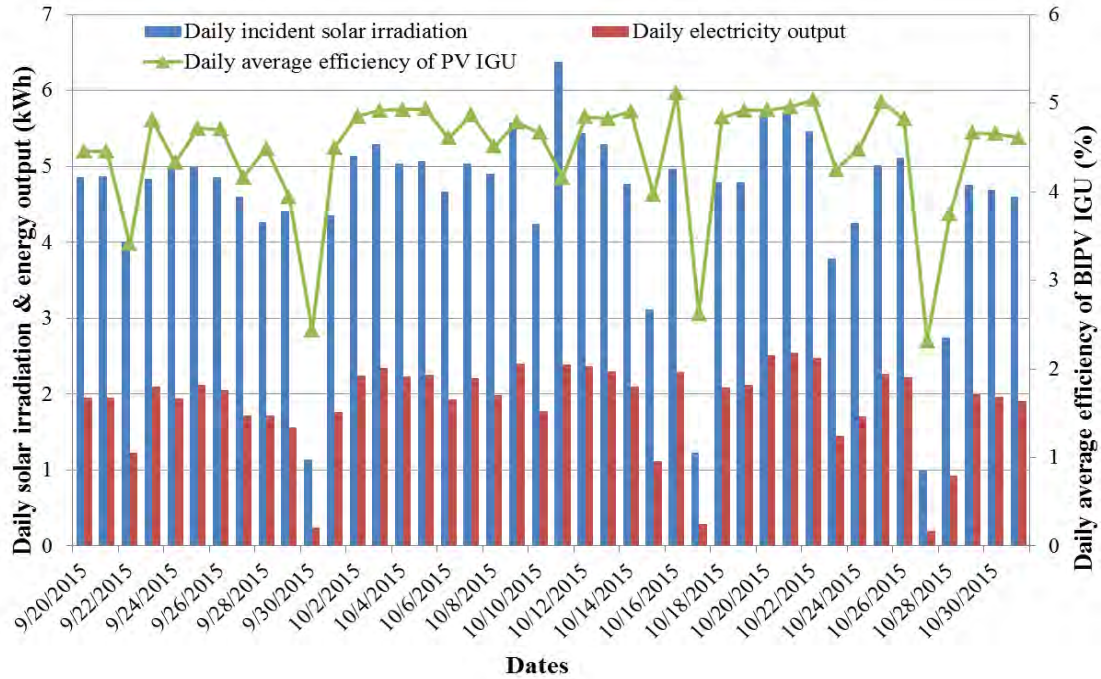


Figure 22 Daily incident solar irradiation and electricity output in October, 2015

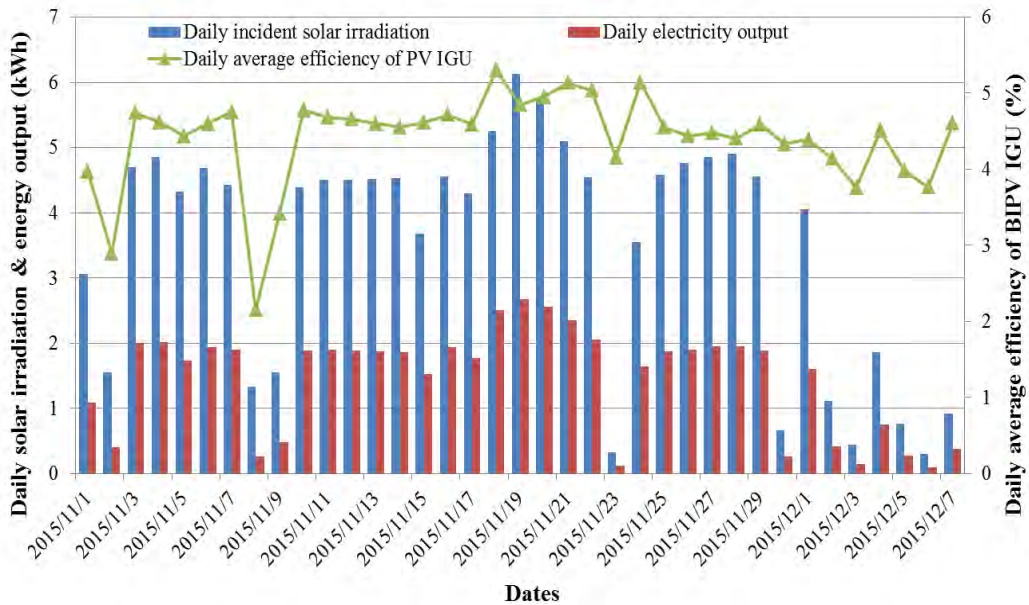
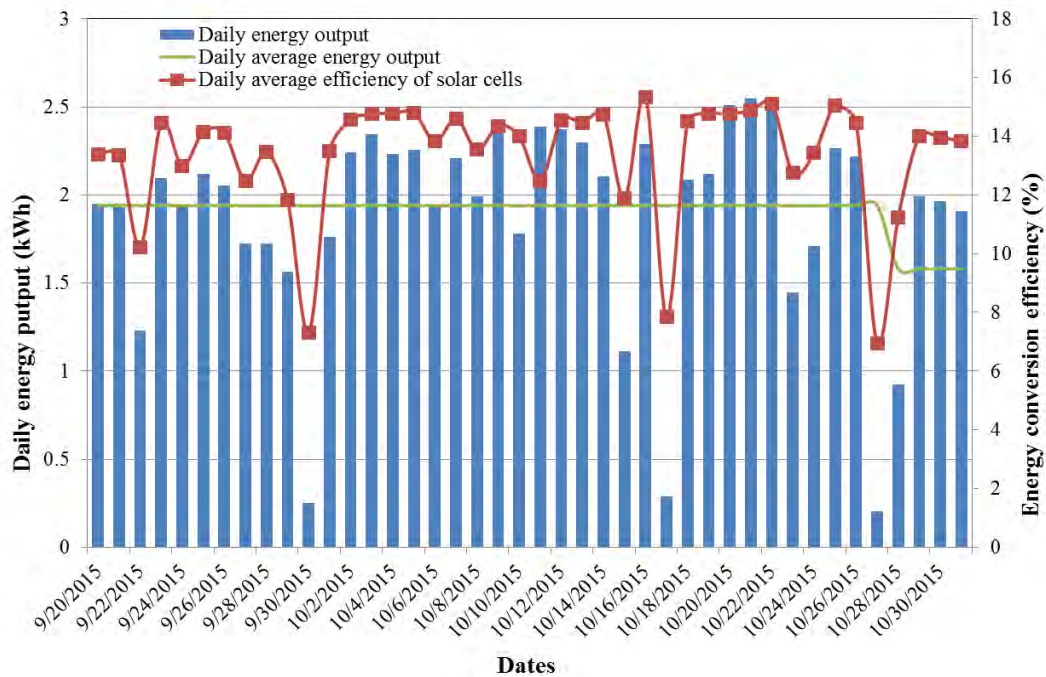
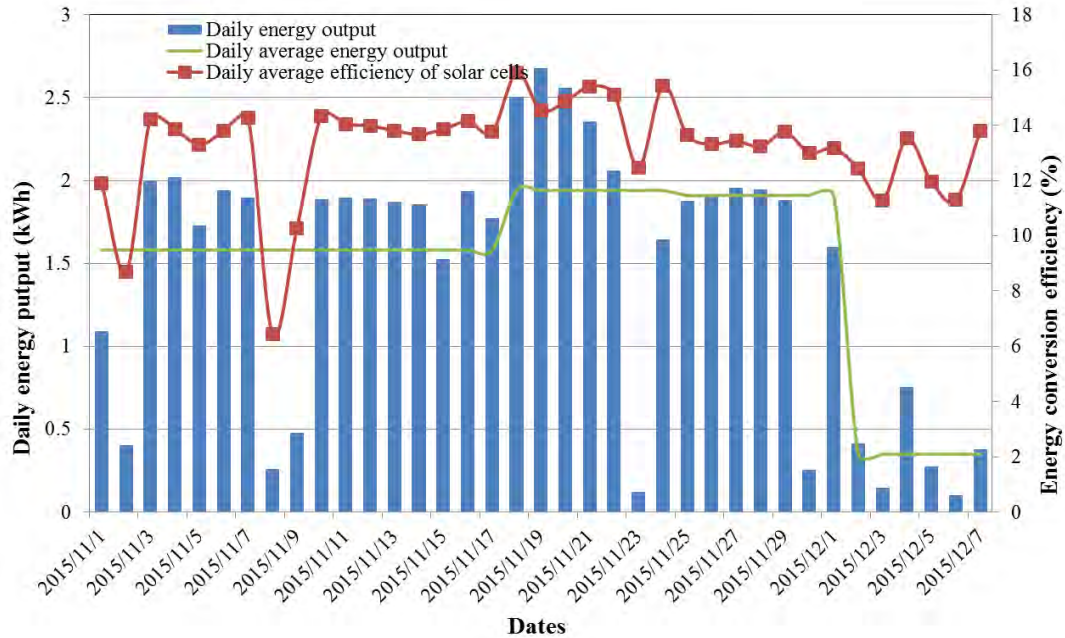


Figure 23 Daily incident solar irradiation and electricity output in November, 2015

Moreover, the daily average electricity outputs at different orientations were calculated and are presented in Figures 24 and 25. They were 1.58kWh, 1.94kWh and 1.91kWh for the southeast, south and southwest orientations, respectively. The BIPV IGU generated almost the same daily average electricity in south and southwest orientations, but 19% less electricity in southeast orientation during the test period. That is not surprising, given that the daily average incident solar irradiation on south and southwest vertical façades were obviously larger than that on southeast façade. Based on this comparison results, a conclusion can be drawn that south and southwest orientations are more suitable for installing BIPV IGU in terms of increasing power generation in Berkeley, California and this conclusion should be also correct for the rest of the United States. As shown in Figures 24 and 25, the daily average efficiency of solar cells was about 15% on sunny days, but it was less than 12% on cloudy days and overcast days.



**Figure 24** Daily energy conversion efficiency & daily average electricity outputs at different orientations from Sep to Oct. 2015



**Figure 25** Daily energy conversion efficiency & daily average electricity outputs at different orientations in Nov. 2015

Figures 26a and 26b present the incident solar irradiation on south vertical façade as well as the power output of the BIPV IGU on typical sunny days in Oct. 2015. It is seen that the maximum incident solar irradiation was about 736W/m<sup>2</sup> and the corresponding power output of the BIPV IGU was 321W on typical sunny days in Oct. 2015.

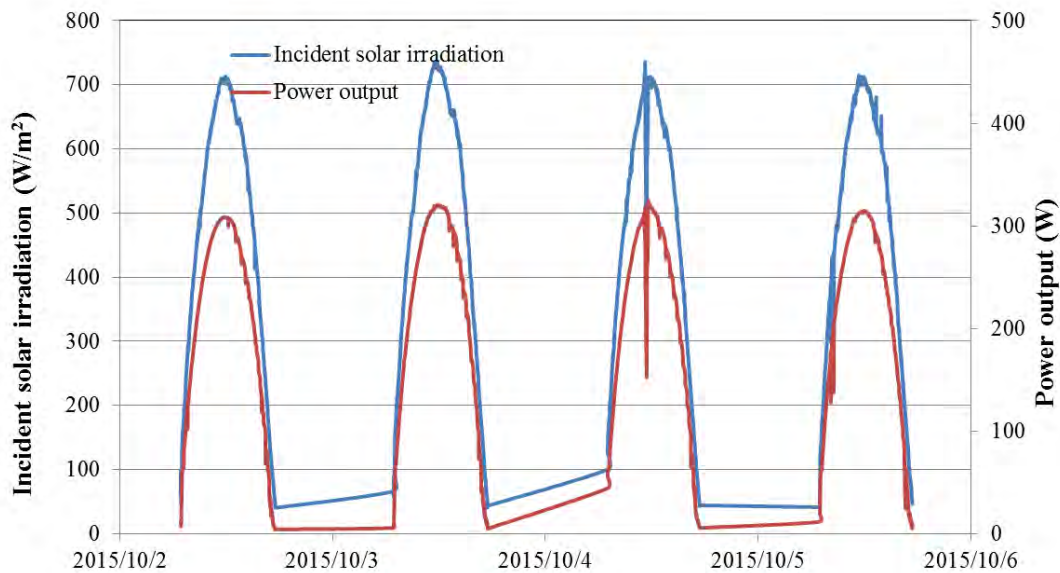


**Figure 26a** Incident solar irradiation and the corresponding power output on typical sunny days (differing axis scales)

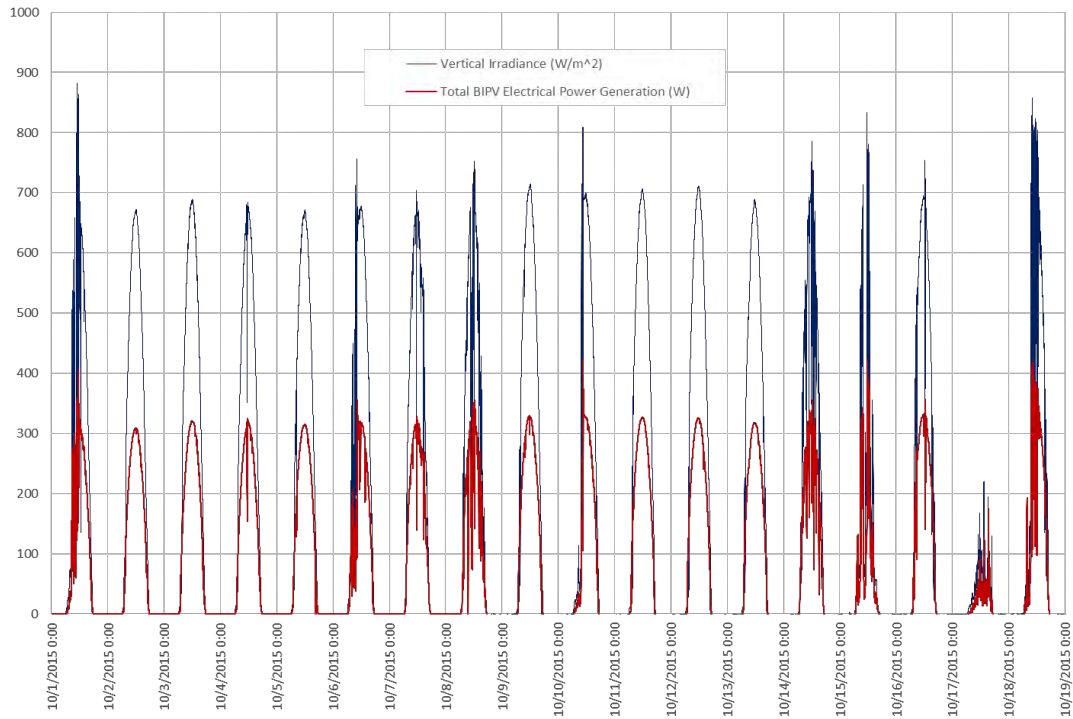


**Figure 26b** Incident solar irradiation and the corresponding power output for October 1-19 (same axis scale)

As mentioned before, the real time power output of the BIPV IGU was not only recorded by the ECU and transferred to the inverter manufacturer's remote database, but also measured by a local electricity meter. However, the ECU only recorded DC power, while the local electricity meter recorded AC power. Both AC power data and DC power data on typical sunny days are compared in [Figure 27](#). The maximum difference between DC power and AC power was 10%. In other words, the total energy loss from DC to AC was 10%, which included the microinverter energy loss, wire loss and so on.

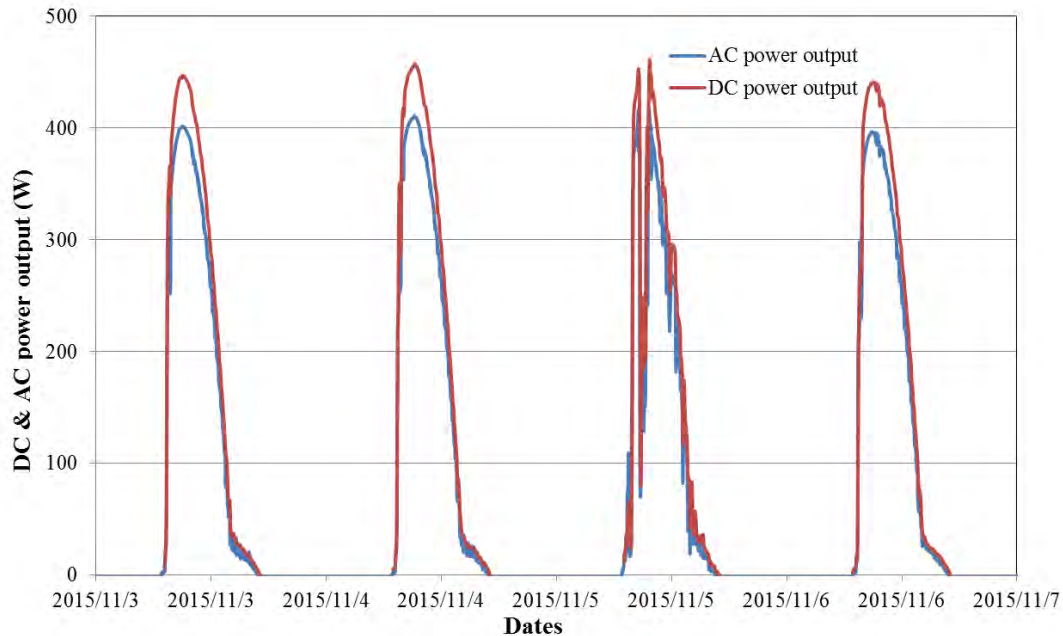


**Figure 27** Comparison of DC power output and AC power output on sunny days

The impacts of solar irradiation level, incident angle and PV module temperature on the energy conversion efficiency of BIPV laminates were also analyzed. As shown in [Figure 28](#), the energy conversion efficiency increased with the solar irradiation increasing, especially when the solar irradiation was above than  $300\text{W}/\text{m}^2$ . Two reasons may explain this phenomenon. On the one hand, low solar irradiation usually corresponds to a large incident angle on sunny days and large incident angle would result in large reflectance for the BIPV laminates and, thus, declining power output and energy conversion efficiency. [Figure 29](#) illustrates the relationship between solar incident angle and energy conversion efficiency during this test. It is obvious that the energy conversion efficiency increased with decreasing incident angle, especially when the incident angle was less than 70 degrees. Also, when the incident angle was less than 70 degrees, the impact on energy conversion efficiency was not obvious. On the other hand, the impact of low irradiation level on energy conversion efficiency can be attributed to solar spectrum distribution. It is well known that solar cells respond only to certain portions of the solar spectrum and their power output changes measurably with variations in the solar spectrum distribution. When solar irradiation is low, usually at early morning and late afternoon, the solar spectrum distribution is definitely different from that at air mass 1.5, and the proportion of the active solar spectral irradiance which could activate electrons in solar cells is also low. However, the energy conversion efficiency of PV modules is calculated based on the total solar irradiation rather than the active solar spectral irradiance, thus it would be lower at low solar irradiation level.

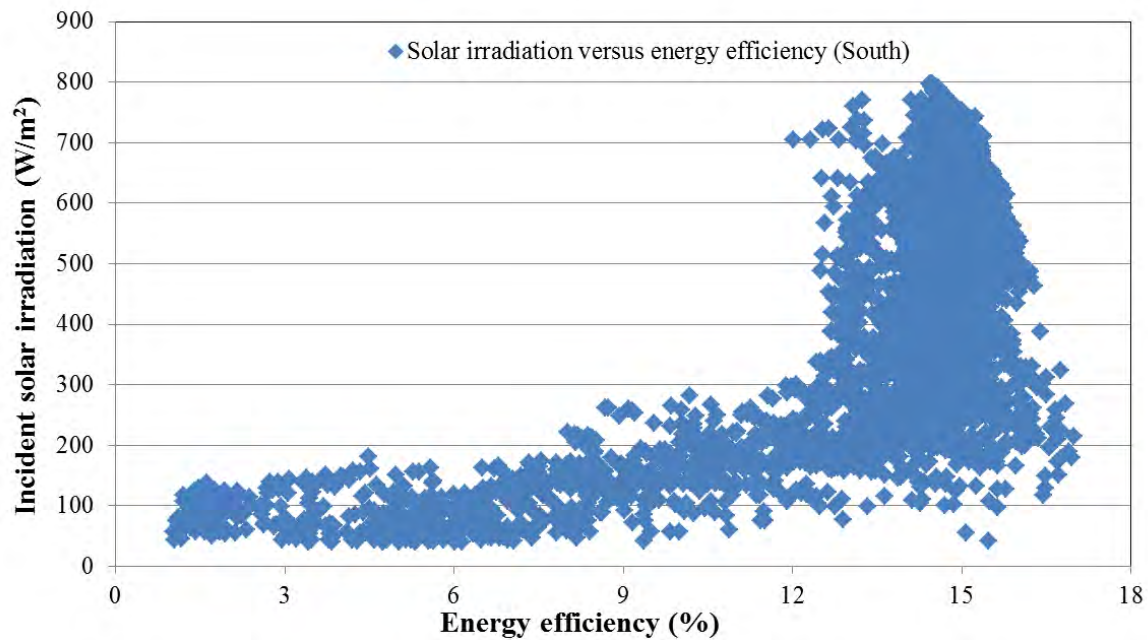


**Figure 28** Relationship between incident solar irradiation and energy conversion efficiency

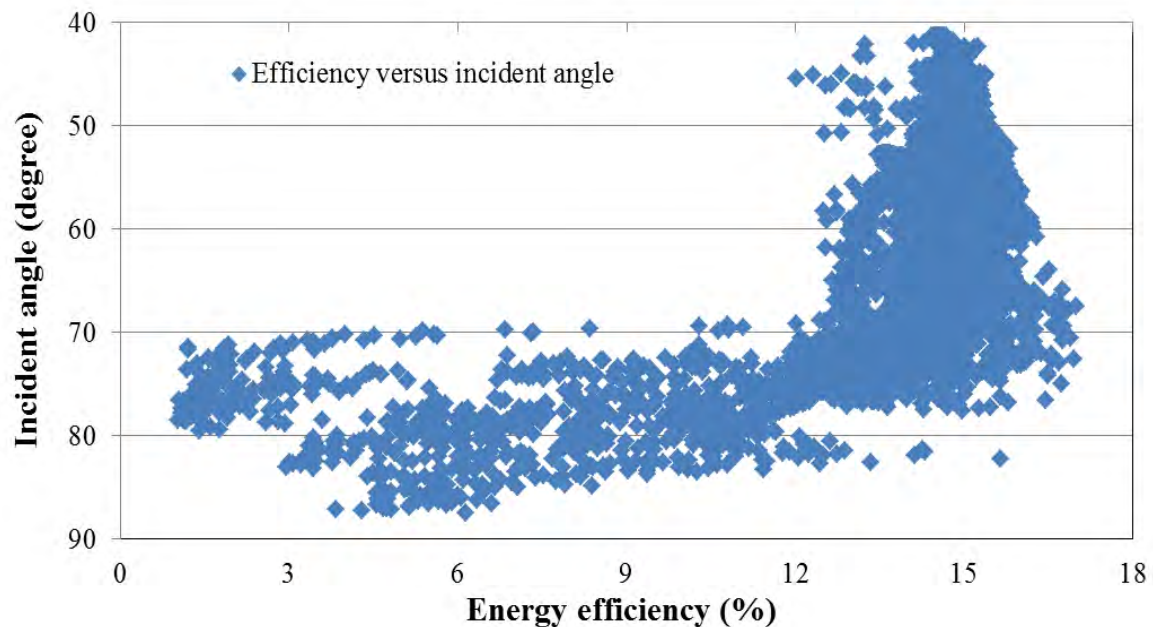


**Figure 29** Relationship between solar incident angle and energy conversion efficiency

**Figure 30** illustrates the relationship between BIPV laminate temperature and energy conversion efficiency of the BIPV IGU during this test. It is seen that the energy conversion efficiency declined with the laminate temperature increasing. Specifically, as the PV laminate temperature increased by 1 degree, the power output of the BIPV IGU declined by 0.42%. Thus, in order to improve the energy conversion efficiency, more attention should be paid to the heat dissipation issue of BIPV IGU in future design.

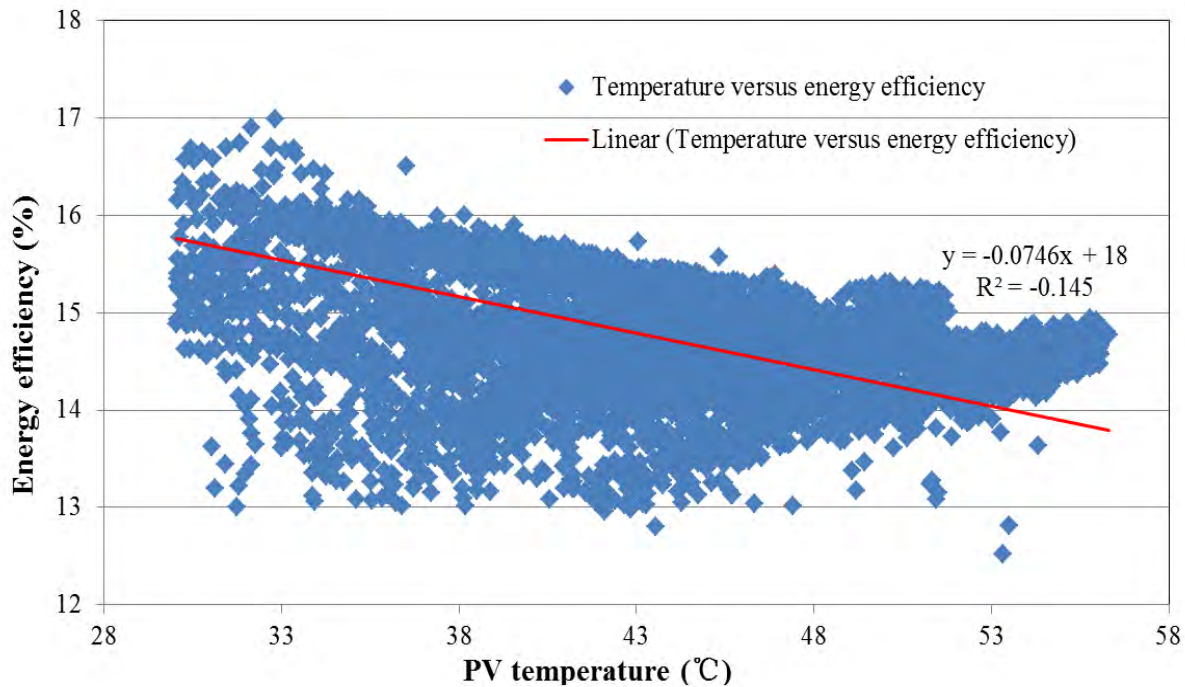


**Figure 30** Relationship between laminate temperature and energy conversion efficiency

For BIPV systems, one of the problems of most concern is the shading effect from various obstructions, such as building itself (window frame, overhang, roof, pillar), adjacent buildings, trees, telephone poles, and so on. Different obstructions cast different patterns of shadow and result in different impacts on the power output. In this test, vertical and horizontal shade tests were conducted to analyze the impacts of the two typical shade conditions on the power generation performance of the BIPV IGU. **Figure 31** shows the vertical shade case and the shadow cast on the BIPV IGU. It is seen that the left side PV string was totally shaded by the vertically installed board at afternoon. To quantitatively analyze the impact of vertical shade on power output of BIPV arrays (there were two BIPV arrays, each array consisted of two BIPV IGUs), a comparison of power outputs between the shaded and unshaded BIPV arrays are conducted and presented in **Figure 32**. It is seen that the power outputs of the both BIPV arrays were the same on each morning when no shadow was cast on the BIPV IGU. However, in the afternoon, the power output of the shaded BIPV array was a little lower than that of the unshaded one.

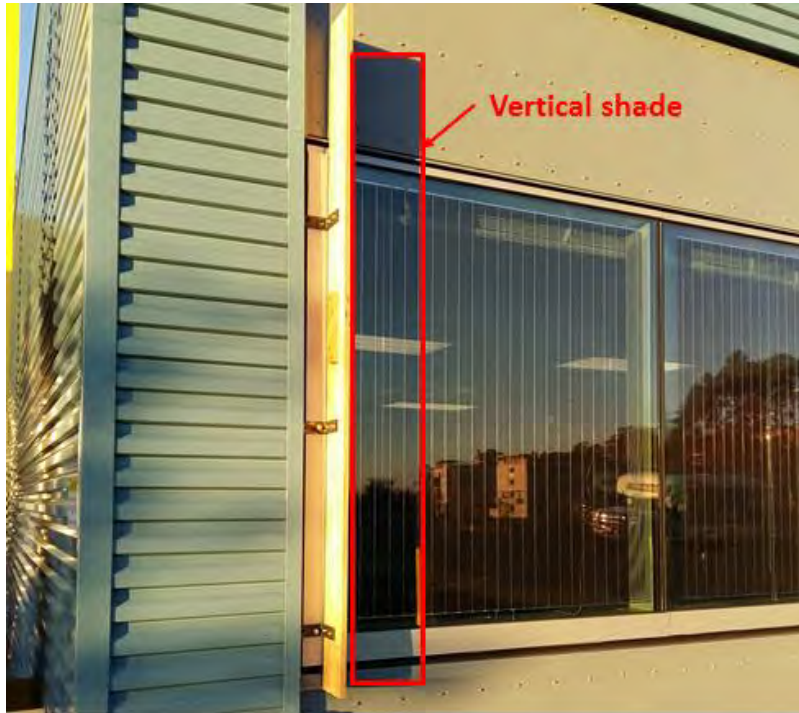


**Figure 31** Vertical shade case and the casted shadow on the BIPV IGU

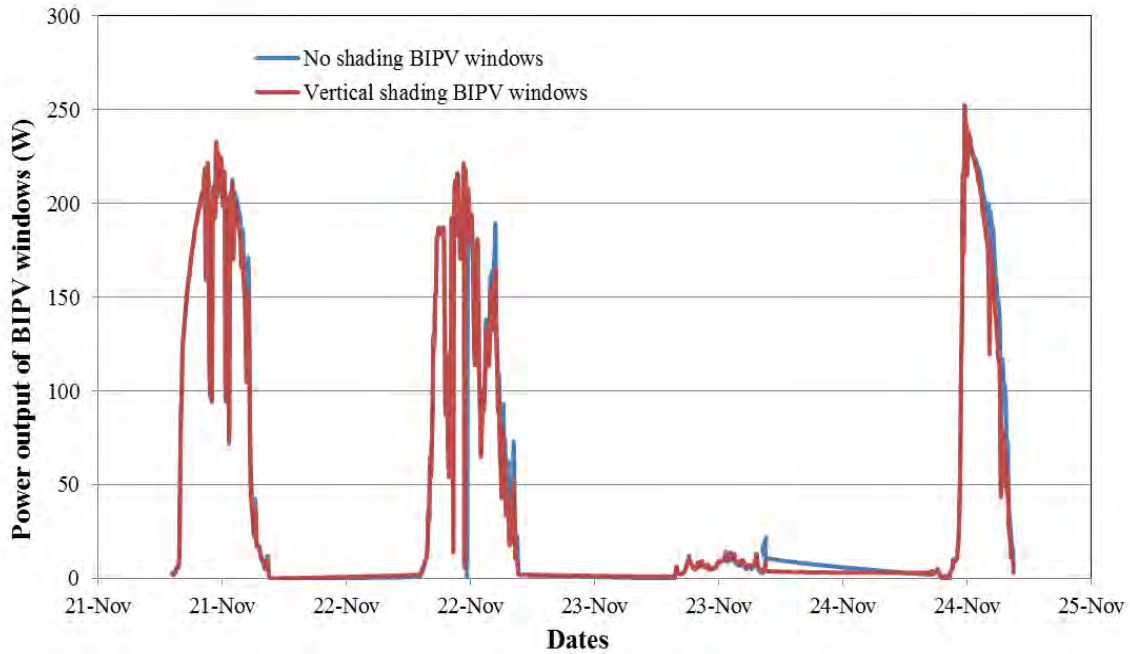


**Figure 32** Comparison of power outputs under vertical shade condition

The total energy output of the shaded BIPV array was 3125Wh, which is lower than that of the unshaded one by only 4%. It seems like that the impact of vertical shading on the power output in this specific case was not considerable. There are two explanations for this. First, when the vertical shade test was conducted, the XR test bed was facing southwest orientation, thus the

vertical shading device only cast shadow on the BIPV IGU in the late afternoon. Because solar irradiation was low at this time of day, there is no significant effect on the total energy output of the BIPV unit. Second, as shown in [Figure 33](#), each PV laminate consisted of 8 columns of PV strings and each of two clusters of 4 PV strings were first connected in parallel and then connected in series. In this case, although the left PV string was totally shaded, the remaining parallel PV strings can operate as usual, thus the total power output was reduced by 1/4 at most. Based on the analysis results, a conclusion can be drawn that for BIPV windows installed facing southwest or west orientation, the left side vertical shade would have a limited effect on the total energy output.

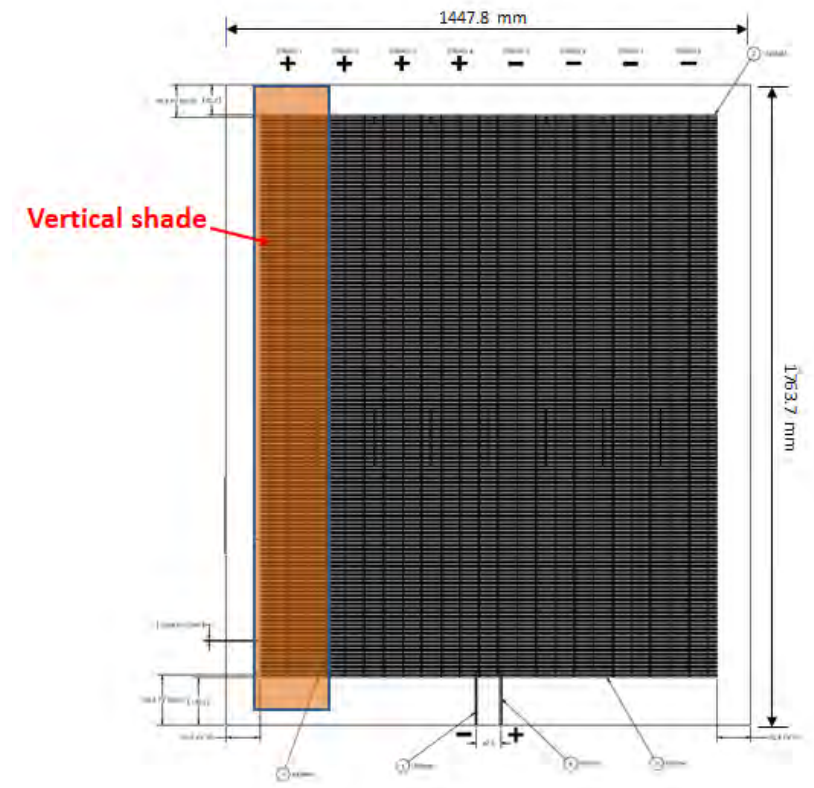


**Figure 33** Vertical shade case & arrangement of PV strings

[Figure 34](#) shows the horizontal shade case and the shadow on the BIPV IGU. As the width of the horizontal shade board was only 200mm, the shadow cast on the BIPV IGU was small. To quantify the impact of horizontal shade on the power output of BIPV arrays, a comparison of power outputs between the shaded and unshaded BIPV arrays are also conducted and presented in [Figure 35](#). It was found that the power output of the shaded BIPV array was much lower than that of the unshaded BIPV array before 2:30PM. Specifically, the power output of the shaded BIPV array was only half of the unshaded BIPV array before 2:00PM. This is because the horizontal shade device casted shadow on the all 8 strings, as shown in [Figure 36](#), which resulted in no current transfer through the shaded BIPV IGU, thus the energy output of the shaded BIPV IGU was zero. However, the other BIPV IGU in the shaded BIPV array operated as usual because there was bypass diode for conducting electricity in the junction box, thus the

total energy output of the shaded BIPV array was half of that of the unshaded BIPV array. After 2:30PM, the power outputs of both the shaded and unshaded BIPV arrays were almost the same as the incident angle of solar irradiation was relatively low at that time and thus almost no shadow was cast on the BIPV IGU.

Please see earlier notes on horizontal shading. This effect is not a 2pm or 2:30pm effect. It is purely sun angle dependent. Typically, in the morning and afternoon, you wouldn't expect any degradation because the Sun angle is low. The degradation will be at midday. These values are very location and season dependent.



**Figure 34** Horizontal shade case and the casted shadow on the BIPV IGU

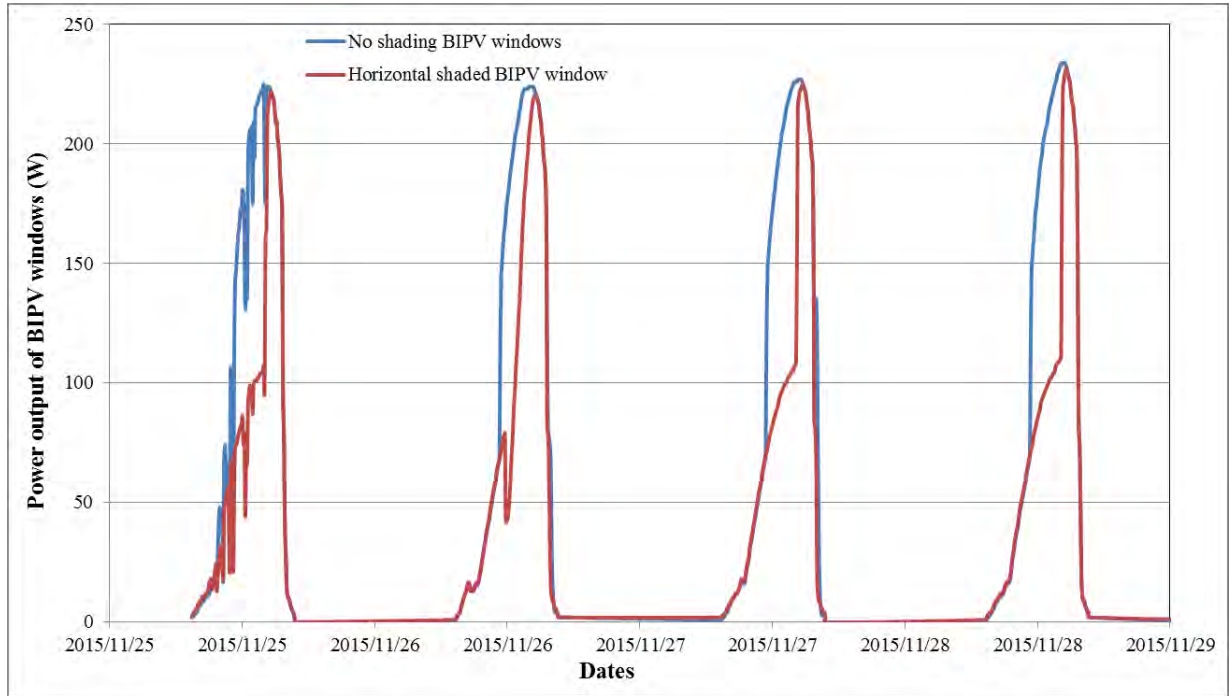


Figure 35 Comparison of power outputs under horizontal shade condition

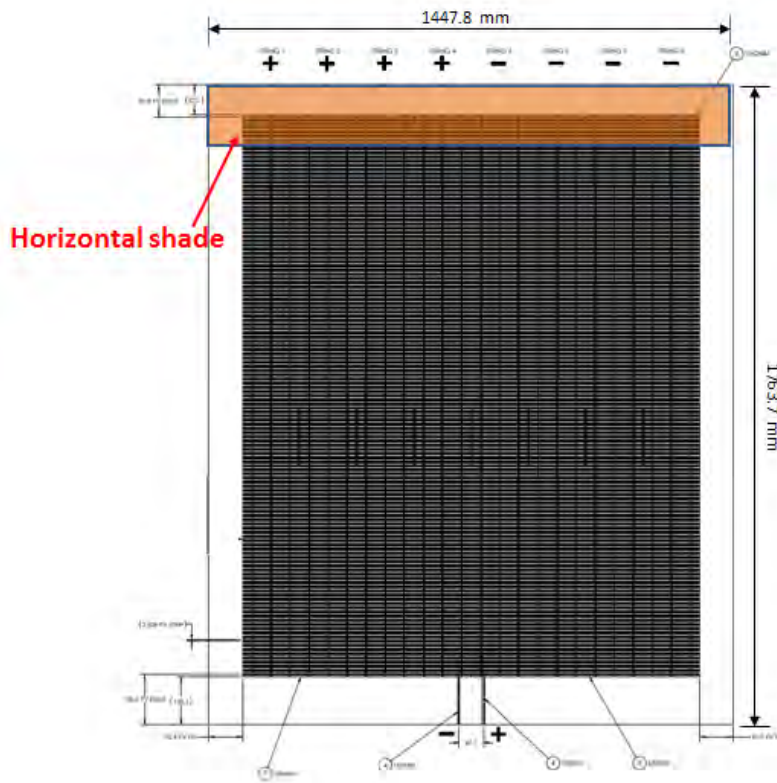


Figure 36 Horizontal shade case & PV strings arrangement

The total energy output of the shaded BIPV array was 3612Wh, which is lower than that of the unshaded one (5027Wh) by 28.1%. Based on the above results, we can conclude that for Solaria PV laminates with a vertical arrangement of PV strings, the impact of horizontal shade on the power output was much larger than that of vertical shade due to the vertical arrangement of PV strings for the BIPV laminates.

In summary, for BIPV design, more attention should be paid on reducing or eliminating any shading as much as possible because in certain circumstances, even a little shadow may result in a severe decrease of power output. If some shading of the BIPV unit is unavoidable, a reasonable arrangement of PV strings should be considered to bring down the energy loss as much as possible. For example, if horizontal shading was unavoidable in this test, to reduce the energy losses caused by this shading, the BIPV IGU strings could be vertically arranged, instead of horizontally.

### 4.3 Predicted Power Generation Performance

The PVWatts software developed by NREL was also used in this study to simulate and predict the annual BIPV electricity generation. The model simulation results were validated and calibrated against the measured data in September and October and the comparison results are listed in the last two rows of Tables 6 and 7. It is seen that the simulated results agree well with the measured data. Thus, this validated model was further used to predict the monthly and annual BIPV electricity generation. Table 8 lists the simulated monthly and annual electricity generation of the BIPV IGU. It is seen that the monthly electricity production of the vertical installed BIPV system is relatively uniform throughout the year. This is due to the interesting coupling of solar angles and incident solar radiation intensity, so when intensity is high, the incident angle is larger and vice versa, resulting in relatively constant output.

**Table 8** Simulated monthly and annual electricity generation of the BIPV IGU using PVWatts

Months	Solar Energy Generation, AC (kWh)	Incident Solar Radiation (kWh/m <sup>2</sup> /day)
January	49.29	3.23
February	39.67	2.91
March	38.17	2.58
April	47.22	3.41
May	35.85	2.57
June	32.78	2.48
July	35.84	2.58
August	44.18	3.13
September	58.58	4.2
October	57.76	3.89
November	56.97	3.93
December	51.19	3.37
<b>Total (annual)</b>	<b>547.5</b>	<b>38.3</b>

The simulation was done for Berkeley using the TMY3 weather data for Oakland, CA, which is neighboring city to Berkeley CA.

The total annual electricity output of this BIPV system is estimated to be 548 kWh for 8.9 m<sup>2</sup> of windows vision area, or 10.8 m<sup>2</sup> of total windows area. If we normalize to glazing vision area, the output is 61.6 kWh/m<sup>2</sup>/yr. It should be noted again that PV cells cover 1/3 of the glazing vision area, so if there was not requirement for transparency (such as in spandrel panels) and coverage would be 100%, the annual power production for Berkeley, CA would be 185 kWh/m<sup>2</sup>/yr. Equivalent traditional roof PV of the same area would produce 232 kWh/m<sup>2</sup>/yr, with much higher production in summer months.

#### 4.4 Thermal Performance & HVAC Electricity Consumption

Compared to the reference IGU, the energy conversion and heat transfer processes occurring in the BIPV IGU were more complicated. Solar irradiation shining on the BIPV IGU is partly reflected by the tempered glass layers and low-e coating and partly absorbed by the solar cells. The remaining incident solar radiation passes through the BIPV IGU and enters the indoor room providing daylighting and solar heat gain. Solar energy absorbed by the solar cells is also partly converted into direct current (DC) electricity and the absorbed remainder is dissipated as waste heat, resulting in an increase of the PV module operating temperature. **Figure 37** illustrates various surface temperature profiles of the BIPV IGU and the reference IGU. It is seen that the outer surface temperatures of both BIPV IGU and reference IGU were very close, but the inner surface temperature difference was relatively large. Due to the high absorptivity of solar irradiation, the inner surface temperature of the BIPV IGU was higher than that of the reference IGU by 7°C at noon.

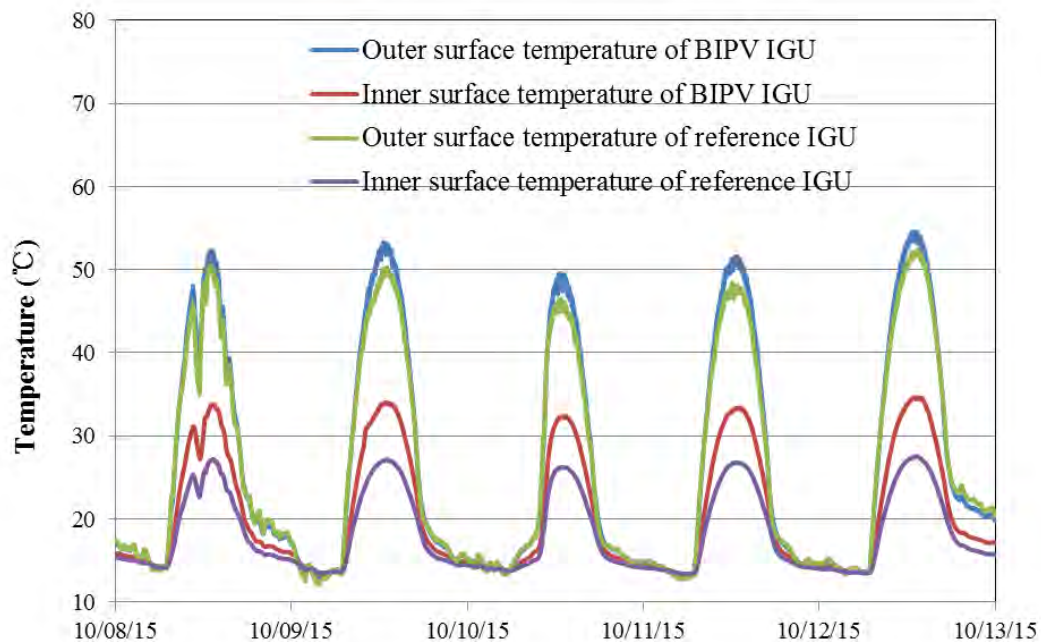


**Figure 37** Comparison of surface temperatures between BIPV IGU and reference IGU

Even though the BIPV IGU had higher inner surface temperature, theoretically speaking, its solar heat gain coefficient (SHGC) should be lower than the reference IGU because of the portion of glazing that is covered by opaque PV cells. Due to the choice of laminate construction, where a low-e coating was embedded in the laminate, one would expect higher SHGC and higher U-factor for BIPV glazing due to the embedding of low-e coating, however the decreased solar transmittance due to opaqueness of PV cells actually decreases overall SHGC and is expected to decrease cooling loads. As shown in [Figure 38](#), the average SHGC of the BIPV IGU and the reference IGU were 0.25 and 0.32, respectively. [Figures 39 and 40](#) present the solar irradiation transmittances of the BIPV IGU and the reference IGU. It is seen that the BIPV IGU has much lower solar irradiation transmittance than the reference IGU. The average solar irradiation transmittance for the BIPV and reference IGUs were 0.11 and 0.23, respectively. U-factor of the BIPV IGU was higher than the reference IGU, as shown in [Figures 41 and 42](#), and the average U-factors for the BIPV and reference IGUs were 3.5 and 1.5, respectively. Thus, BIPV IGU would expect higher heating loads due to the higher U-factor.

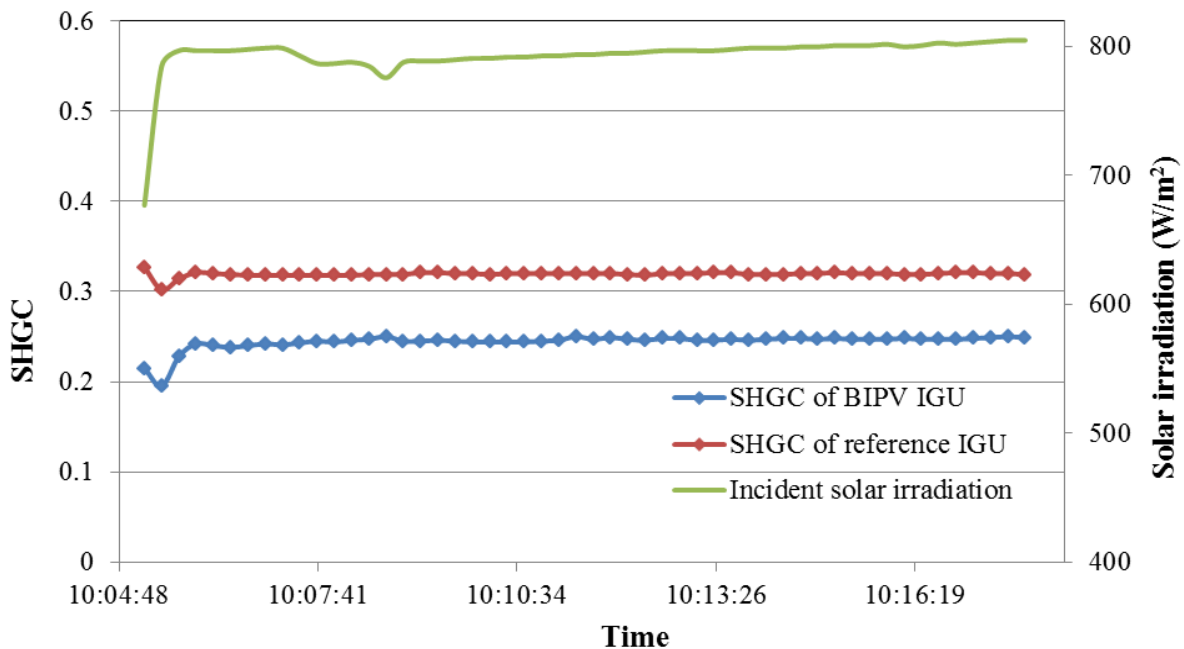


**Figure 38** Comparison of SHGCs between BIPV IGU and reference IGU

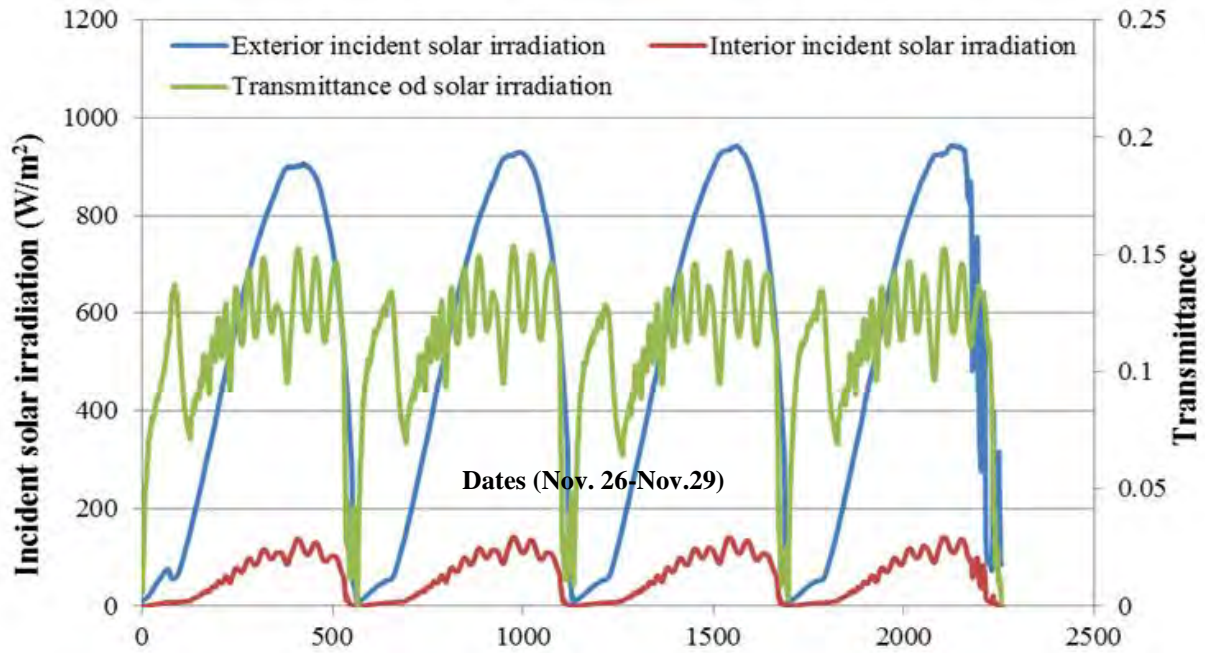


Figure 39 Solar irradiation transmittance of BIPV IGU

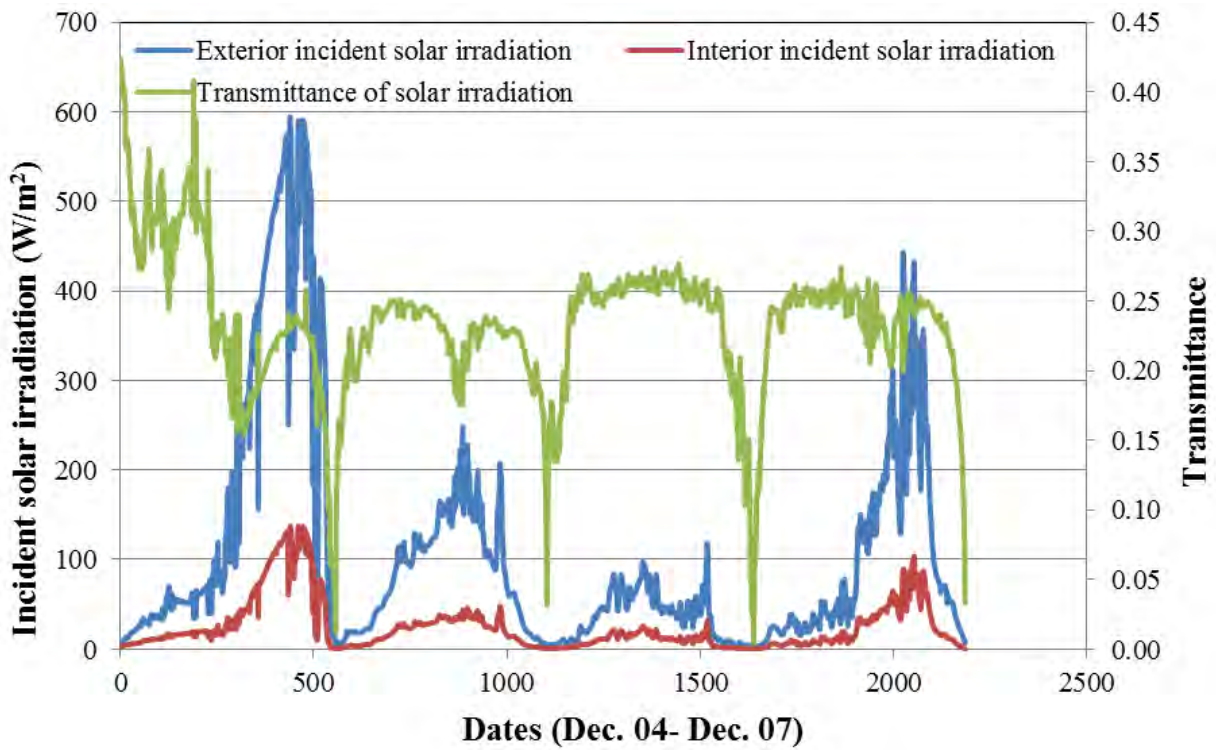


Figure 40 Solar irradiation transmittance of reference IGU

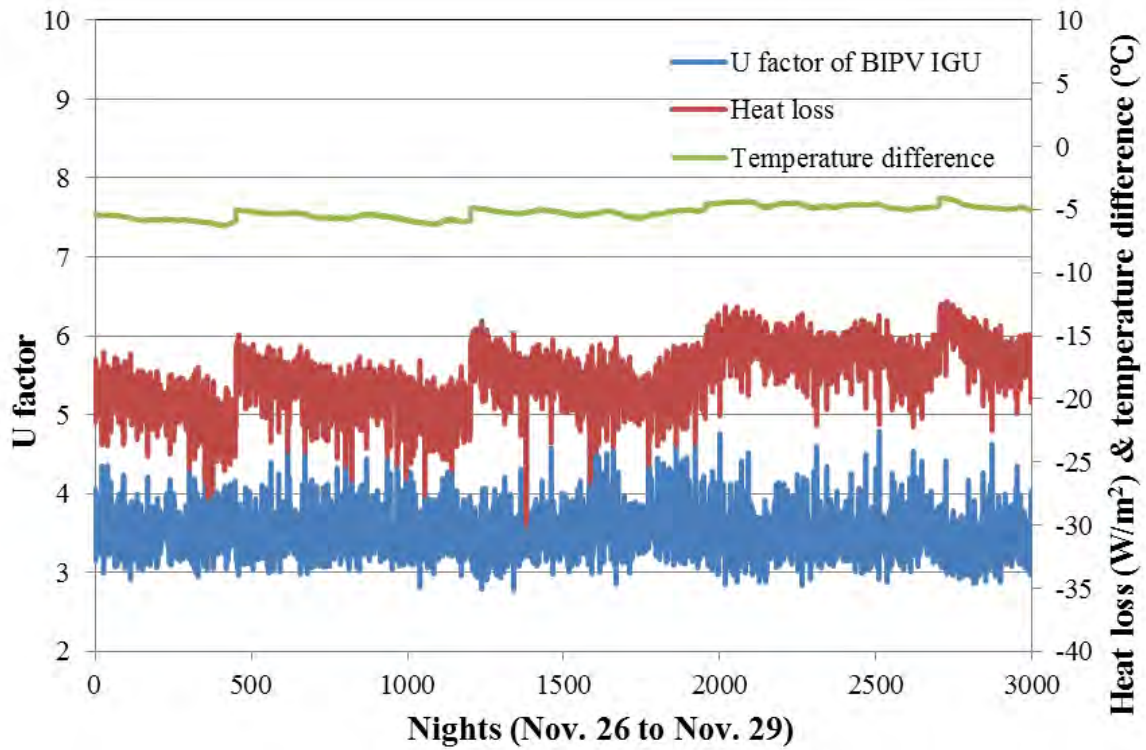


Figure 41 U-factor of the BIPV IGU (average U-factor is 3.5)

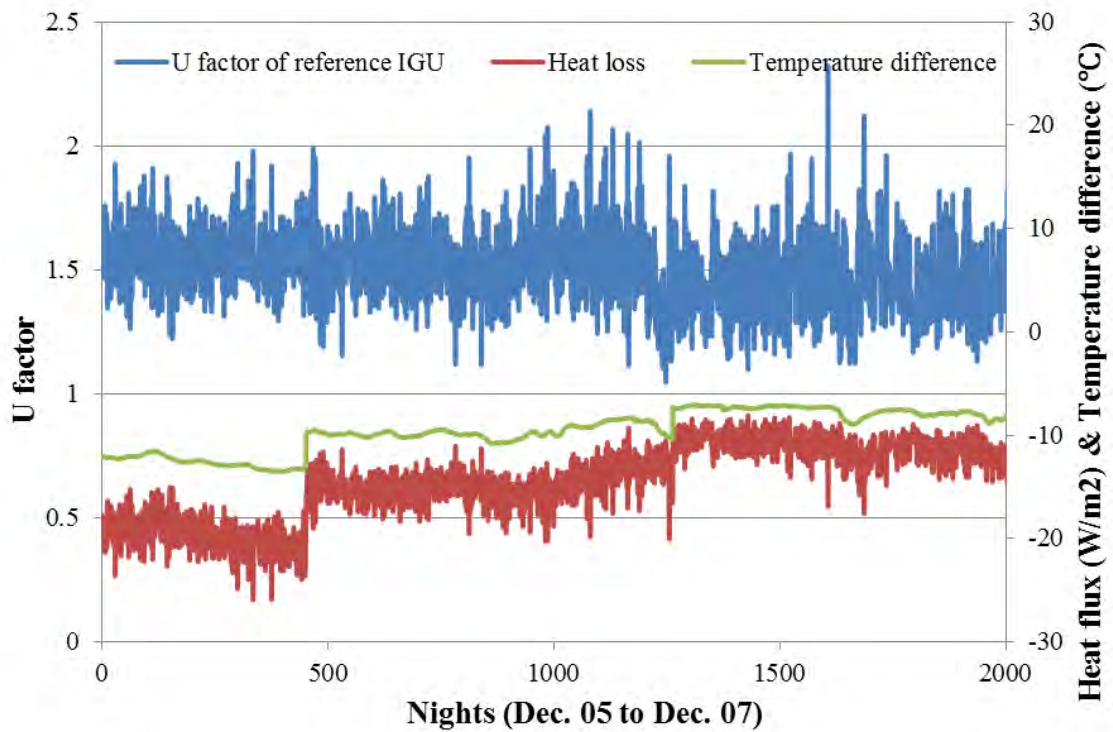
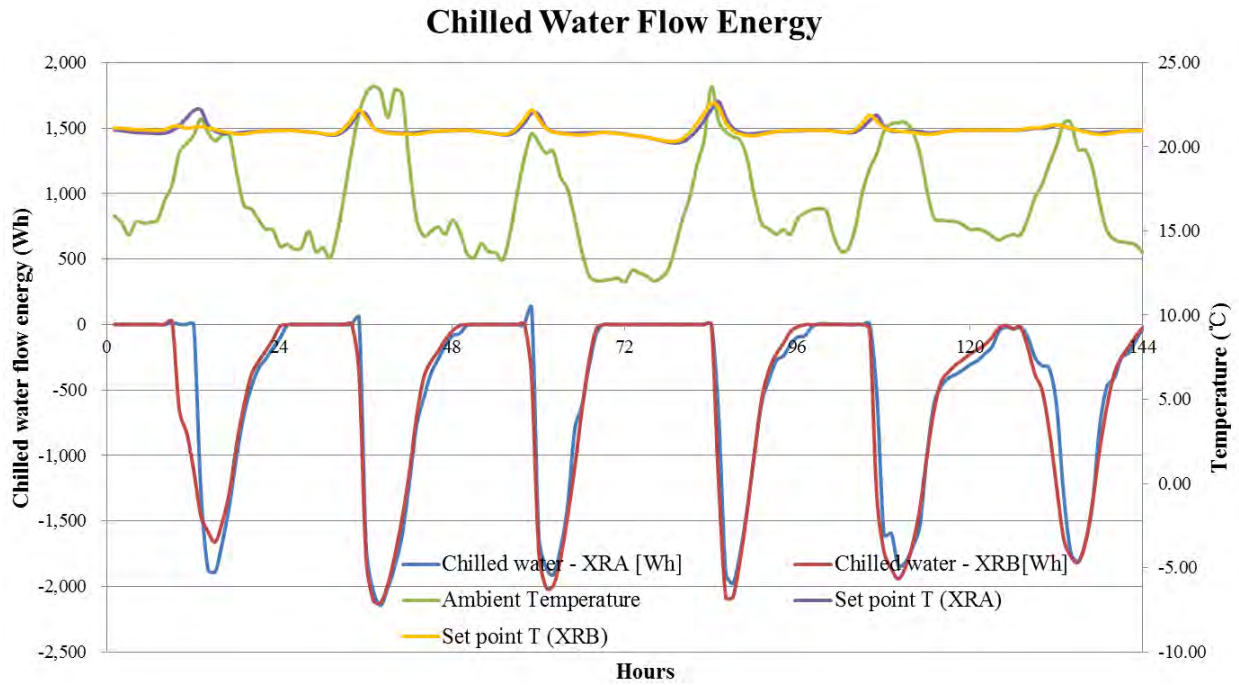


Figure 42 U-factor of the reference IGU (average U-factor is 1.5)

#### 4.4.1 Testing Results: South Orientation

During the entire test period, various parameters related to HVAC electricity consumption in both test cells (XRA and XRB) were measured and recorded. The measured parameters included water flow rates of heating and chilled water, supply and return water temperature in heating and chilled water loops, air flow velocity in supply and return ductworks, supply and return air flow temperature, as well as the real-time electricity consumption of water pumps and air handling units. Based on the above data, the HVAC electricity uses in both XRA (where BIPV IGU was installed) and XRB (where reference IGU was installed) were calculated.

A comparison of chilled water energy consumption in both XRA and XRB from Oct. 01 to Oct. 06, 2015 is presented in [Figure 43](#). During this period, the XR test bed was facing due south, which means that both the BIPV IGU and the reference IGU were facing south. The indoor air set point temperatures in both XRA and XRB were 21 °C. Both the venetian blinds behind the BIPV IGU and the reference IGU were pulled down. As shown in [Figure 43](#), the chilled water energy consumption in XRA was a little less than that in XRB and the total chilled water energy consumptions for XRA and XRB were 73,295Wh and 78,857Wh, respectively. Thus, the XRA test cell equipped with BIPV IGU reduced 7.1% chilled water energy consumption compared to the XRB during this period. Assuming the coefficient of performance (COPs) of chiller plants was 3.0, the electricity use of chiller plants for XRA and XRB can be calculated. Finally, the total HVAC electricity use was calculated by counting up the electricity uses of chiller plants, air handling units and water pumps in both XRA and XRB. A comparison of HVAC electricity uses in XRA and XRB is shown in [Figure 44](#). The total HVAC electricity uses of XRA and XRB were 98,807Wh and 105,184Wh, respectively. Thus, due to the lower SHGC, the BIPV IGU reduced 6.1% HVAC electricity use compared to the reference IGU under the experimental conditions of south orientation, 21°C set point temperature and both blinds pulled down.



**Figure 43** Comparison of chilled water energy consumption between XRA and XRB from Oct. 01 to Oct. 06, 2015 (South orientation, 21°C set point temperature, both venetian blinds down)

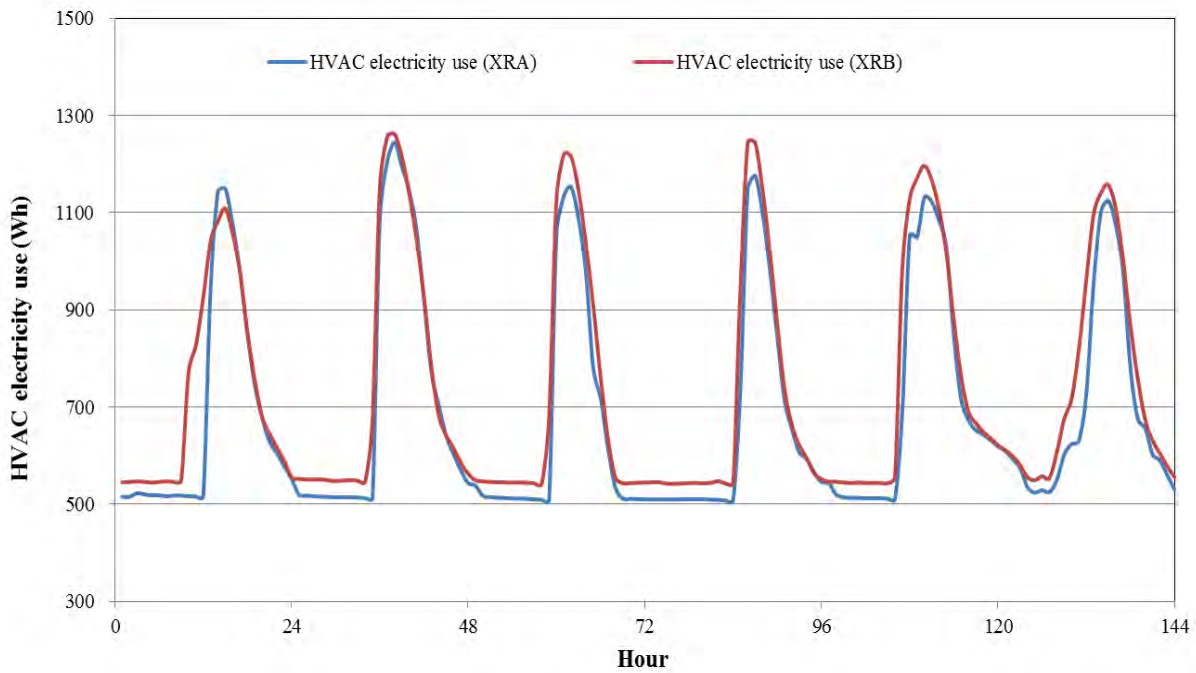


**Figure 44** Comparison of HVAC electricity uses between XRA and XRB from Oct. 01 to Oct. 06, 2015 (South orientation, 21°C set point temperature, both venetian blinds down)

From Oct. 20 to Oct. 23, 2015, the indoor air set point temperature in both XRA and XRB were adjusted to 17°C, and the venetian blinds were pulled up in both test beds. In this experimental case, a comparison of chilled water energy consumption in both XRA and XRB is presented in Figure 45. It can be observed that the chilled water energy consumption in XRA was less than that in XRB and the total chilled water energy consumptions for XRA and XRB were 95,420 Wh and 121,018 Wh, respectively. Therefore, the XRA test cell equipped with BIPV IGU reduced 21.1% chilled water energy consumption compared to XRB during this period. The total HVAC electricity usage for XRA and XRB during this period is presented in Figure 46. The **total HVAC electricity** usage reflects coefficient of performance (COP) of the system, which is typically on the order of 3 or higher. For XRA and XRB test beds the total HVAC-related electricity use, including fans and pumps was 66,075 Wh and 75,822 Wh, respectively. Thus, the BIPV IGU reduced HVAC electricity use by 12.9% compared to the reference IGU under the experimental conditions (south orientation, and both venetian blinds were pulled up).

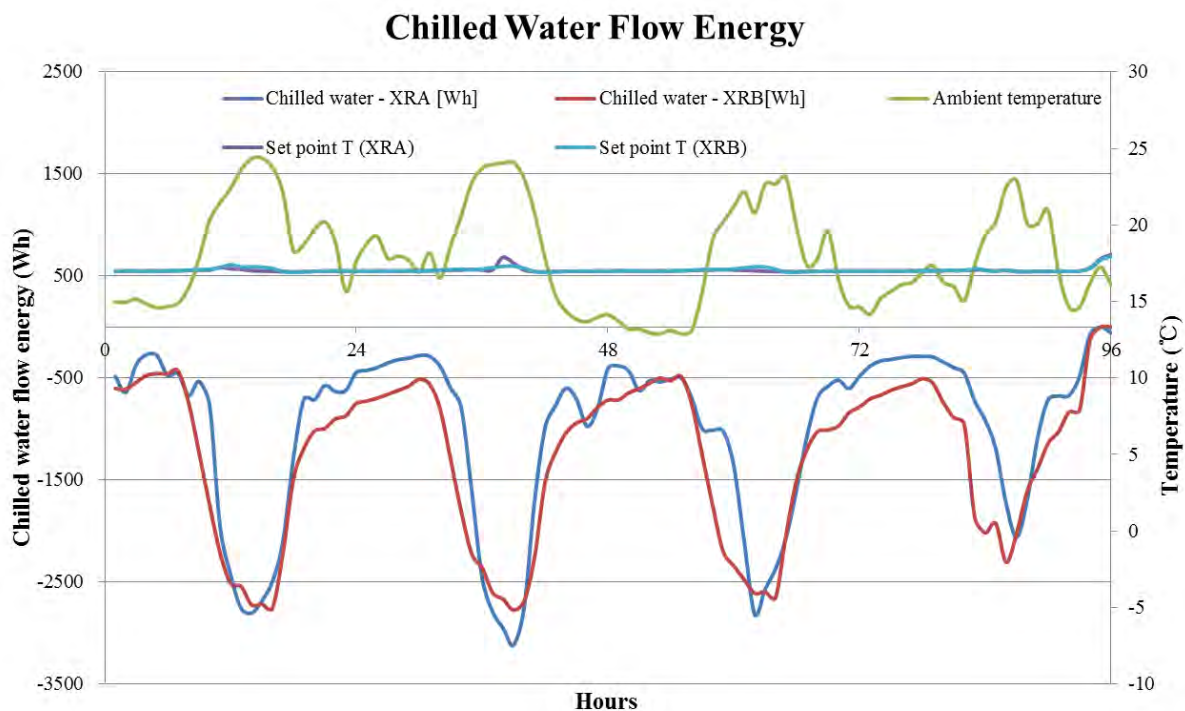


**Figure 45** Comparison of chilled water energy consumption between XRA and XRB from Oct. 20 to Oct. 23, 2015 (South orientation, 17°C set point temp., both blinds up)

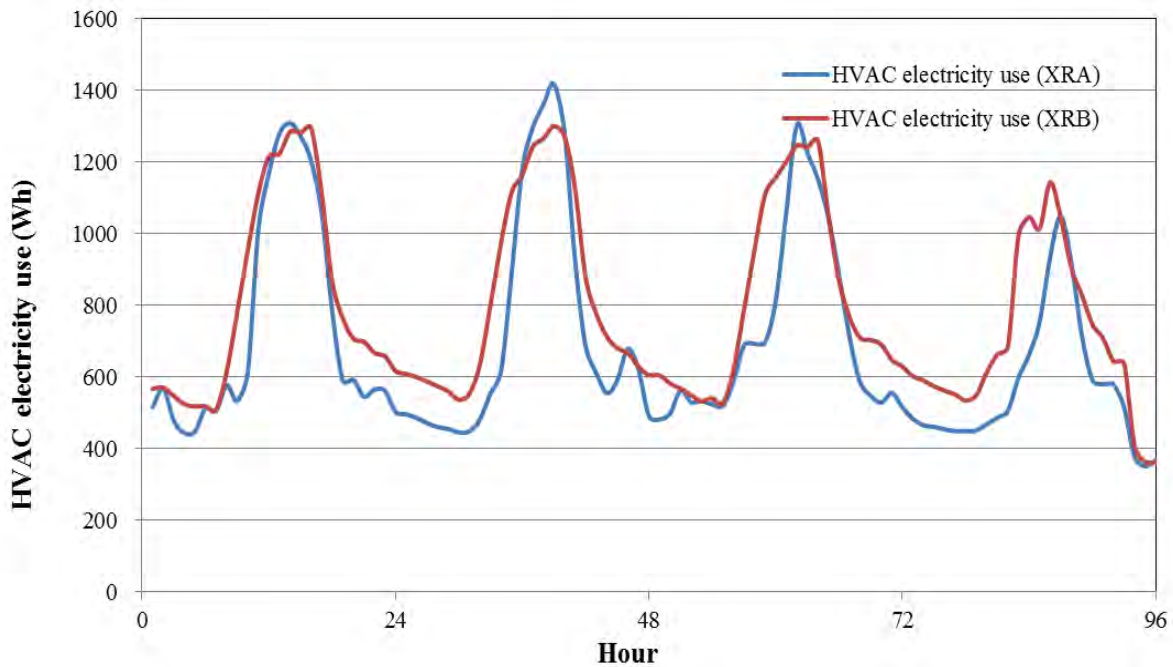


**Figure 46** Comparison of HVAC electricity uses between XRA and XRB from Oct. 20 to Oct. 23, 2015 (South orientation, 17°C set point temp., both blinds up)

From Oct. 24 to Oct. 27, 2015, the indoor air set point temperature in both XRA and XRB were adjusted to 18°C, while the other conditions were unchanged. In this experimental case, the chilled water energy consumption in XRA was also obviously less than that in XRB, as shown in [Figure 47](#), and the total chilled water energy consumption of XRA and XRB was 64,749 Wh and 83,598 Wh, respectively. The XRA test cell equipped with BIPV IGU reduced 22.5% chilled water energy consumption compared to XRB during this period. The HVAC electricity usage in XRA and XRB during this period is presented in [Figure 48](#). The total HVAC electricity usage in XRA and XRB were 55,648 Wh and 63,103 Wh, respectively. Thus, the BIPV IGU reduced 11.8% HVAC electricity use compared to the reference IGU under the experimental conditions of south orientation, 18°C set point temperature and both venetian blinds were pulled up.

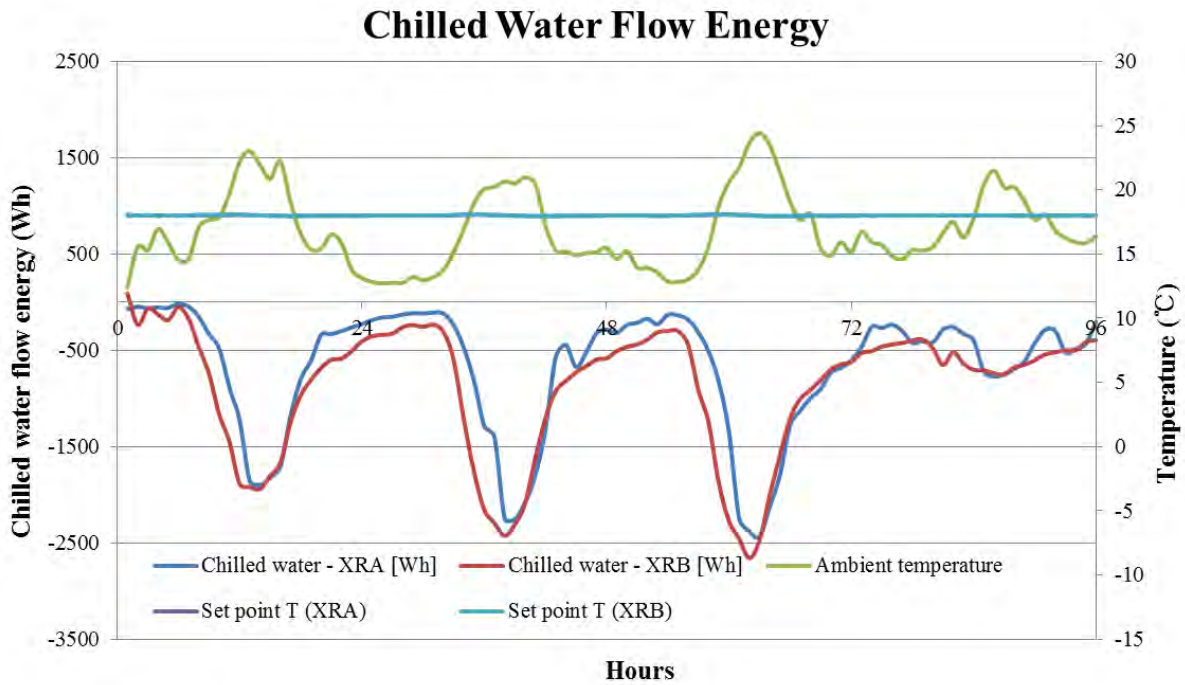


**Figure 47** Comparison of chilled water energy consumption between XRA and XRB from Oct. 24 to Oct. 27, 2015 (South orientation, 18°C set point temp., both blinds up)

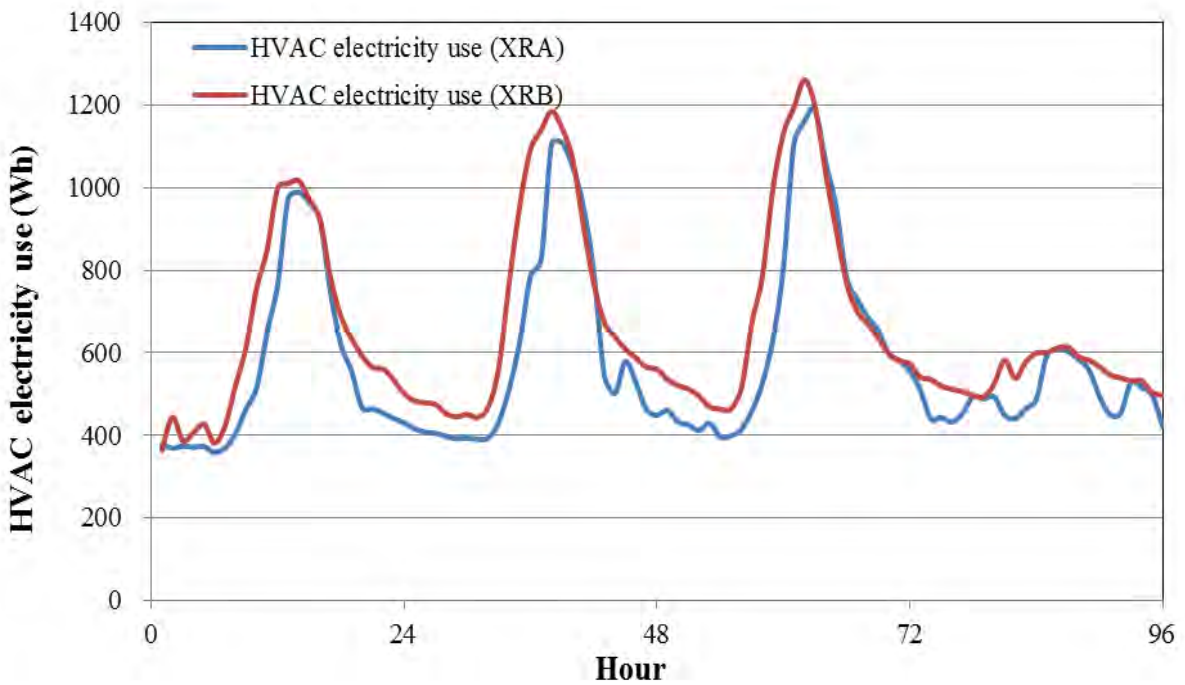


**Figure 48** Comparison of HVAC electricity uses between XRA and XRB from Oct. 24 to Oct. 27, 2015 (South orientation, 18°C set point temp., both blinds up)

From Nov. 18 to Nov. 22, 2015, the orientation of the XR test bed was still pointed to south orientation, the set point temperature was kept at 18°C and both venetian blinds in XRA and XRB were pulled up. In this case, the chilled water energy consumption in XRA was much lower than that in XRB, as shown in Figure 49, and the total chilled water energy consumptions in XRA and XRB were 60,988 Wh and 98,111 Wh, respectively. The XRA test cell equipped with BIPV IGU reduced chilled water energy by 37.8% compared to XRB in this case. The HVAC electricity usage in XRA and XRB during this period is presented in Figure 50. The total HVAC electricity usage in XRA and XRB was 62,942 Wh and 76,734 Wh, respectively. The BIPV IGU reduced 18.0%.

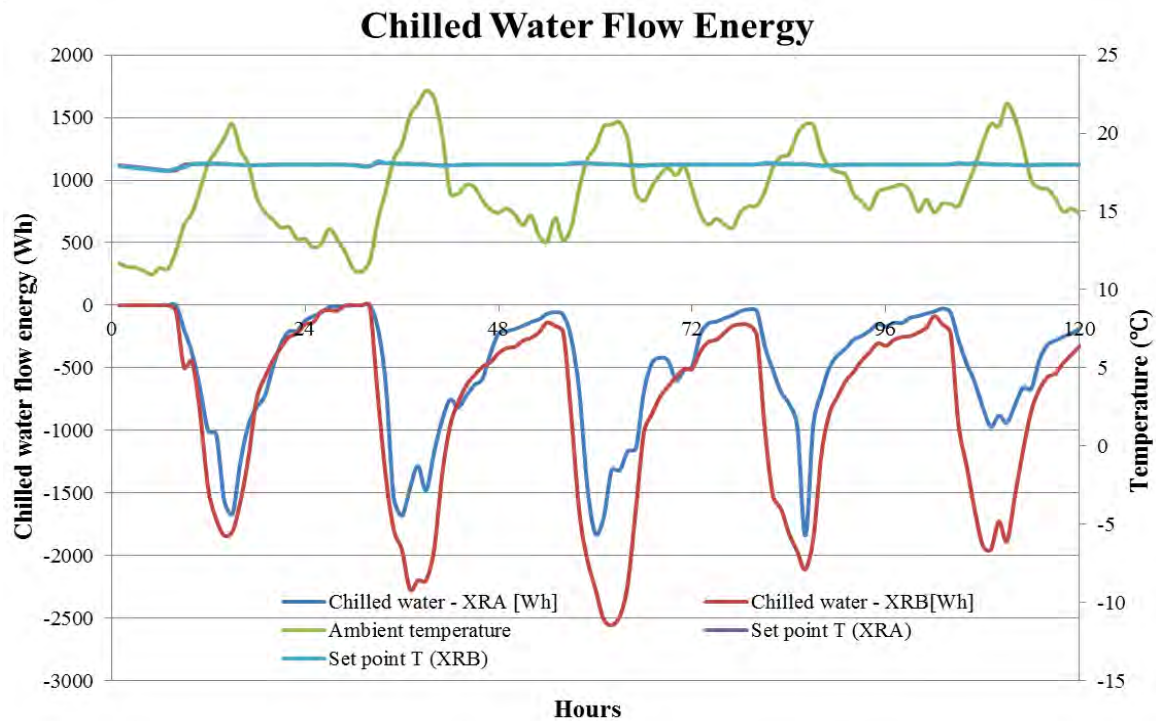


**Figure 49** Comparison of chilled water energy consumption between XRA and XRB from Nov. 18 to Nov. 22 (South orientation, 18°C set point temp., both blinds up)

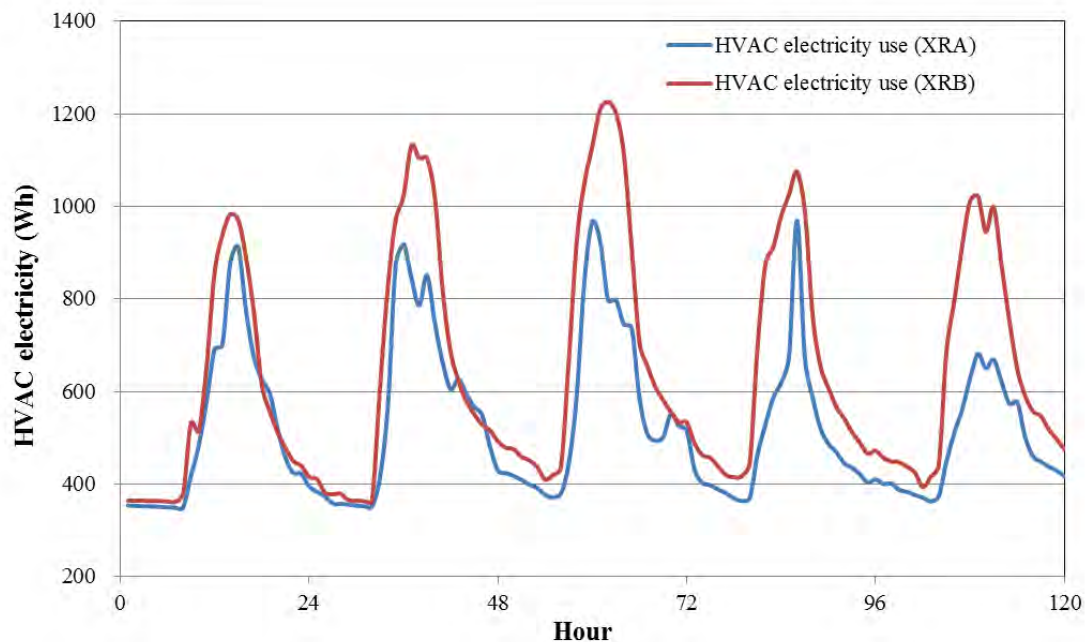


**Figure 50** Comparison of HVAC electricity uses between XRA and XRB from Nov. 18 to Nov. 22, 2015 (South orientation, 18°C set point temp., both blinds up)

#### 4.4.2 Testing Results: Southeast Orientation

The main purpose of rotating the test bed to different orientations was to measure and evaluate the overall energy performance (power, thermal and daylighting performance) of the BIPV IGU such that to further identify the optimum orientation in terms of energy-efficient for installation.

From Oct. 28 to Oct. 30 2015, the orientation of the XR test bed was rotated to the southeast orientation, the set point temperature was kept at 18°C and the venetian blinds in both XRA and XRB were pulled up. In this experimental case, the chilled water energy consumption in XRA was a little less than that in XRB, as shown in [Figure 51](#), and the total chilled water energy consumptions in XRA and XRB were 57,166 Wh and 59,794 Wh, respectively. The XRA test cell equipped with BIPV IGU reduced only 4.4% chilled water energy consumption compared to XRB in southeast orientation. The HVAC electricity usage in XRA and XRB during this period is presented in [Figure 52](#). The total HVAC electricity usage in XRA and XRB was 44,929 Wh and 46,318 Wh, respectively. The BIPV IGU reduced HVAC electricity use by only 3.0% compared to the reference IGU under the experimental conditions of southeast orientation, 18°C set point temperature and both venetian blinds were pulled up. The above results showed that the BIPV IGU facing southeast orientation had much lower HVAC energy saving potential compared to the reference IGU than the south-facing orientation.

This outcome has two explanations. When the XR test bed rotated to the southeast orientation, on the one hand, the west wall of the XRA test cell received more solar heat gain which resulted in an increase of cooling load, on the other hand, as the XR test bed was close to another test

bed, a part of the reference IGU was shaded by the adjacent test bed at morning, as shown in Figure 53, thus the solar heat gain of the reference IGU was obviously reduced in southeast orientation.

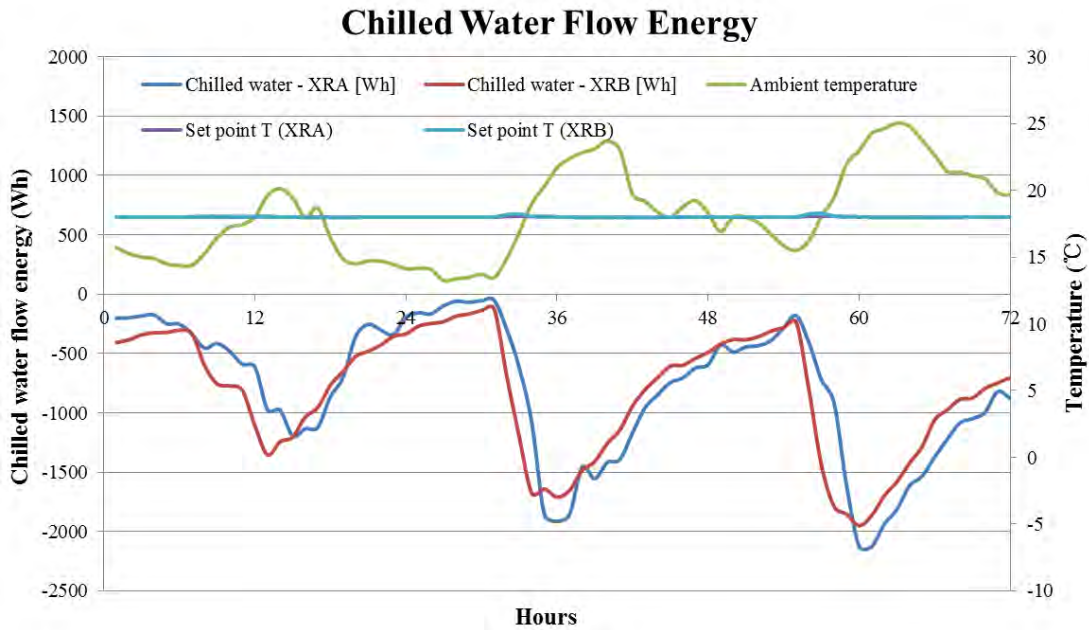


Figure 51 Comparison of chilled water energy consumption between XRA and XRB from Oct. 28 to Oct. 30, 2015 (Southeast orientation, 18°C set point temp., both blinds up)

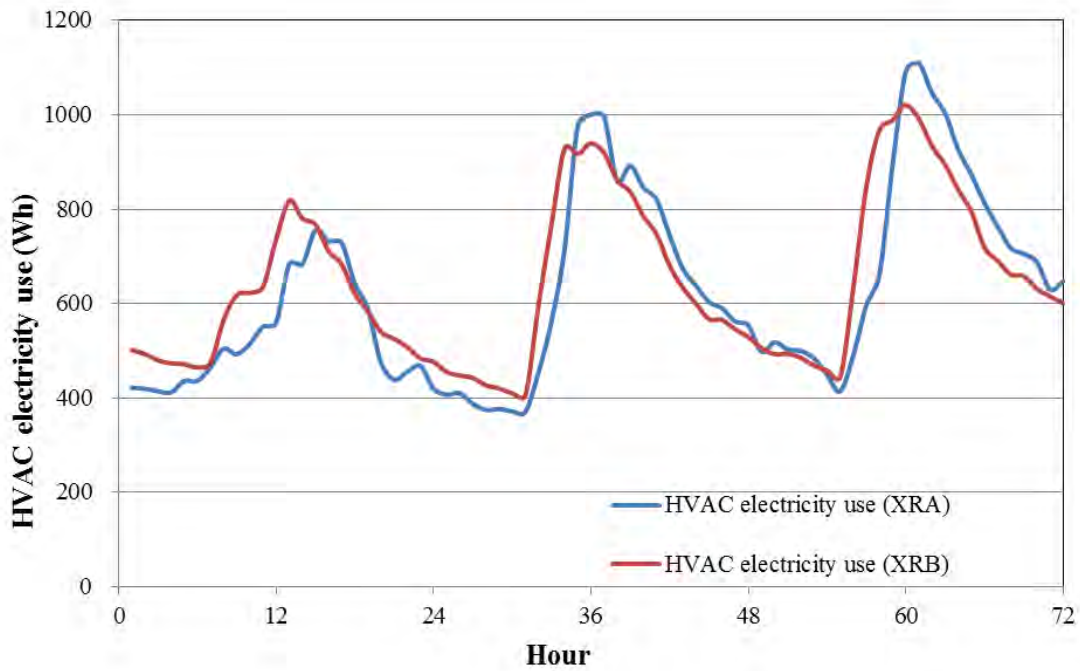
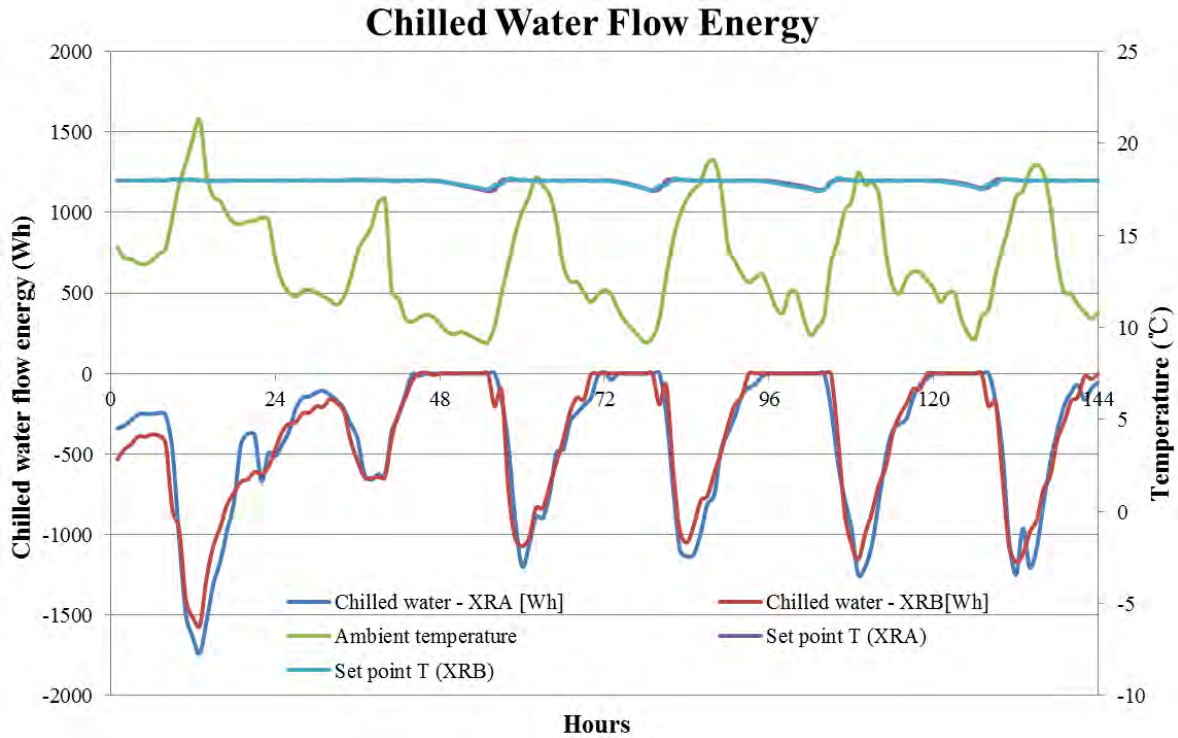


Figure 52 Comparison of HVAC electricity uses between XRA and XRB from Oct. 28 to Oct. 30, 2015 (Southeast orientation, 18°C set point temp., both blinds up)



**Figure 53** The reference IGU is shaded by an adjacent test bed when turned to southeast orientation

From Nov. 01 to Nov. 06, 2015, both venetian blinds in XRA and XRB were pulled down while the other conditions were unchanged. In this case, the chilled water energy consumption in XRA was a little higher than that in XRB, as shown in [Figure 54](#), and the total chilled water energy consumptions in XRA and XRB were 56,996 Wh and 56,562 Wh, respectively. The XRA test cell equipped with BIPV IGU consumed 0.8% more chilled water energy compared to XRB during this period. Compared to XRB, XRA even though had higher chilled water energy consumptions, its HVAC electricity use was still lower than that of XRB, as shown in [Figure 55](#), due to the less electricity uses for air handling units and water pumps. The total HVAC electricity uses in XRA and XRB were 70,036 Wh and 71,629 Wh, respectively. The BIPV IGU reduced 2.2% HVAC electricity use compared to the reference IGU under the experimental conditions of southeast orientation, 18°C set point temperature and both venetian blinds were pulled down.



**Figure 54** Comparison of chilled water energy consumption between XRA and XRB from Nov. 01 to Nov.06, 2015 (Southeast orientation, 18°C set point temp., both blinds down)

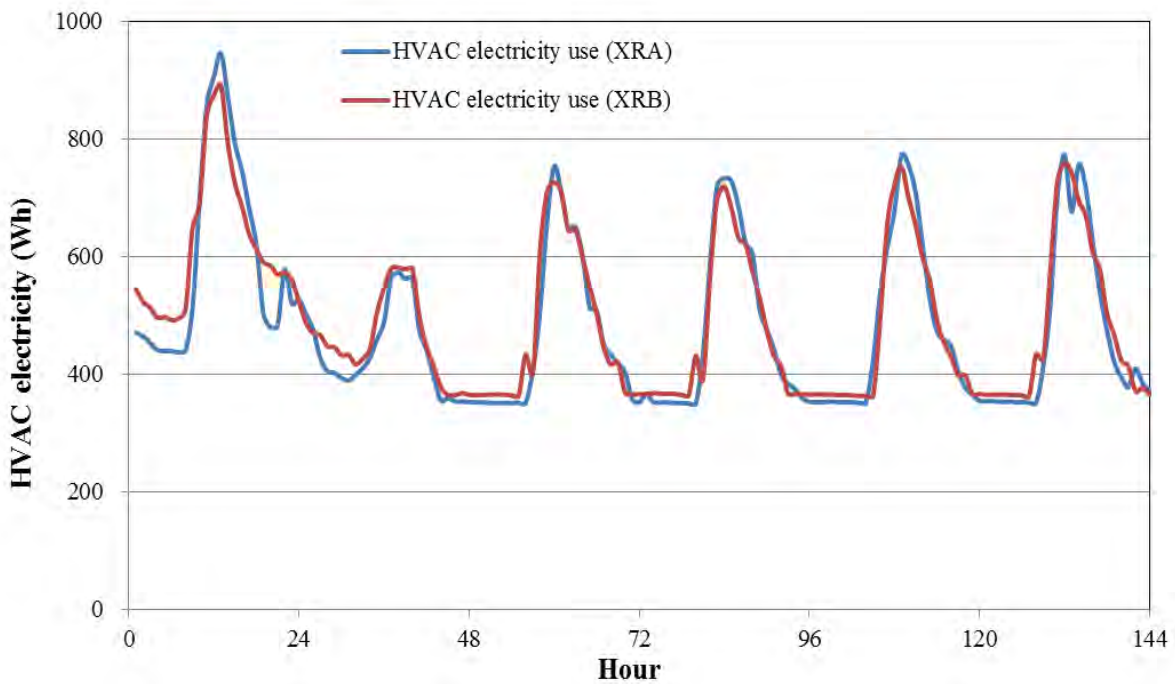


**Figure 55** Comparison of HVAC electricity uses between XRA and XRB from Nov. 01 to Nov. 06, 2015 (Southeast orientation, 18°C set point temp., both blinds down)

#### 4.4.3 Testing Results: West Orientation

From Dec. 05 to Dec. 08 2015, the test bed was rotated to the west orientation and the indoor air set point temperature was adjusted to 25°C for heating. In this case, the hot water energy consumption in XRA was much higher than that in XRB due to higher U-factor, and lower SHGC, thus reducing the beneficial solar heat gain in heating mode, as shown in [Figure 56](#). The total hot water energy consumption in XRA and XRB was 99,858 Wh and 67,711 Wh, respectively. The XRA test cell equipped with BIPV IGU consumed 47.5% more hot water energy compared to XRB during this period. Compared to XRB, XRA consumed more HVAC electricity use for space heating, as shown in [Figure 57](#). The total HVAC electricity usage in XRA and XRB was 62,180 Wh and 52,136 Wh, respectively. The BIPV IGU consumed 19.3% more HVAC electricity compared to the reference IGU under the experimental conditions of west orientation, 25°C set point temperature and both venetian blinds were pulled up.

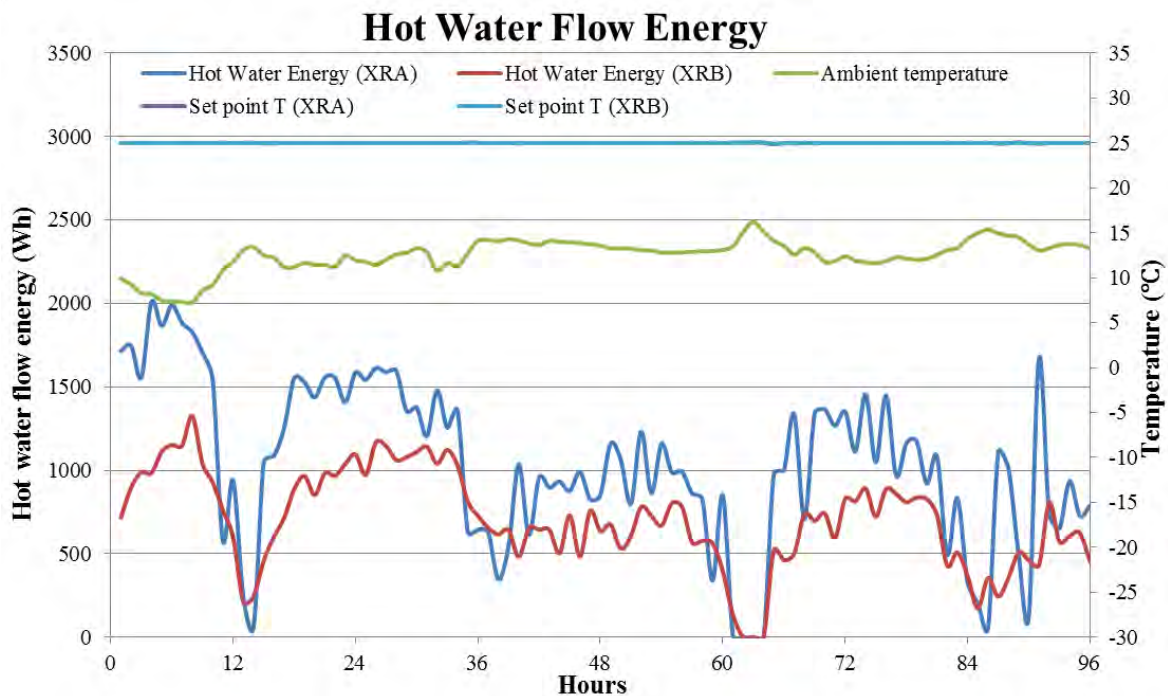


**Figure 56** Comparison of hot water energy consumption between XRA and XRB from Dec. 05 to Dec.08, 2015 (West orientation, 25°C set point temp., both blinds up)

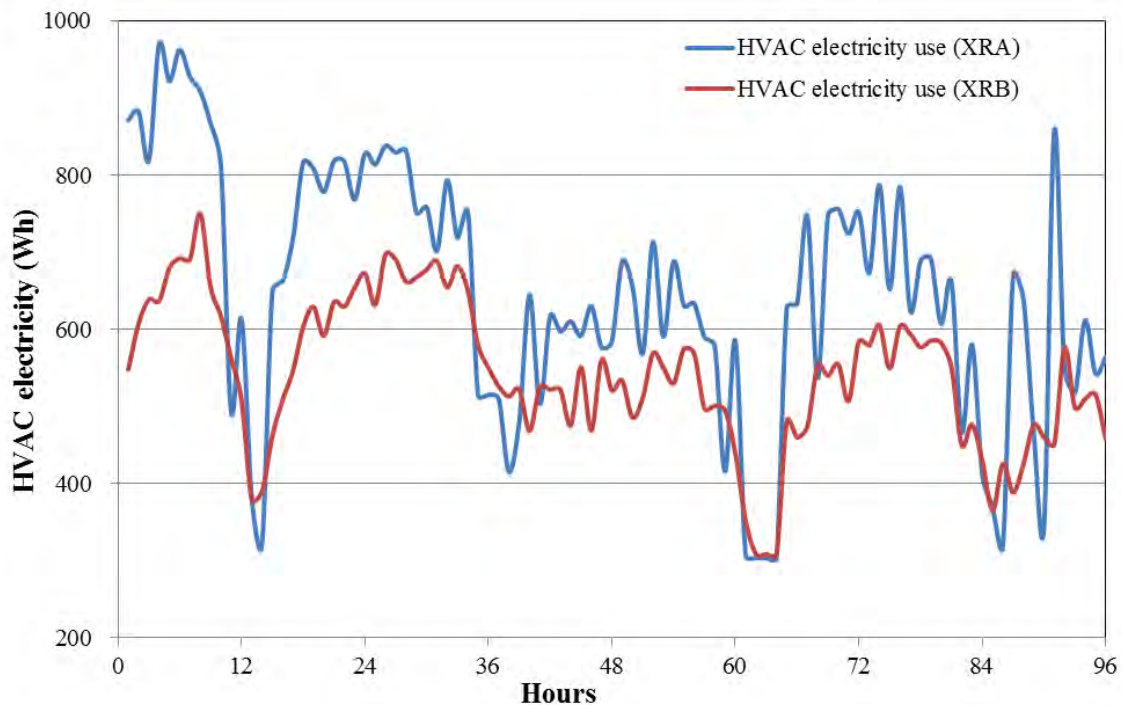


**Figure 57** Comparison of HVAC electricity usage between XRA and XRB from Dec. 05 to Dec.08, 2015 (West orientation, 25°C set point temp., both blinds up)

In order to have a complete understanding on the HVAC energy saving potential of the BIPV IGU, an overview of energy saving results under different orientations, different set point temperatures and different shade positions are listed in [Table 9](#). In general, the BIPV IGU had much higher HVAC energy saving potential in south orientation than in southeast orientation. The average HVAC electricity saving for the south facing BIPV IGU was 11.6%, but it was only 2.6% for southeast facing. Eliminating the two countervailing influences discussed above, an energy saving potential of about 10% might be expected for the southeast orientation. Due to a high U-factor, the thermal insulation performance of the BIPV IGU was worse than that of the reference IGU. For space heating, the test cell equipped with BIPV IGU consumed 19.3% more HVAC electricity than the test cell installed with reference IGU. In addition, the shade position also affected the HVAC energy saving of the BIPV IGU. The BIPV IGU had higher energy saving potential in the case of both venetian blinds being pulled up, followed by blinds in XRA being pulled up but in XRB being pulled down, and the lowest savings came from the case where both blinds were pulled down.

**Table 9** Overview of energy saving results of the BIPV IGU under different conditions

Test periods	Orientation	Set point temp.	Blinds position	Chilled (Hot) water energy (Wh)	HVAC electricity use (Wh)	Energy saving of BIPV IGU
10/01-10/06	South	21 °C	Both down	XRA:73,295 XRB:78,857	XRA:98,807 XRB:105,184	6.1%
10/20-10/23	South	17 °C	Both up	XRA:95,420 XRB:121,018	XRA:66,075 XRB:75,822	12.9%
10/24-10/27	South	18 °C	Both up	XRA:64,749 XRB:83,598	XRA:55,648 XRB:63,103	11.8%
10/28-10/30	Southeast	18 °C	Both up	XRA:57,166 XRB:59,794	XRA:44,929 XRB:46,318	3.0%
11/01-11/06	Southeast	18 °C	Both down	XRA:56,996 XRB:56,562	XRA:70,036 XRB:71,629	2.2%
11/18-11/22	South	18 °C	Both up	XRA:60,988 XRB:98,111	XRA:62,942 XRB:76,734	18%
12/05-12/08	West	25 °C (heat)	Both up	XRA:99,858 XRB:67,711	XRA:62,180 XRB:52,136	-19.3%
<b>Sub-Totals</b>						<b>Totals</b>
XRA				508,472	460,617	969,089
XRB				565,651	490,926	1,056,577
% Saving A vs. B				-10.1%	-6.2%	-8.3%

## 4.5 Daylighting Performance

The objective of this analysis is to evaluate the trade-offs associated with the BIPV glazing between daylight, glare, and lighting energy use.

### 4.5.1 Visual comfort

Hemispherical field-of-view luminance measurements were made in two locations at seated eye height 4 ft. above the floor parallel to and facing the window (Figures 58-59). These locations represent a conservative, worst case evaluation of discomfort glare from the window. The venetian blinds were either fully raised or fully lowered with a slat angle that just blocked direct sunlight. The electric lighting was set to a fixed lighting level of 300 lux, providing a stable ambient lighting level so that visual discomfort could be evaluated with an adequate baseline for visual adaptation.

Measurements were made using commercial-grade digital cameras (Canon 60D) equipped with an equidistant fisheye lens (Sigma E 4.5 mm f/2.8). Bracketed low dynamic range (LDR) images were taken automatically at 10-min intervals then converted into a calibrated high dynamic range (HDR) image, which was then used to assess discomfort glare.

The Daylight Glare Probability (DGP) index was used to evaluate discomfort glare. This index was derived through a comprehensive statistical analysis of HDR data and subjective response in a full-scale private office testbed that was retrofit with a variety of daylighting measures [11]. The 10-min interval DGP values were used to calculate summary values for the day from 8 AM to 6 PM local time, which were then compared to the four classified levels of glare tolerance as shown in Table 10.

**Table 10** Daylight Glare Probability (DGP) classification

Max DGP of 95% office time	and	Average DGP of 5% office time	Class	Meaning
$\leq 0.35$ ("imperceptible" glare)	and	$\leq 0.38$ ("perceptible" glare)	A	Best
	and	$> 0.38$	B	Good
$\leq 0.40$ ("perceptible" glare)	and	$\leq 0.42$ ("disturbing" glare)	B	Good
	and	$> 0.42$	C	Reasonable
$\leq 0.45$ ("disturbing" glare)	and	$\leq 0.53$ ("intolerable" glare)	C	Reasonable
	and	$> 0.53$	Discomfort	Discomfort
$> 0.45$			Discomfort	Discomfort

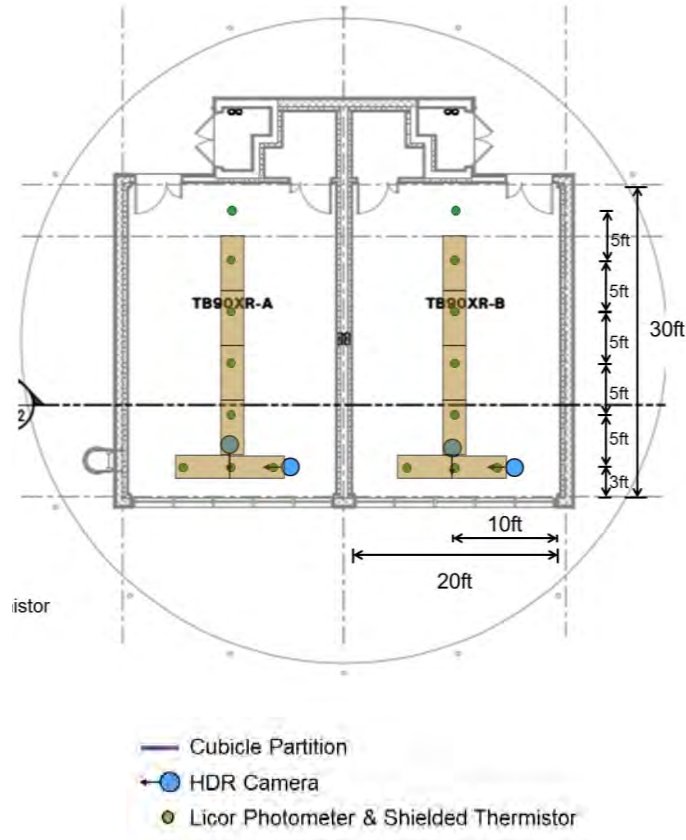


**Figure 58** Location of sensors in the reference and test rooms.



**Figure 59** (Left) Fisheye view from seated height looking toward the window at 3 ft. from the window; (right) fisheye view from seated height looking parallel to the window at 3 ft. from the window.

#### 4.5.2 Lighting energy

Lighting energy use due to daylight dimming was determined based on measured illuminance levels at the workplane and the dimming profile of LED and fluorescent fixtures, derived from a parallel FLEXLAB study. The LED installed lighting power density was 0.51 W/ft<sup>2</sup>. The dimming profile from full power was linear, where 64.9 W was required to produce 300 lux at the workplane in each 10 ft. deep zone. The T5 fluorescent system had an installed LPD of 0.59 W/ft<sup>2</sup>, with 123.6 W required to produce 300 lux in each zone. Sensors at a distance of 8 ft., 18 ft. and 28 ft. from the window were used to determine daily lighting energy use between 8 AM and 6 PM local time.

#### 4.5.3 Daylight adequacy

Workplane illuminance was measured in the center of the space at incremental distances of 5 ft. from the window wall. For each of the 10 ft. deep window, center or rear zones, illuminance data from each of the two sensors were binned based on three ranges of illuminance: 0-100 lux, 100-2000 lux, and greater than 2000 lux for the period from 8 AM to 6 PM local time. For each bin, the useful daylight illuminance (UDI) was then calculated, defined by the percentage of day that daylight was within the defined binned range. A daylighting system that is able to deliver daylight to the workplane within the range of 100-2000 lux for 100% of the day in all areas of the room would be considered to be successful in providing adequate daylight.

#### 4.5.4 Discomfort glare and lighting energy use

Results for discomfort glare, daylight adequacy, and lighting energy use are given in [Tables 11-14](#) for the monitored period. A few observations can be made from these data:

- For the seated view looking toward the window, discomfort glare from the window was inadequately controlled over the entire period irrespective of reference or test condition, window orientation and whether the blinds were raised or lowered.
- For the seated view looking parallel to the window, glare was controlled adequately by the test condition (BIPV) with blinds lowered and on occasion in both rooms on cloudy days.
- Daily lighting energy use for the south-facing orientation was increased with the BIPV with blinds case by 250 Wh/day (116%) or 519 Wh/day (116%) on average compared to the reference room with blinds if dimmable LED or fluorescent lighting was used over the 30 ft. deep space, respectively (Figure 61).
- The BIPV with blinds admitted less useful daylight than the reference case with blinds in the rear zone furthest from the window: daylight illuminance levels were between 100-2000 lux for 77% of the day with BIPV with blinds case versus 90% with the reference with blinds case.

Discomfort glare was expected to be lower with the BIPV window compared to the reference window due to the combined effect of both the visible transmittance of the transparent glass

and the lower percentage of transparent window area. [Figures 60 and 61](#) and [Tables 12 and 13](#) show the range in DGP over the monitored period for the various measured cases. This data supports this supposition.

The reduction in transmitted daylighting was also expected to result in increased lighting energy use and less indoor brightness. Lighting energy use data shown in [Figure 62](#) also supports this supposition and demonstrates the magnitude of the performance tradeoffs when using the BIPV technology.

A combination of a lower transmittance glazing and/or a more closed slat angle will be needed to bring overall discomfort levels in both rooms to below the “just perceptible” glare level of 0.35, if the most conservative view point near the window is used for the assessment. As a result of reducing glare further, lighting energy use will increase in both rooms but the magnitude of the increase will likely be lower than the between-room differences measured in this study. Therefore, for a rough, conservative estimate of the net energy production and assuming that fluorescent lighting will remain prevalent in the existing building stock for the next decade: the increase in lighting energy use is about 519 Wh while the average BIPV production for this same period is 1940 Wh/day. The net energy production is therefore 1421 Wh/day if differences in HVAC energy use are not accounted for. For an LED lighting case, the increase lighting energy would be approximately half that of the fluorescent case, about 250 Wh, resulting in a net energy production of 1681 Wh/day when factoring in solar electricity production.

**Table 11** Daily lighting energy use (Wh) and percentage savings

Date	Light	Blinds		Sky condition	Fluorescent Lighting energy use (Wh)			LED Lighting energy use (Wh)		
		A	B		room A BIPV	room B-ref	Savings	room A BIPV	room B-ref	Savings
10/3/2015	off	down	down	Clear	952	418	-128%	453	198	-129%
10/4/2015	off	down	down	Clear	977	436	-124%	466	206	-126%
10/5/2015	off	down	down	Clear	955	428	-123%	455	202	-126%
10/6/2015	off	down	down	Clear	934	497	-88%	453	233	-94%
10/7/2015	off	down	down	Clear	909	395	-130%	432	187	-131%
10/8/2015	on	down	down	Dynamic	1041	508	-105%	501	239	-110%
10/9/2015	on	down	down	Clear	999	430	-132%	477	205	-132%
10/10/2015	on	down	down	Clear	1527	1005	-52%	760	505	-51%
10/11/2015	on	down	down	Clear	970	436	-122%	461	208	-122%
10/12/2015	on	down	down	Clear	966	433	-123%	460	206	-123%
10/13/2015	on	down	down	Clear	879	395	-123%	411	187	-120%
10/14/2015	on	down	down	Clear	849	354	-140%	405	169	-139%
10/15/2015	on	up	down	Dynamic	1105	1137	3%	547	565	3%
10/16/2015	on	up	down	Clear	479	429	-12%	234	209	-12%
10/17/2015	on	up	down	Overcast	1835	2010	9%	917	1003	9%
10/18/2015	on	up	down	Dynamic	583	607	4%	285	296	4%
10/19/2015	on	up	down	Dyn+Clear	588	638	8%	294	312	6%
10/20/2015	on	up	up	Clear	395	125	-216%	191	58	-229%
10/21/2015	on	up	up	Clear	432	126	-242%	208	59	-250%
10/22/2015	on	up	up	Clear	354	130	-172%	169	61	-175%
10/23/2015	on	up	up	Dynamic	787	430	-83%	384	204	-88%
10/24/2015	on	up	up	Dynamic	571	280	-104%	275	136	-103%
10/25/2015	on	up	up	Clear	587	359	-64%	291	176	-65%
10/26/2015	on	up	up	Clear	497	256	-94%	241	123	-96%
10/27/2015	on	up	up	Cloudy	1978	1455	-36%	997	722	-38%

**Table 12** Daylight glare probability (DGP) levels for a seated view looking normal to the window

Date	Light	Blinds		Sky condition	Camera 1 -facing window					
		A	B		Room A-BIPV		Room B-Reference			
					Mean 5%	Max 95%	Class	Mean 5%	Max 95%	Class
10/1/2015	off	down	down	Dyn+Clear	0.460	0.437	C	0.738	0.653	Discomfort
10/2/2015	off	down	down	Clear	0.425	0.424	C	0.624	0.623	Discomfort
10/3/2015	off	down	down	Clear	0.437	0.436	C	0.648	0.646	Discomfort
10/4/2015	off	down	down	Clear	0.434	0.432	C	0.642	0.640	Discomfort
10/5/2015	off	down	down	Clear	0.437	0.435	C	0.648	0.645	Discomfort
10/6/2015	off	down	down	Clear	0.685	0.437	Discomfort	0.834	0.832	Discomfort
10/7/2015	off	down	down	Clear	0.447	0.444	C	0.686	0.676	Discomfort
10/8/2015	on	down	down	Dynamic	0.464	0.459	Discomfort	0.718	0.708	Discomfort
10/9/2015	on	down	down	Clear	0.438	0.437	C	0.654	0.653	Discomfort
10/10/2015	on	down	down	Clear	0.474	0.446	C	0.721	0.675	Discomfort
10/11/2015	on	down	down	Clear	0.444	0.443	C	0.666	0.665	Discomfort
10/12/2015	on	down	down	Clear	0.441	0.439	C	0.659	0.658	Discomfort
10/13/2015	on	down	down	Clear	0.452	0.451	Discomfort	0.688	0.686	Discomfort
10/14/2015	on	down	down	Clear	0.498	0.489	Discomfort	0.796	0.772	Discomfort
10/15/2015	on	up	down	Dynamic	0.872	0.869	Discomfort	0.785	0.717	Discomfort
10/16/2015	on	up	down	Clear	0.872	0.871	Discomfort	0.747	0.736	Discomfort
10/17/2015	on	up	down	Overcast	0.542	0.459	Discomfort	0.420	0.399	C
10/18/2015	on	up	down	Dynamic	0.877	0.874	Discomfort	0.821	0.798	Discomfort
10/19/2015	on	up	down	Dyn+Clear	0.881	0.878	Discomfort	0.771	0.753	Discomfort
10/20/2015	on	up	up	Clear	0.873	0.872	Discomfort	0.846	0.844	Discomfort
10/21/2015	on	up	up	Clear	0.873	0.872	Discomfort	0.844	0.842	Discomfort
10/22/2015	on	up	up	Clear	0.874	0.872	Discomfort	0.842	0.841	Discomfort
10/23/2015	on	up	up	Dynamic	0.875	0.873	Discomfort	0.853	0.851	Discomfort
10/24/2015	on	up	up	Dynamic	0.876	0.872	Discomfort	0.846	0.845	Discomfort
10/25/2015	on	up	up	Clear	0.875	0.873	Discomfort	0.848	0.843	Discomfort
10/26/2015	on	up	up	Clear	0.878	0.876	Discomfort	0.863	0.857	Discomfort
10/27/2015	on	up	up	Cloudy	0.478	0.405	C	0.654	0.614	Discomfort

**Table 13** Daylight glare probability (DGP) levels for a seated view looking parallel to the window

Date	Light	Orientation	Blinds		Sky Condition	Room A - BIPV			Room B - Reference		
			room A-BIPV	room B-Ref.		Mean (%)	Max (%)	Class	Mean (%)	Max (%)	Class
10/1/15	off	South	Down	Down	Dyn+Clear	0.329	0.306	A	0.450	0.416	C
10/2/15	off	South	Down	Down	Clear	0.349	0.304	A	0.413	0.409	C
10/3/15	off	South	Down	Down	Clear	0.357	0.311	A	0.475	0.417	C
10/4/15	off	South	Down	Down	Clear	0.376	0.308	A	0.458	0.418	C
10/5/15	off	South	Down	Down	Clear	0.329	0.311	A	0.492	0.420	C
10/6/15	off	South	Down	Down	Clear	0.360	0.323	A	0.496	0.422	C
10/7/15	off	South	Down	Down	Clear	0.330	0.318	A	0.519	0.441	C
10/8/15	on	South	Down	Down	Dynamic	0.325	0.322	A	0.455	0.447	C
10/9/15	on	South	Down	Down	Clear	0.354	0.339	A	0.498	0.445	C
10/10/15	on	South	Down	Down	Clear	0.414	0.339	C	0.491	0.455	Discomfort
10/11/15	on	South	Down	Down	Clear	0.382	0.353	C	0.539	0.465	Discomfort
10/12/15	on	South	Down	Down	Clear	0.422	0.352	C	0.545	0.474	Discomfort
10/13/15	on	South	Down	Down	Clear	0.366	0.350	A	0.544	0.475	Discomfort
10/14/15	on	South	Down	Down	Clear	0.357	0.339	A	0.548	0.476	Discomfort
10/15/15	on	South	UP	Down	Dynamic	0.677	0.586	Discomfort	0.476	0.455	Discomfort
10/16/15	on	South	UP	Down	Clear	0.864	0.857	Discomfort	0.594	0.523	Discomfort
10/17/15	on	South	UP	Down	Overcast	0.488	0.385	C	0.360	0.351	B
10/18/15	on	South	UP	Down	Dynamic	0.871	0.859	Discomfort	0.594	0.515	Discomfort
10/19/15	on	South	UP	Down	Dyn+Clear	0.863	0.839	Discomfort	0.620	0.479	Discomfort
10/20/15	on	South	UP	UP	Clear	0.876	0.872	Discomfort	0.902	0.900	Discomfort
10/21/15	on	South	UP	UP	Clear	0.875	0.873	Discomfort	0.902	0.899	Discomfort
10/22/15	on	South	UP	UP	Clear	0.873	0.868	Discomfort	0.900	0.899	Discomfort
10/23/15	on	South	UP	UP	Dynamic	0.829	0.825	Discomfort	0.875	0.857	Discomfort
10/24/15	on	South	UP	UP	Dynamic	0.842	0.830	Discomfort	0.877	0.871	Discomfort
10/25/15	on	South	UP	UP	Clear	0.877	0.871	Discomfort	0.903	0.899	Discomfort
10/26/15	on	South	UP	UP	Clear	0.865	0.842	Discomfort	0.901	0.884	Discomfort
10/27/15	on	South	UP	UP	Cloudy	0.255	0.236	A	0.334	0.305	A

**Table 14** Percentage of day (8AM-6PM) that the daylight levels are within a specified range of illuminance (usable daylight index (UDI)) for the center zone 10-20 ft. from the window

Date	Light	Blinds		Sky condition	UDI (% of day) – room A BIPV Center zone			UDI (% of day) – room B Reference Center zone		
		A	B		0-100	100-2000	>2000 lux	0-100	100-2000	>2000 lux
10/1/2015	off	down	down	Dyn+Clear	100%	0%	0%	87%	13%	0%
10/2/2015	off	down	down	Clear	2%	98%	0%	0%	100%	0%
10/3/2015	off	down	down	Clear	2%	98%	0%	0%	100%	0%
10/4/2015	off	down	down	Clear	3%	97%	0%	0%	100%	0%
10/5/2015	off	down	down	Clear	3%	97%	0%	0%	100%	0%
10/6/2015	off	down	down	Clear	2%	98%	0%	0%	100%	0%
10/7/2015	off	down	down	Clear	3%	97%	0%	1%	99%	0%
10/8/2015	on	down	down	Dynamic	4%	96%	0%	1%	99%	0%
10/9/2015	on	down	down	Clear	4%	96%	0%	1%	99%	0%
10/10/2015	on	down	down	Clear	29%	71%	0%	19%	81%	0%
10/11/2015	on	down	down	Clear	6%	94%	0%	2%	98%	0%
10/12/2015	on	down	down	Clear	5%	95%	0%	1%	99%	0%
10/13/2015	on	down	down	Clear	5%	95%	0%	1%	99%	0%
10/14/2015	on	down	down	Clear	3%	97%	0%	1%	99%	0%
10/15/2015	on	up	down	Dynamic	11%	89%	0%	13%	87%	0%
10/16/2015	on	up	down	Clear	3%	97%	0%	3%	97%	0%
10/17/2015	on	up	down	Overcast	27%	73%	0%	32%	68%	0%
10/18/2015	on	up	down	Dynamic	3%	96%	2%	4%	95%	0%
10/19/2015	on	up	down	Dyn+Clear	7%	93%	0%	9%	91%	0%
10/20/2015	on	up	up	Clear	1%	99%	0%	0%	76%	24%
10/21/2015	on	up	up	Clear	1%	99%	0%	0%	75%	25%
10/22/2015	on	up	up	Clear	1%	99%	0%	0%	72%	28%
10/23/2015	on	up	up	Dynamic	3%	97%	0%	0%	79%	21%
10/24/2015	on	up	up	Dynamic	4%	96%	0%	1%	71%	28%
10/25/2015	on	up	up	Clear	8%	92%	0%	3%	69%	28%
10/26/2015	on	up	up	Clear	3%	97%	0%	1%	69%	30%
10/27/2015	on	up	up	Cloudy	28%	72%	0%	10%	90%	0%

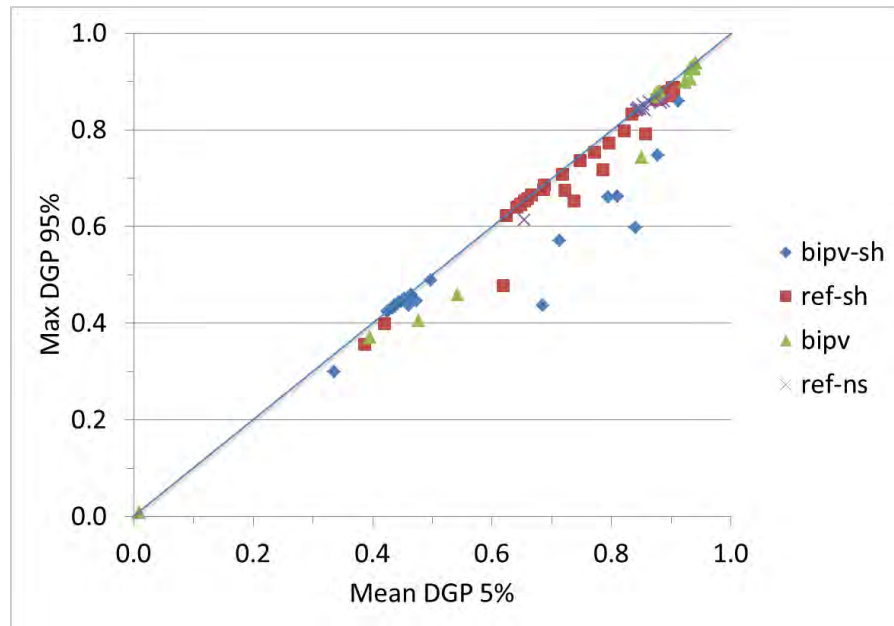


**Figure 60** South-facing window: DGP evaluation for a seated view facing window, 3 ft. from window. Mean DGP in the top 5% of daily values (x-axis) and maximum DGP in the lower 95% of daily values (y-axis). BIPV with shades (bipv-sh), reference case with shades (ref-sh), BIPV with no shades (bipv), and reference case with no shades (ref-ns). A DGP value of 0.35 corresponds to a “just perceptible” level of glare.

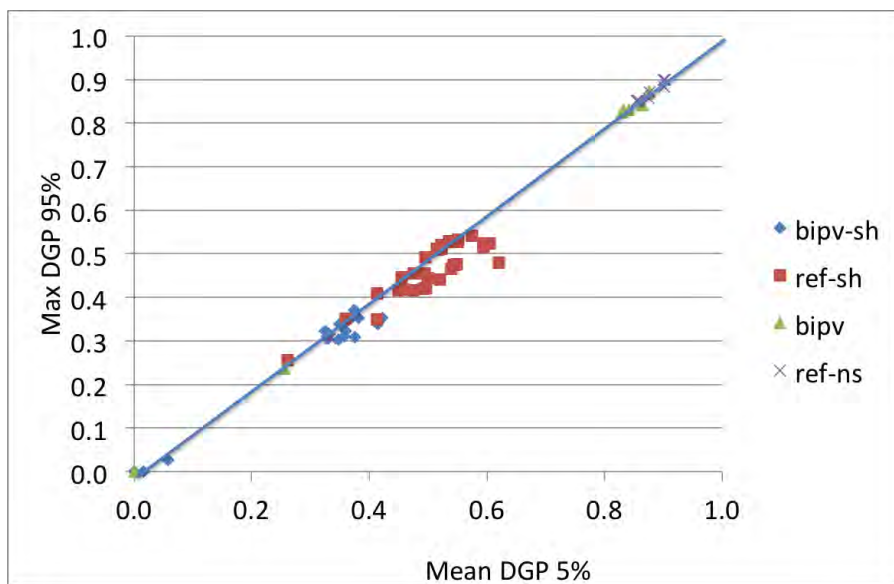


**Figure 61** South-facing window: DGP evaluation for a seated view parallel to a window, 3 ft. from window. Mean DGP in the top 5% of daily values (x-axis) and maximum DGP in the lower 95% of daily values (y-axis). BIPV with shades (bipv-sh), reference case with shades (ref-sh), BIPV with no shades (bipv), and reference case with no shades (ref-ns). A DGP value of 0.35 corresponds to a “just perceptible” level of glare.

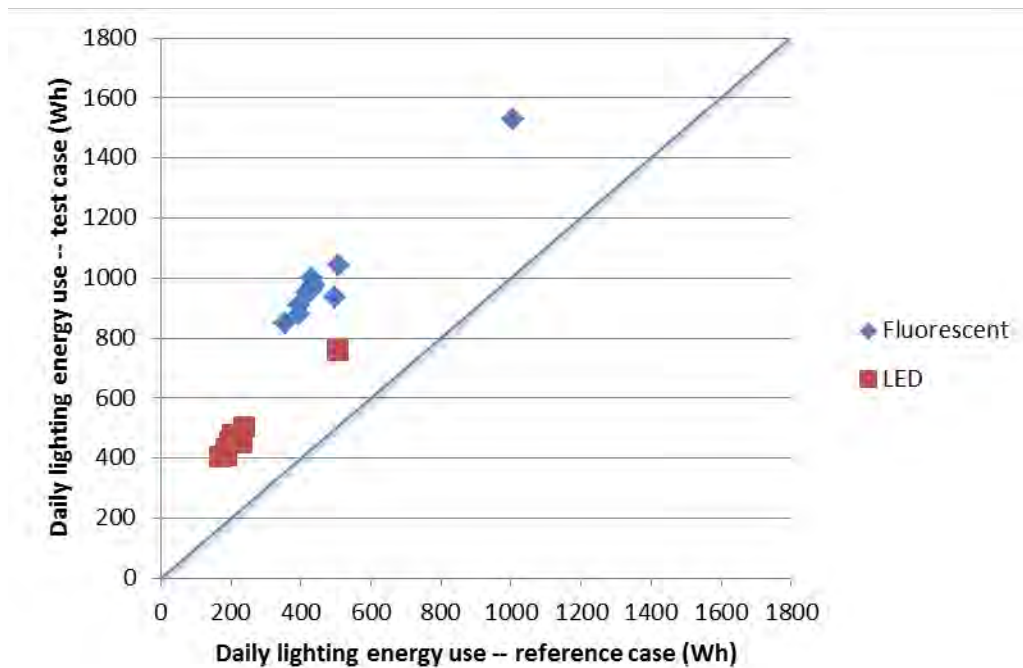


**Figure 62** Daily lighting energy for south facing window with reference glazing and blinds versus BIPV test case with blinds. Data are given for dimmable LED and fluorescent lighting systems.

The BIPV alone, without blinds, is more effective at reducing glare compared to the unshaded reference window but only when sky conditions are overcast and/or the sun's orb is not within the field of view. On a cloudy day of October 27, 2015, for example, the mean DGP value for the upper 5% of the day was 0.478 with the BIPV window compared to 0.654 for the reference window. On a sunny day of October 26, 2015, glare is high in both test cells with the mean DGP-5% at intolerable levels of 0.878 versus 0.863 for the BIPV and reference windows, respectively. Even so, the visible transmittance of the glass in both cases would need to be reduced, or other forms of shading introduced to bring the DGP levels to acceptable levels (<0.35). The DGP values in this example are given for the view facing the window.

As a benchmark for design, the "effective aperture" (EA) of the window wall is a parameter that defines the daylight potential of unshaded glazing. EA is defined here as the product of the window-to-wall area ratio, visible transmittance of the glass at normal incidence, and percentage of transparent area of the window (Table 15). In this test, the window-to-wall area ratio is 0.40, which is the largest window area allowed by the prescriptive energy efficiency codes. An EA of 0.30 or more is usually sufficient to achieve daylight "saturation" (i.e., additional annual lighting energy use reductions will not occur with greater window area or more transparent glazing) in a 15-ft deep private office. In this field test, the EA of the reference window without blinds is 0.26 whereas the EA of the BIPV window without blinds is 0.19. When blinds are used, the EA is lowered in both cases even further. To improve daylighting

and manage glare, alternate technologies should be considered if these parameters are of primary concern.

**Table 15** Effective aperture (EA) of the reference and test case windows

	Tvis	Open	WWR	EA
Reference	0.64	1.00	0.4	0.256
BIPV	0.73	0.66	0.4	0.193

#### 4.6 Comparison of Overall Energy Performance

To have a complete understanding on the overall energy saving potential of the BIPV IGU, an overview of energy consumption and energy generation results are listed in [Table 16](#). It is seen that even though the lighting electricity use of the test cell installed with BIPV IGU is higher than that installed with the reference IGU, the increment was relatively small compared to the amount of power generation of the BIPV window. In addition, the BIPV IGU also reduced net HVAC energy use by about 10% factoring in both reduced cooling due to its lower SHGC and higher heating energy use from a higher U-factor. Thus, the overall energy performance of the BIPV IGU is considerably better than that of the reference IGU. The BIPV IGU saved 15.9% net total electricity use compared with the reference IGU during the test period.

**Table 16** Comparison of electricity uses between XRA and XRB during the test period

Dates	XRA (BIPV IGU)				XRB (Reference IGU)			Energy saving	
	HVAC electricity use (kWh)	Lighting electricity use (LED) (kWh)	BIPV IGU Power generation (kWh)	Net electricity use (kWh)	HVAC electricity use (kWh)	Lighting electricity use (LED) (kWh)	Net electricity use (kWh)	Total energy saving in XRA (kWh)	Energy saving in XRA (%)
10/1/2015	16.14	1.75	1.76	16.13	17.40	1.57	18.97	2.85	15.00
10/2/2015	17.36	0.43	2.24	15.55	18.04	0.21	18.25	2.70	14.78
10/3/2015	15.76	0.45	2.34	13.87	16.92	0.20	17.11	3.24	18.95
10/4/2015	15.79	0.47	2.23	14.02	16.73	0.21	16.94	2.92	17.23
10/5/2015	17.10	0.46	2.25	15.31	18.13	0.20	18.33	3.02	16.50
10/6/2015	16.65	0.45	1.94	15.17	17.97	0.23	18.20	3.03	16.64
10/7/2015	25.85	0.43	2.21	24.08	27.85	0.19	28.04	3.96	14.14
10/8/2015	29.61	0.50	1.99	28.13	31.04	0.24	31.28	3.15	10.08
10/9/2015	31.25	0.48	2.40	29.32	29.83	0.21	30.03	0.71	2.35
10/10/2015	29.11	0.76	1.78	28.09	28.78	0.50	29.29	1.20	4.09
10/11/2015	28.16	0.46	2.39	26.23	29.08	0.21	29.29	3.06	10.46
10/12/2015	29.18	0.46	2.37	27.27	30.66	0.21	30.87	3.59	11.64
10/13/2015	25.57	0.41	2.30	23.68	29.09	0.19	29.28	5.59	19.11

Dates	XRA (BIPV IGU)				XRB (Reference IGU)			Energy saving	
	HVAC electricity use (kWh)	Lighting electricity use (LED) (kWh)	BIPV IGU Power generation (kWh)	Net electricity use (kWh)	HVAC electricity use (kWh)	Lighting electricity use (LED) (kWh)	Net electricity use (kWh)	Total energy saving in XRA (kWh)	Energy saving in XRA (%)
10/14/2015	21.09	0.40	2.10	19.39	23.35	0.17	23.52	4.12	17.53
10/15/2015	18.38	0.55	1.11	17.82	18.55	0.56	19.11	1.29	6.77
10/16/2015	18.85	0.23	2.29	16.80	19.88	0.21	20.09	3.29	16.37
10/17/2015	13.03	0.92	0.29	13.66	15.54	1.00	16.54	2.88	17.40
10/18/2015	13.37	0.28	2.09	11.57	15.62	0.30	15.91	4.34	27.29
10/19/2015	16.04	0.29	2.12	14.22	18.05	0.31	18.37	4.15	22.59
10/20/2015	17.64	0.19	2.51	15.32	19.61	0.06	19.67	4.35	22.11
10/21/2015	17.51	0.21	2.55	15.17	19.88	0.06	19.94	4.76	23.89
10/22/2015	17.25	0.17	2.48	14.94	19.55	0.06	19.62	4.68	23.83
10/23/2015	13.68	0.38	1.45	12.61	16.78	0.20	16.98	4.37	25.72
10/24/2015	13.43	0.28	1.71	11.99	15.35	0.14	15.49	3.50	22.59
10/25/2015	14.47	0.29	2.26	12.49	16.94	0.18	17.12	4.62	27.01
10/26/2015	15.85	0.24	2.22	13.87	17.67	0.12	17.79	3.92	22.04
10/27/2015	11.91	1.00	0.21	12.70	13.14	0.72	13.86	1.16	8.40
10/28/2015	12.70	0.51	0.93	12.29	14.04	0.35	14.39	2.10	14.61
10/29/2015	15.20	0.39	1.99	13.59	15.43	0.20	15.63	2.04	13.04
10/30/2015	17.03	0.42	1.96	15.49	16.84	0.24	17.08	1.59	9.33
10/31/2015	15.77	0.57	1.91	14.43	16.95	0.37	17.32	2.89	16.67
11/1/2015	14.31	0.91	1.09	14.13	14.87	0.80	15.67	1.54	9.84
11/2/2015	10.54	1.24	0.40	11.37	11.05	1.04	12.08	0.71	5.90
11/3/2015	11.20	0.76	2.00	9.95	11.48	0.53	12.01	2.06	17.13
11/4/2015	11.25	0.77	2.02	10.00	11.20	0.54	11.74	1.73	14.78
11/5/2015	11.35	0.77	1.73	10.38	11.33	0.58	11.91	1.52	12.77
11/6/2015	11.39	0.76	1.94	10.21	11.70	0.53	12.23	2.02	16.51
11/7/2015	12.08	0.59	1.90	10.77	12.24	0.53	12.76	1.99	15.59
11/8/2015	9.46	1.00	0.26	10.21	9.90	1.08	10.98	0.77	7.04
11/9/2015	8.47	1.04	0.48	9.04	8.81	1.07	9.88	0.84	8.52
11/10/2015	9.62	0.61	1.89	8.34	9.81	0.54	10.36	2.01	19.41
11/11/2015	10.34	0.60	1.90	9.04	10.33	0.53	10.86	1.82	16.72
11/12/2015	10.80	0.61	1.89	9.52	10.83	0.53	11.36	1.85	16.24
11/13/2015	11.41	0.60	1.87	10.14	11.37	0.53	11.90	1.76	14.81
11/14/2015	11.10	0.57	1.86	9.82	11.51	0.51	12.03	2.21	18.35
11/15/2015	9.74	0.63	1.53	8.85	10.66	0.62	11.28	2.43	21.56
11/16/2015	9.10	0.64	1.93	7.81	9.47	0.54	10.01	2.20	21.96

## 5. CONCLUSIONS

Based on the above comparative test results, the following conclusions can be drawn:

1. BIPV windows are characterized with both functions of building energy efficiency and distributed renewable energy generation because they not only produce power, but they also reduce solar heat gain and daylighting glare.
2. Compared to the low-e reference IGU, the test cell with BIPV IGU had lower overall energy use. On average BIPV IGU showed approximately 15.9% energy saving potential for the test period. Due to the higher U-factor and lower SHGC, however, the test cell with BIPV IGU consumed more energy for heating, thus lowering overall potential for energy savings. The higher U-factor was the result of the inappropriate placement of low-e coating in the BIPV IGU, which can be remedied in future installations.
3. Discomfort glare is lower with the BIPV window compared to the reference window due to the combined effect of both the visible transmittance of the transparent glass and the lower percentage of transparent window area. However, a combination of a lower transmittance glazing and/or suitable shading system will be needed to bring overall discomfort levels in both rooms to below the “just perceptible” glare level of 0.35
4. The increase in lighting energy use due to lower availability of daylight is anywhere between 250 Wh/day (LED lighting) to 520 Wh/day (fluorescent lighting)
5. The Solaria BIPV IGU has acceptable visual appearance, both looking from indoors and outdoors. View through the BIPV window does not appear significantly obstructed and it has overall appearance of fritted striped glazing.
6. BIPV window has relatively high energy conversion efficiency due to high efficiency crystalline silicon solar cells being used. The daily average energy conversion efficiency of the BIPV IGU was about 5% on sunny days, but it was much lower on overcast days because the crystalline silicon solar cells have lower efficiency under low irradiation level. The daily average electricity outputs at different orientations were 1.58kWh, 1.94kWh and 1.91kWh for the southeast, south and southwest orientations, respectively. Thus, south and southwest orientations are more suitable for installing BIPV IGU in terms of increasing power generation.
7. Micro-inverters are used in Solaria BIPV windows because they can track each PV module’s maximum power point alone and thus it is more productive than the conventional string inverter. Moreover, micro-inverters are less dependent on the impacts of partial exterior shading, PV modules’ mismatching and different installation orientations. BIPV systems employing micro-inverters are safer than the systems using conventional string inverters because the voltage of micro-inverter are much lower than that of string inverter. Alternatively strings inverters with module level electronics can be used
8. Electricity production on vertical window surfaces yield relatively uniform monthly energy throughout the year. This is due to the interesting coupling of solar angles and incident

solar radiation intensity, so when intensity is high, incident angle is low (i.e., closer to normal) and vice versa, resulting in relatively constant output.

9. More attention should be paid on reducing various exterior shading due to negative impact on power production. If shading is unavoidable in some cases, a reasonable arrangement of PV strings should be considered to bring down the energy loss as much as possible. For example, if horizontal shading is anticipated, shift PV cells down towards the bottom of the window and/or eliminate one cell from the top of the window. Alternatively, different electrical layout can be considered and/or use of micro-inverters.
10. Use of crystalline silicon solar cells for the Solaria BIPV modules resulted in a higher temperature coefficient during the test. For every degree centigrade of PV laminate temperature increase, the power output declined by 0.42%. This is in line with temperature-coefficient-of-power of crystalline silicon solar cells. In order to improve the energy conversion efficiency, lower PV temperatures are desired.

## 6. RECOMMENDATIONS

The following recommendations are offered:

1. The junction box of each BIPV laminate is suggested to be placed in the upper side of window frame because rain water may get into the lower side of window frame and then cause a short circuit to the junction box. In addition, if the junction box is placed in upper side of frame, occupants are unable to touch it, thus it will be safer.
2. More attention should be paid on reducing various exterior shading due to negative impact on power production. If shading is unavoidable in some cases, a reasonable arrangement of PV strings should be considered to bring down the energy loss as much as possible. For example, if the horizontal shading is present, the BIPV IGU should be installed rotated by 90 degrees, so that partial shading does not shut down entire window power production. An onsite exterior shading study is recommended prior to BIPV design.
3. A study on daylighting performance and visual comfort under different transmittances is recommended to be conducted to identify the optimal transmittance which can not only achieve the acceptable visual comfort and daylighting performance, but also maximize the overall energy performance of BIPV IGU including power generation, reduction of HVAC energy use and lighting energy use.
4. The U-factor of the BIPV IGU tested on FLEXLAB was relatively high due to the inappropriate placement of low-e coating. If the low-e coating is deposited on the forth surface (facing the IGU cavity) in future designs (see Figure 12), its energy performance would be further improved and the energy saving potential would be larger.

## 7. REFERENCES

- [1] Arasteh, D., S. Selkowitz, J. Apte, Zero Energy Windows, Proceedings of the 2006 ACEEE Summer Study on Energy Efficiency in Buildings, August 13-18, 2006, Pacific Grove, CA, <<http://gaia.lbl.gov/btech/papers/60049.pdf>>
- [2] 2010 Buildings Energy Data Book. US Department of Energy, Building Technologies Program, Energy Efficiency and Renewable Energy. Tables 1.1.1 and 1.2.3.
- [3] Apte J, Arasteh D (2006). Window-Related Energy Consumption in the US Residential and Commercial Building Stock. Berkeley, CA, Lawrence Berkeley National Laboratory: LBNL-60146
- [4] U.S. Energy Information Administration (2012). Annual Energy Outlook 2012- with Projections to 2035. DOE/EIA-0383(2012)
- [5] Nelson Ng. The design and manufacture of vacuum glazing. The University of Sydney. <<http://www.physics.usyd.edu.au/app/research/vacuumglazing/>>
- [6] H. Weinsäcker, H.-P. Ebert, J. Fricke. VIG - Vacuum Insulation Glass. 7th International Vacuum Insulation Symposium 2005.
- [7] Chris Woodford. "Smart" windows (electrochromic glass), 2014 <<http://www.explainthatstuff.com/electrochromic-windows.html>>
- [8] <<http://www.commercialwindows.org/thermochromic.php>>
- [9] GPG report. A Pilot Demonstration of Electrochromic and Thermochromic Windows in the Denver Federal Center, Building 41, Denver, Colorado.
- [10] EPTP, 2014. Building Integrated Photovoltaics—A New Design Opportunity For Architects. European Photovoltaic Technology Platform. <[http://www.aie.eu/files/RES%20TF/BIPV\\_web.pdf](http://www.aie.eu/files/RES%20TF/BIPV_web.pdf)>
- [11] Wienold J., J. Christoffersen (2006). Evaluation methods and development of a new glare prediction model for daylight environments with the use of CCD cameras. *Energy and Buildings* 38(7): 743- 757.